

**Clinical and Laboratory studies to
support the First-in-Human trial of a
novel poly(ADP-ribose) polymerase
inhibitor in combination with
temozolomide**

NEWCASTLE UNIVERSITY LIBRARY

203 02878 1

MED Thesis M811

Ruth Plummer

MD Thesis

July 2004

Abstract

Poly(ADP-ribose)polymerase (PARP) is a nuclear enzyme involved in the repair of DNA single strand breaks via the Base Excision Repair pathway (BER).

Temozolomide, a DNA alkylating agent recently licensed for the treatment of gliomas and melanoma, produces DNA lesions which are targets for BER. Preclinical studies demonstrate that PARP inhibitors increase the cytotoxicity and antitumour activity of temozolomide suggesting that PARP inhibitors may have a clinical role as chemopotentiating agents.

This thesis describes the protocol development of a First-in-Human phase I clinical trial of AG014699, a potent PARP inhibitor, in combination with temozolomide in patients with advanced solid malignancies discussing the rationale for the study design, definition of pharmacodynamic (PD) endpoints and starting dose. A two part trial escalating first the dose of AG014699 then that of temozolomide was designed with PD endpoints for part 1 and classical toxicity endpoints for part 2.

The development and validation of two PARP activity assays to measure enzyme activity and inhibition in human peripheral blood lymphocytes (PBLs) and homogenised tumour biopsies are discussed. An established tumour cell line (L1210) was evaluated to provide Quality Assurance, and preparation, storage and transport stability of samples investigated. The first assay developed relied upon measuring incorporation of [³²P] NAD⁺ into poly(ADP-ribose) (PAR), this assay proved robust but depended upon the availability of large numbers of PBLs, limiting its clinical application. An alternative assay based on detection of PAR with a monoclonal antibody and electronic digitisation of the chemiluminescence signal was validated and then assessed in a phase II mechanistic study of temozolomide alone in patients with advanced malignant melanoma. This small study provided additional validation for the assay and also data on DNA damage and repair after temozolomide which can be used as control data to interpret the pharmacodynamic results of the First-in-Human study.

Contents

Chapter 1	Introduction	1-34
1.1	Background	2
1.2	DNA repair mechanisms	3
	1.2.1 Base excision repair	5
	1.2.2 Mismatch repair	6
1.3	Poly(ADP-ribose) polymerase (PARP)	7
1.4	Role of PARP-1 in DNA repair	11
	1.4.1 Base excision repair	11
	1.4.1 Interactions of PARP-1 and p53	14
1.5	Role of PARP-1 in apoptotic and necrotic cell death	16
1.6	Development of PARP-1 inhibitors	18
1.7	Development of AG014699	22
1.8	Temozolomide	25
	1.8.1 Chemistry and mechanism of action	25
	1.8.2 Repair of temozolomide induced DNA damage	27
	1.8.8.1 N ⁷ -methylguanine and N ³ -methyladenine repair	27
	1.8.8.2 O ⁶ -alkylguanine DNA-alkyltransferase and MMR	27
	1.8.3 Temozolomide and PARP-1 inhibition	29
	1.8.4 Clinical use of temozolomide	31
1.9	Summary	33
Chapter 2	Protocol development of Phase I clinical protocol for First-in-Human use of a PARP inhibitor in combination with a cytotoxic agent	35-57
2.1	Introduction	36
2.2	Preclinical efficacy study	37
	2.2.1 Efficacy	37
	2.2.2 PK and PD	40
	2.2.2.1 PK/PD at efficacious dose	40
	2.2.2.2 Pk/PD at toxic dose	42
2.3	Protocol development	43
	2.3.1 Summary of protocol design	43
	2.3.2 Dosing plan for the two parts of the study	46
	2.3.3 Single agent dosing with AG014699	47
	2.3.4 Study objectives and endpoints	48
2.4	Preclinical toxicology and starting dose	50
2.5	Definition of pharmacodynamic endpoints	53
2.6	Precursor study rationale and links with PARP inhibitor study	56
2.7	Conclusion	57
Chapter 3	Laboratory Methods	58-77
3.1	Materials	59
	3.1.1 General laboratory chemicals	59
	3.1.2 Tissue culture reagents	59
	3.1.3 Clinical supplies	59
	3.1.4 Radiochemicals	60

3.1.5	Antibodies	60
3.1.6	Other reagents	60
3.2	Tissue culture and preparation of QC samples	60
3.2.1	Methods	60
3.2.2	Preparation of QC samples for [³² P] assay	61
3.2.3	Preparation of QC samples for immunoblot	61
3.3	Lymphopreparation of human PBLs	62
3.4	Preparation of tissue/tumour homogenates	63
3.4.1	Collection and storage of tumour samples	63
3.4.2	Homogenisation of tissue	63
3.5	[³² P] NAD ⁺ incorporation PARP activity assay in PBLs	64
2.5.1	Stock solutions preparation and storage	64
2.5.2	Assay procedure	65
3.6	[³² P] NAD ⁺ incorporation PARP activity assay in tumour/tissue homogenate	68
3.6.1	Stock solutions and storage	68
3.6.2	Assay procedure	68
3.7	Immunoblot assay for measuring PAR formation in human PBLs	70
3.7.1	Stock solutions	70
3.7.2	Preparation of PAR standards	71
3.7.3	Assay procedure	72
3.8	Immunoblot assay for measuring PAR formation in homogenised tumour/tissue	75
3.8.1	Stock solutions	75
3.8.2	Assay procedure	75
3.9	Statistical analyses	77

Chapter 4	Validation of [³²P] NAD⁺ incorporation assay for PARP activity in clinical samples	78-108
4.1	Introduction	79
4.2	Measurement of PARP activity in human PBLs	81
4.2.1	Lymphopreparation and permeabilisation	81
4.2.1.1	Lymphopreparation	81
4.2.1.2	Permeabilisation	83
4.2.2	Demonstration of PARP inhibition in human PBLs	87
4.3	Establishment of QC samples	88
4.4	Validation of sample storage and handling	89
4.4.1	PARP-1 activity in fresh versus frozen L1210 cells	90
4.4.2	Preservation of PARP-1 inhibition with Frozen storage	92
4.4.3	Comparison of frozen storage temperature	94
4.4.4	Enzyme stability in PBLs	96
4.4.5	Temporal fluctuation in PBL PARP activity	97
4.4.6	Assessment of enzyme integrity after transportation of samples	99
4.5	Assay validation for use with human tumour samples	100

4.5.1	Confirmation of activation in the absence of added oligonucleotide	101
4.5.2	Effect of freezing and storage of tissue samples	102
4.5.3	PARP inhibition with AG014699 in tissue	103
4.6	Intra-assay variability	104
4.7	Discussion	105
Chapter 5	Development and validation of immunoblot PARP activity assay	109-145
5.1	Introduction	110
5.2	PAR detection in L1210 and PBL cell preparations	112
5.3	Identification and characterisation of a poly(ADP-ribose) standard curve	118
5.4	Modifications to the assay protocol during validation experiments	124
5.5	Immunoblotting for tumour/tissue samples	129
5.6	Investigation of the nature of 10H antibody binding chemiluminescence detection	133
5.7	Evaluation of PARP knockout cells or animal tissue using immunoblot	136
5.8	Discussion	141
Chapter 6	Clinical and laboratory results for a phase II mechanistic study of temozolomide in advanced malignant melanoma	146-173
6.1	Introduction	147
6.2	Study design	150
6.2.1	Protocol design	150
6.2.2	Sampling schedule and methods	151
6.2.3	Laboratory methods	153
6.3	Patient demographics and clinical data	155
6.3.1	Patient demographics	153
6.3.2	Treatment and toxicity summary	157
6.3.3	Response data	158
6.4	Plasma temozolomide pharmacokinetics	159
6.5	PARP activity in human PBLs and the effect of temozolomide	161
6.6	PARP activity in homogenised human tumour biopsies	164
6.7	Investigation of DNA damage and repair	165
6.7.1	COMET assay for DNA breaks	165
6.7.2	ATase	166
6.8	Discussion	168
Chapter 7	Summary	174-179
7.1	Introduction	175
7.2	Protocol development	175
7.3	Pharmacodynamic assay validation	176
7.4	Assay evaluation within a phase II clinical trial	178
7.5	Conclusions and future directions	178
References		180-190

Acknowledgments

Firstly, and most importantly, I would like to thank Nicola, Hilary and Herbie for the supervision, advice and enthusiasm they have given me throughout this project. I have the unusual privilege of having been supervised through two doctoral projects where my supervisors have also become friends. The final stages of assay development were assisted and made more fun by the appointment of Chris Jones as the “PARP clinical fellow” and my first MD student.

I am very grateful to Suzanne Kyle who provided expert help and taught me much, Mike Batey with whom I learnt to lymphoprep, April Clark for her technical assistance and Huw Thomas for his help with the animal experiments.

Alex Bürkle generously supplied the 10H antibody used and also supported our endeavours to modify his immunoblot assay for clinical use. His colleague Ragen Pfeiffer provided much practical help.

Alan Boddy has tolerated my inexperience on all matters pharmacokinetic with good humour, Barbara Dukacz and Mark Verrill provided much constructive comment whilst acting as internal assessors for the project.

Financial support was provided by Cancer Research UK and Pfizer GRD. I am particularly grateful for the help and enthusiasm given to development of the clinical PARP project by Heidi Steinfeldt, Steve Reich (Pfizer GRD) and Lesley Robson (Cancer Research UK).

Finally I would like to thank my husband, Chris, and children, David, Michael and Emily, who have tolerated months of a distracted mummy who never wanted to play in the evenings.

Chapter 1

Introduction

1.1 Background

Cancer is a major cause of morbidity and mortality in both children and adults. The disease has enormous implications both for sufferers and their families in terms of physical, emotional and financial changes in their lives. For the National Health Service the treatment of tumours and care of patients in the terminal phases of the disease have major resource implications. In the last year total deaths from cancer have overtaken those for heart disease as the major cause of adult mortality.

Improvement in cancer survival has been identified by the government as a key area for action (1992). There are estimated to be >250,000 new diagnoses and >150,000 deaths per year in the United Kingdom (www.cancerresearchuk.org).

Treatments for cancer include surgery, radiotherapy, cytotoxic chemotherapeutic drugs, biological agents, the newer targeted therapies – the signal transduction modifying agents and supportive/palliative care. The majority of patients will receive a combination of these treatment modalities for their tumour over the course of the disease.

Over the last 50 years there have been great advances in the use of cytotoxic chemotherapy, and high cure rates are achieved in a number of childhood cancers, lymphoma and germ cell tumours. However the majority of adult solid tumours are incurable with chemotherapy alone, and in the metastatic setting this treatment remains palliative. The efficacy of cytotoxic drugs is limited by toxicity, in particular myelosuppression, lack of specificity and cancer cell drug resistance. A variety of resistance mechanisms have been described or proposed, including decreased drug uptake into cells, increased drug efflux (for example multi-drug resistance mediated by P-glycoprotein expression), inactivation of the drug, alteration of the cellular target, development of tolerance and repair of the drug-induced DNA damage (DeVita, Hellman et al. 1997).

The development of better agents with which to treat cancer is a major goal both for the pharmaceutical industry and also within academic research laboratories. It is estimated that in the field of anticancer drug development there are approximately 500 compounds in development (Budman, Calvert et al. 2003). New agents are identified

by screening natural products against tumour cell line panels, target identification and rational drug design, or the use of computational drug design to improve existing drugs or identify new compounds.

One potential target for the improvement in the efficacy of existing cytotoxic chemotherapy would be inhibition of the DNA repair machinery. It is known that the DNA damage caused by many chemotherapeutic agents is rapidly repaired, both in normal tissues and the tumour. Inhibition of this repair in conjunction with administration of DNA damage either by chemotherapy or radiotherapy could be a mechanism for improving treatment outcomes.

The Drug Development Unit within the Northern Institute for Cancer Research has been developing inhibitors of poly(ADP-ribose)polymerase (PARP) including PARP-1, an enzyme involved in DNA repair, as a mechanism for potentiating the cytotoxicity of both chemotherapy agents and radiation. The work reported in this thesis has been performed within the Drug Development Unit and included establishing optimum study design and the pharmacodynamic endpoints of PARP-1 inhibition. This introduction gives an overview of DNA repair mechanisms, PARP-1 and its role in DNA repair, the preclinical development of a potent PARP inhibitor and discusses the development of temozolomide, an oral monofunctional DNA alkylating agent, which will be used in combination in the First-in-Human study of the PARP-1 inhibitor in cancer.

1.2 DNA repair mechanisms

Throughout the life of a mammalian cell there are various situations in which DNA may be damaged, either by exogenous toxins, exposure to ionising radiation and from endogenous sources such as products of cellular metabolism. It is estimated that the average rate of damage is about 10^4 events per cell per day (Ames and Gold 1991). It is therefore essential that the cell has mechanisms in place to preserve its genomic integrity. There are reported to be at least 5 distinct pathways by which the cell can detect and repair much of this damage; direct repair, mismatch repair (MMR), base excision repair (BER), nucleotide excision repair (NER), non-homologous end joining

(NHEJ) and homologous recombinational repair (HRR) (reviewed in (Lindahl, Karran et al. 1997; Hansen and Kelly 2000; Christmann, Tomicic et al. 2003).

Direct repair describes the mechanism where the modified base is repaired by direct reversal of the alteration without removal of the base itself. The main component of the direct repair pathway is the alkyltransferase protein which will be discussed in detail in section 1.9 in relation to temozolomide.

Nucleotide excision repair is thought to be coupled with transcription, sometimes termed “transcription-coupled repair” (TCR) and involves at least 11 proteins (reviewed in (Wood 1996; Lindahl, Karran et al. 1997). A helix distorting lesion is recognised by a three protein complex, other proteins are recruited and the DNA backbone incised by XPF and XPG nucleases. An oligonucleotide of 25-32 bases is released and the gap filled and DNA re-ligated. Its evolutionary role is thought to be linked to the correction of UV (sunlight) damage to DNA (Lindahl, Karran et al. 1997), and inherited lesions in this pathway are responsible for the photosensitivity disorder xeroderma pigmentosum.

Double strand breaks are repaired by homologous recombination repair (HRR) or non-homologous end-joining (NHEJ), the major proteins in these pathways being Rad 51, NBS, MREII, XRCC3 and BRCA1 and BRCA2 (HRR); and Ku70, Ku86 and DNA-PK in NHEJ (reviewed in (Bernstein, Bernstein et al. 2002).

The study reported here involves progress towards a phase I study of a PARP inhibitor in combination with temozolomide, a DNA methylating agent used in the treatment of melanoma and brain tumours ((Newlands, Stevens et al. 1997). Temozolomide methylates DNA at O⁶-guanine, N⁷-guanine and N³-adenine in a ratio 1:14:2. O⁶-methylguanine is repaired by O⁶-alkylguanine-DNA alkyltransferase (OGAT, ATase, MGMT) but if unrepaired becomes a target for MMR. N⁷-methylguanine and N³-methyladenine are repaired by BER. PARP-1 is known to have a role in BER. Hence these three mechanisms of DNA repair are discussed in more detail below.

1.2.1 Base excision repair

The base excision repair pathway is divided into short patch and long patch repair. Despite these names BER involves removal of relatively short stretches of DNA, between 1 and 15 nucleotides. Short patch base excision repair involves removal of one base only whilst long patch repair removes 2-15 nucleotides; however they share a common pathway. It is thought that short patch repair is involved in the repair of methylation induced DNA damage whereas long patch repair corrects oxidative damage (Hansen and Kelly 2000) these mechanisms having evolved to correct endogenous DNA damage (Lindahl, Karran et al. 1997).

Short patch BER involves the removal of the incorrect or damaged base by a DNA glycosylase, in eukaryotes 3-methyladenine DNA glycosylase (MPG) repairs N⁷-methylguanine, N³-methyladenine and N³-methylguanine adducts, all of which are formed by temozolomide ((Friedberg, Walker et al. 1995). Removal of the damaged base generates an apurinic/apyrimidinic (AP) site which is cleaved by an AP endonuclease/3' phosphodiesterase leaving a single strand break. Replacement of the damaged base and religation of the DNA involves recruitment of a complex including DNA polymerase β , DNA ligase I or III/XRCC I (X-ray repair cross-complementing 1), PARP-1 (Masson, Niedergang et al. 1998) and/or PARP-2 (Schreiber, Ame et al. 2002). The steps in the process are summarised in figure 1.1 (adapted from (Lindahl, Karran et al. 1997), the role of PARP-1 in the process will be discussed in more detail below.

Long-patch repair is thought to be involved in the repair of oxidised or reduced AP sites and is thought to be a minor, sub-pathway. 2-15 bases are excised, subsequent repair involving DNA polymerases δ , ϵ and β , PCNA/RF-C, FEN I and DNA ligase I (Hansen and Kelly 2000). There is no known role for PARP-1 in this process.

Figure 1.1

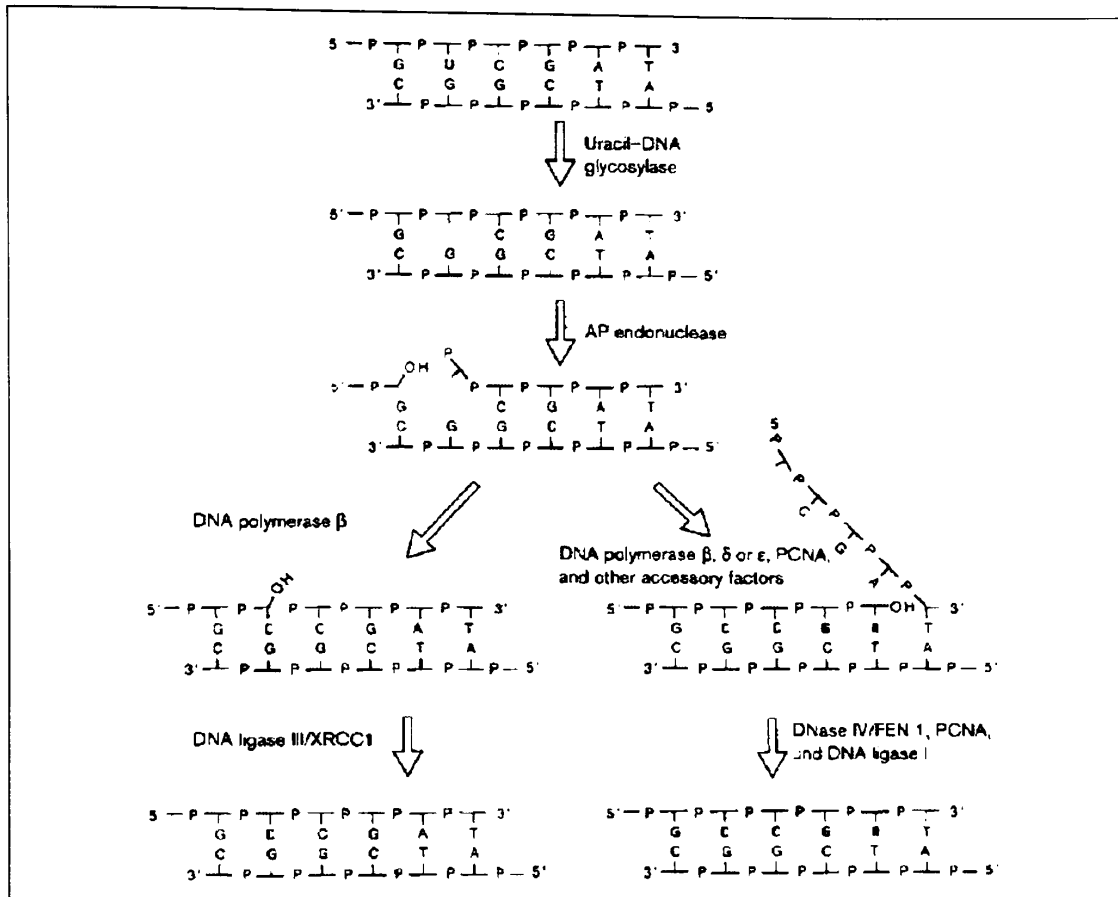


Figure 1.1 Schematic representations of the steps involved in BER, the common initial pathway dividing into short-patch repair on the left and long-patch repair on the right.

1.2.2 Mismatch repair

Mismatch repair (MMR) recognises incorrectly paired oligonucleotides resulting in their excision and the generation of a 100-1000 nucleotide gap in the daughter strand with the incorrectly paired base, leaving the correct (in most cases) template strand intact. The gap in the daughter strand is filled and the DNA ligated to complete the repair process. MMR repair is defective in some inherited forms of cancer (Hereditary non-polyposis coli, HNPCC; (Lynch, Smyrk et al. 1996)) and in a number of sporadic cancers and is thought to lead to genetic instability and resistance to DNA damage by a number of chemotherapeutic agents including temozolomide, 6-thioguanine, cisplatin and carboplatin (Fink, Aebi et al. 1998).

MMR repair was initially studied in bacteria and the major members of the pathway characterised in *Escherichia coli* as MutS, MutL and MutH. Homologues of these enzymes have now been characterised in mammalian species and are termed the MSH and MLH genes, MSH1-6 (Fishel and Wilson, 1997) which act as heterodimers. MLH 1 inactivation is common in human tumours. MSH2 and MSH6 heterodimers preferentially recognise single base mispairs (Drummond, Li et al. 1995) and bind to the O⁶-methylguanine residues formed by temozolomide. However it is the mispaired thymine residue in the daughter strand which is excised and the O⁶-methylguanine residue is left intact for further mis-pairing (Fink, Aebi et al. 1998). Loss of MMR confers “methylation tolerance” and resistance to temozolomide. The consequences of this are discussed in section 1.8 and the interaction between MMR and PARP-1 inhibitor in section 1.8.4

1.3 Poly(ADP-ribose)polymerase (PARP)

Poly(ADP-ribosyl)ation of nuclear and intra-cellular proteins occurs in most eukaryotic cells in response to a variety of cellular stresses and was first reported in 1963 (Chambon, Weil et al. 1963). It is now known that this process is due to a family of enzymes known as poly(ADP-ribose) polymerase or PARP enzymes, 18 members of the family have been identified so far. PARP 1, 2, 3, V-PARP and Tankyrase being the most intensively investigated (reviewed in (Smith 2001), with PARP-1 (EC 2.4.2.30) the most abundant and best characterised.

All the members of the family cloned so far show marked homology (25-60% homology with PARP-1), with the NAD⁺ binding cleft being highly conserved (Simonin 1993), figure 1.2 adapted from (Smith 2001). PARP-1 (EC 2.4.2.30) is very highly conserved between species; in particular the catalytic region shows 100% homology between vertebrates and 92% homology among all species (de Murcia and Menissier de Murcia 1994).

Figure 1.3

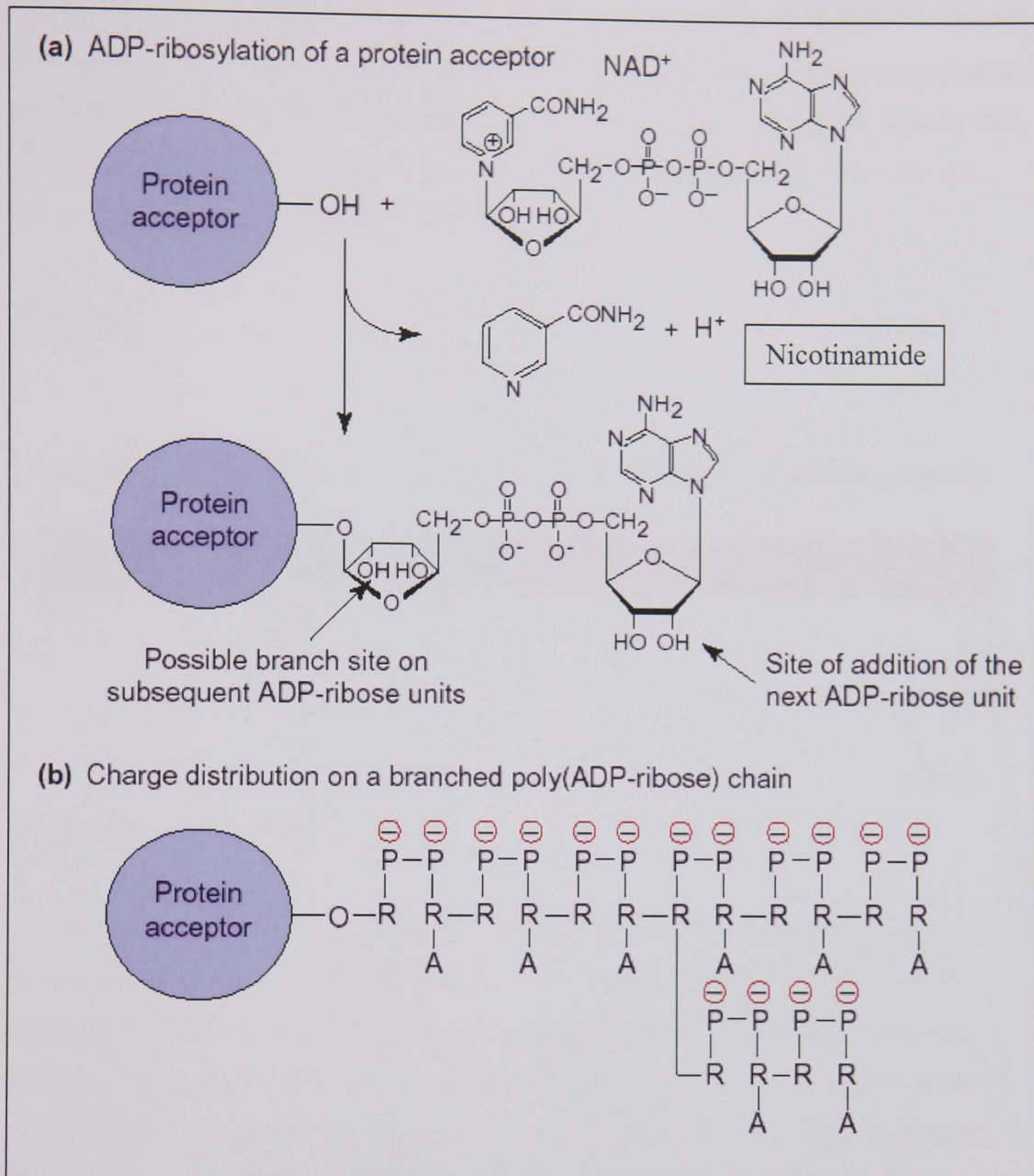


Figure 1.3 Catalytic mechanism of PARP enzymes. a) PARP cleaves NAD^+ releasing nicotinamide and covalently attaches linear and branched polymers of ADP-ribose, which may >100 units long, to acceptor proteins. b) charge distribution on polymer

PARP-1 is a protein of 1014 amino acid residues, which has three functional domains (figure 1.4 from (Burkle 2001); the DNA binding fragment (DBD) which contains two zinc finger motifs involved in DNA strand break recognition and a nuclear location signal, the central auto-modification domain which includes a BRCA-1 C-terminal

domain (BRCT) and the C-terminal catalytic fragment which binds NAD^+ (reviewed in (Shall 2002)). In humans the gene coding for PARP-1, designated ADPRT, lies on chromosome 1q41-1q42 (Cherney, McBride et al. 1987). The crystal structure of the purified catalytic fragment of chicken PARP-1 has been identified (Ruf, Murcia et al. 1996). Human PARP-1 can now be produced from c-DNA cloned in baculovirus expression vectors (Knight and Chambers 2001).

Figure 1.4

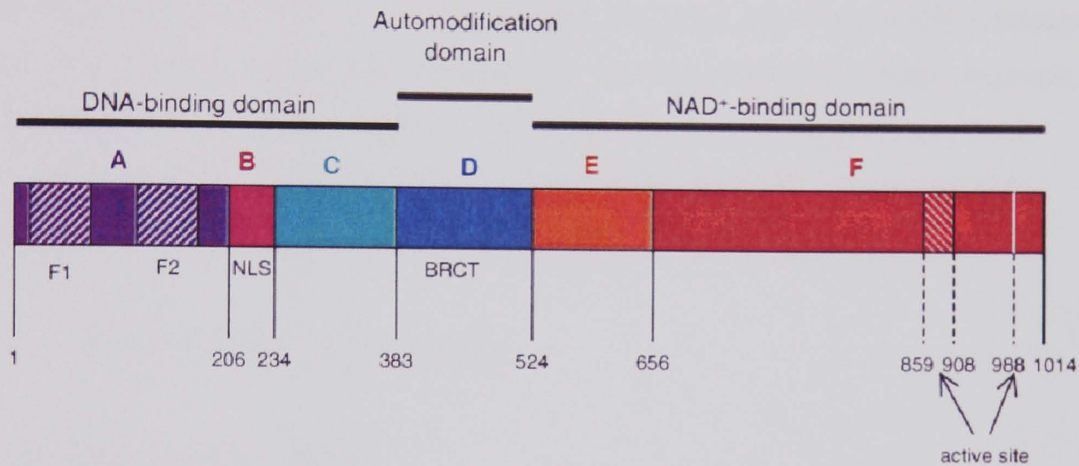


Figure 1.4 Functional domains of PARP-1

PARP-1 is a very abundant nuclear enzyme being present at the density of one enzyme molecule per 1 kb DNA (Burkle 2001). It is constitutively expressed in eukaryotic cells but has low basal activity unless activated by genotoxic stresses. DNA binding increases the activity of the enzyme 500-fold. PARP-1 binds to DNA strand breaks via the two zinc fingers at the aminoterminal DBD, its activity being dependent on such binding (Boulikas 1991). The enzyme acts as a homodimer (Mendoza-Alvarez and Alvarez-Gonzalez 1993) catalysing the transfer of ADP-ribose from the substrate NAD^+ to nuclear acceptors. These acceptors include histones, topoisomerases, DNA polymerases I and II, Ca^{2+} and Mg^{2+} -endonucleases and DNA ligases, p53, but in particular the PARP-1 enzyme itself (reviewed in (Davidovic, Vodenicharov et al. 2001)). Long polymers of up to 200 units, often highly branching, are formed. Modified PARP-1 is released from the DNA, this is presumed to be due to the electrostatic repulsion of the now highly negatively charged complex and results in inactivation of the enzyme. The polymer is rapidly degraded by poly (ADP-ribose) glycohydrolase (PARG) (Davidovic, Vodenicharov et al. 2001; Rossi, Denegri

et al. 2002) releasing PARP-1 for further activation. Although it was originally proposed that PARP could not remove the final ADP-ribose residue, this being removed by ADP-ribosyl protein lyase (Oka, Ueda et al. 1984), recent studies using purified PARG and PARG inhibitors suggest that PARG alone can degrade the entire polymer (Jacobson M, PARP Conference, Lisbon, 2003).

There is much debate over the potential roles of PARP-1 and poly(ADP-ribosylation) in the cells. The rapid production of polymer in response to DNA damage has led to the suggestion that PARP-1 plays an important part in the signalling of DNA damage and, in fact, acts as a “molecular nick sensor”, recruiting appropriate repair enzymes (de Murcia and Menissier de Murcia 1994). There is compelling evidence for the involvement of PARP-1 in BER and increasing data suggesting a more complex function in the regulation of DNA repair and induction of apoptosis.

1.4 Role of PARP-1 in DNA repair

1.4.1 Base excision repair

The fact that poly(ADP-ribosylation) plays a role in the recovery of proliferating cells from DNA damage was demonstrated over 20 years ago (Durkacz, Omidiji et al. 1980) . It is known that PARP-1 is involved in the process of base excision repair (BER) and PARP-1 is part of the base excision repair complex (Molinete, Vermeulen et al. 1993; Lindahl, Satoh et al. 1995; Dantzer, Schreiber et al. 1999). PARP-1 is activated within minutes of DNA damage (Bernardi, Negri et al. 1995) and the synthesis of poly(ADP-ribose) has been shown to be directly proportional to the number of single and double DNA strand breaks (D'Amours, Desnoyers et al. 1999). PARP-1 has been shown to bind to single strand breaks via the second zinc finger (f II), a single strand break introduces flexibility into the damaged region of DNA, and a characteristic “V”-shape to the molecule is seen on dark-field electron microscopy. PARP-1 binds specifically to the centre of this “V”, accentuating the distortion (de Murcia and Menissier de Murcia 1994) and potentially easing access for the other elements of the BER pathway.

The polymer complex formed is very short lived, having a half life in vivo of approximately 1 minute (Alvarez-Gonzalez and Althaus 1989). The close association with PARG means that there is a dynamic system where PARP-1 is rapidly activated by the DNA damage, polymer is formed, down stream processes are activated and PARP-1 is released from the DNA. The polymer is then rapidly degraded by PARG to free PARP-1, in the case of automodification, for further activation. The number of PARP-1 molecules per cells means that the enzyme is ideally placed to act as a “nick sensor”, and then be released to detect other DNA damage (Masutani, Nozaki et al. 1995). This process causes a rapid depletion of cellular NAD⁺ and imposes a high energy cost on the cell indicating its importance

It is proposed that PARP-1 has a role in regulating the response to DNA damage via a “shuttling model”, where the enzyme is closely associated with DNA, detects and binds to strand breaks (Sato and Lindahl 1992). This causes PARP activation and formation of negatively charged polymer. Automodification of the enzyme means it becomes progressively more negatively charged, a “point of repulsion” is reached when it no longer can associate with DNA. Polymer is removed from the released enzyme by PARG allowing further shuttling to signal DNA damage (Lindahl, Sato et al. 1995; D'Amours, Desnoyers et al. 1999). PARP-1 binds strongly to DNA, having a high affinity for single strand breaks but also blunt ended DNA double strand breaks, where it is proposed it may act to prevent inappropriate recombination prior to DNA repair (D'Silva, Pelletier et al. 1999).

Poly(ADP-ribosylation) of histones also occurs in response to DNA damage. Attachment of the negatively charged polymer leads to electrostatic repulsion and opening up of the chromatin and allowing access of the BER complex, followed by subsequent degradation of PAR and re-association of the histones with DNA (reviewed in (D'Amours, Desnoyers et al. 1999) suggesting another mechanism by which this enzyme is involved in DNA repair.

Further evidence to support a role for PARP-1 in BER has come from the studies by Masson and colleagues (Masson, Niedergang et al. 1998) where a two-hybrid system was used to demonstrate the close physical association of PARP-1 and XRCC1, which is a scaffold protein in the BER complex. XRCC1 is known to interact with

DNA ligase III and DNA polymerase β , and the identification of its third partner as PARP-1 has led to a new model comprising the BER multi-protein complex (figure 1.5).

Studies where PARP-1 activity has been reduced, either by chemical inhibitors, trans-dominant inhibition of PARP-1 by overexpression of the PARP DNA binding domain (DBD), depletion of PARP by antisense-RNA or mutation of the PARP-1 gene and the generation of PARP-1 knockout mice, have provided more evidence for a role of PARP-1 in BER. Data from studies with all of these mechanisms of PARP inhibition have shown increased sensitivity to agents that cause DNA damage that is repaired by BER – alkylating agents, ionising radiation, oxidative damage but not those repaired by other pathways, for example ultraviolet light.

HeLa cell lines depleted in PARP have been generated by induction of PARP-antisense RNA expression. These cells perform very limited DNA repair in response to methylmethanesulfonate (which generates single strand breaks) induced DNA damage (Ding and Smulson, 1994). Overexpression of the DBD has been established in a number of cell lines. This causes trans-dominant inhibition of PARP-1 possibly by blocking the DNA binding of the enzyme. This inhibition causes increased sensitivity to DNA alkylating agents (N⁷-nitro-N-nitrosoguanidine, MNNG) (Molinete, Vermeulen et al. 1993) and ionizing radiation (Kupper, Muller et al. 1995) with a reduction in PARP activation, an increase in cell doubling time, G₂/M accumulation and reduction in cell survival (Schreiber, Molinete et al. 1992). All these data provide further evidence for a critical role of PARP in BER repair of DNA damage (reviewed in (Dantzer, Schreiber et al. 1999).

PARP^{-/-} (PARP-1 knockout mice) have been developed in three laboratories by homologous recombination in embryonic stem cells (Wang, Auer et al. 1995; de Murcia, Niedergang et al. 1997; Masutani, Nozaki et al. 1999) disrupting exons 2, 4 and 1 respectively. These animals are phenotypically normal but are substantially deficient in BER and hypersensitive to ionising radiation and DNA alkylating agents (de Murcia, Niedergang et al. 1997; Wang, Stingl et al. 1997; Masutani, Nozaki et al. 1999) and have altered responses to cellular stress (Wang, Stingl et al. 1997). Cell lines from these animals show increased genomic instability (Simbulan-Rosenthal,

Haddad et al. 1999). In a cell-free DNA repair assay extracts from mouse embryonic fibroblasts (MEF) from PARP^{-/-} animals showed impaired repair of DNA single-strand breaks associated with a reduced expression of factors involved in long patch BER (Sanderson and Lindahl 2002). All these data indicate that there is an alteration in BER in these animals (Shall and de Murcia 2000).

Production of poly(ADP-ribose) polymers has been demonstrated in PARP^{-/-} cells (Shieh, Ame et al. 1998). The subsequent identification of the many other members of the PARP family, has helped explain these results. It has been shown that PARP-2 is also a DNA damage-dependent poly(ADP-ribose) polymerase (Ame, Rolli et al. 1999) and that this family member is involved in BER (Schreiber, Ame et al. 2002) and it is likely that the polymer production in response to DNA damage observed in PARP^{-/-} cells (Shieh, Ame et al. 1998) is due to this enzyme. PARP^{-/-} cells can repair irradiation induced DNA damage in an NAD⁺-independent manner. Addition of purified PARP-1 to this cell free system led to a restoration of the NAD⁺-dependent process of BER (Vodenicharov, Sallmann et al. 2000). PARP-1 deficient cells have impaired short patch BER (50% normal) and dramatically reduced long patch repair (80-90% reduction).

In summary, PARP-1 is now known to be a critical part of the BER pathway, binding to the single strand break, signalling damage to other members of the repair pathway and then being released to detect and signal further damage (figure 1.5). It has recently been proposed that the degradation of poly(ADP-ribose) is the unique source of ATP used by DNA ligase during base excision repair (Oei and Ziegler 2000).

1.4.2 Interactions of PARP-1 and p53

There is increasing evidence for an interaction between PARP-1 and p53 (a tumour suppressor protein) to promote effective repair of DNA damage and it is known that p53 is an acceptor protein for poly(ADP-ribosylation) (reviewed in (Bernstein, Bernstein et al. 2002). Human PARP-1 and p53 have been shown to form a complex which does not involve their active domains (Wesierska-Gadek, Wojciechowski et al. 2003). Mice deficient in p53 and PARP-1 have a high frequency of epithelial carcinomas and brain tumours suggesting that there may be an interaction to maintain

genome integrity. p53 is also known to act in BER by stabilising the interaction between DNA polymerase β , Ref-1 and abasic DNA (Offer, Milyavsky et al. 2001).

The intimate association of PARP-1 and p53, may indicate a more subtle role in modulating the role of p53 in apoptotic cell death (Chiarugi 2002). It is known that poly(ADP-ribosylation) occurs in response to an apoptotic stimulus (Bernardi, Negri et al. 1995). Poly(ADP-ribosylation) of p53 alters its binding to DNA (Malanga, Pleschke et al. 1998), PARP^{-/-} MEFs show decreased p53 accumulation and activation following ionising radiation (Valenzuela, Guerrero et al. 2002) whereas irradiation of PARP^{+/+} cells strongly induces p53 (reviewed in (Bouchard, Rouleau et al. 2003). Trans-dominant inhibition of PARP-1 by over expression of the DBD attenuated p21 induction and suppresses the p53-mediated G1 arrest response to ionising radiation (Wieler, Gagne et al. 2003); similar results having been previously observed using chemical inhibitors (Masutani, Nozaki et al. 2000).

These data have led to a more complex model for regulation of BER (figure 1.5 from (Hoeijmakers 2001), p53 committing cells to cell cycle arrest and DNA repair or apoptosis depending on the extent of DNA damage.

Figure 1.5

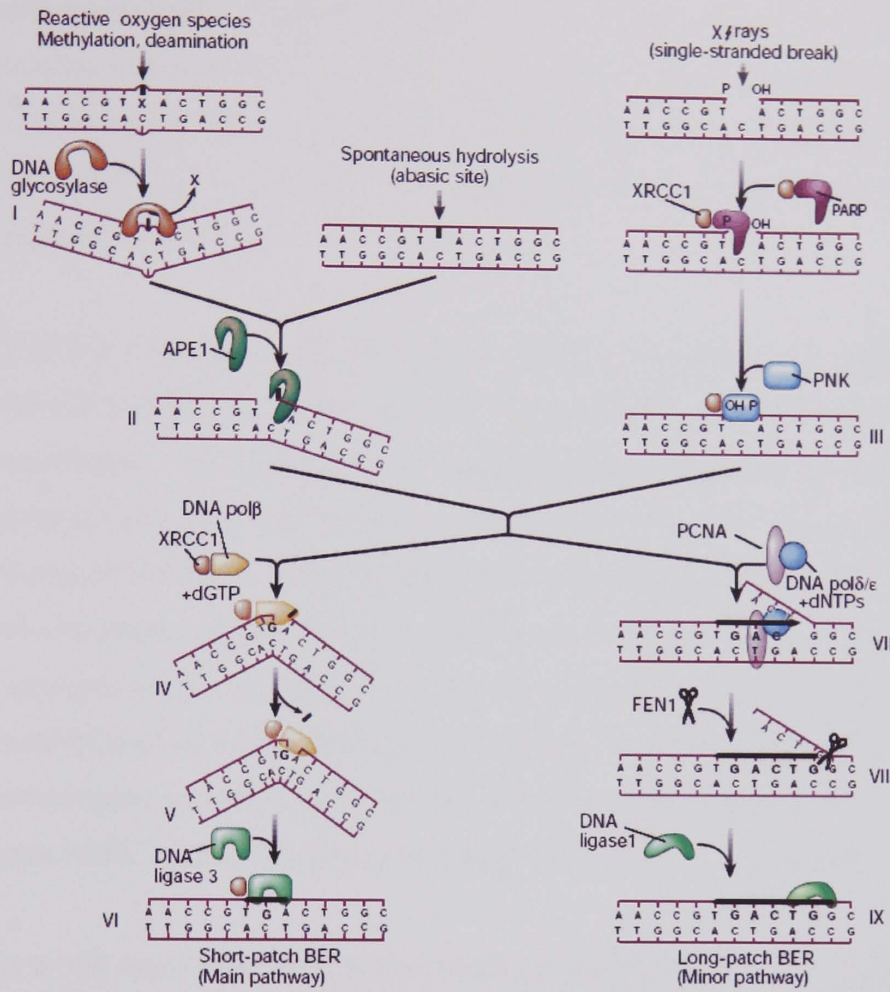


Figure 1.5 Schematic diagram of BER. Damaged base is excised by glycosylase; recruitment of signalling enzymes and Ref-1, an AP endonuclease, generates a single strand break. The BER complex, including PARP-1 is recruited and repair occurs.

1.5 Role of PARP-1 in Apoptotic and Necrotic Cell death

PARP-1 activation is protective in proliferating cells because of its role in DNA repair, however in non-proliferating cells excessive activation of the enzyme leads to cell death. Exposure of quiescent cells to ischaemia or bacterial endotoxins causes widespread liberation of reactive oxygen species (ROS). Consequent DNA damage leads to over activation of PARP-1, NAD⁺ depletion and necrotic or at least caspase-independent, non-apoptotic, cell death. Maintenance of NAD⁺ prevents this type of

cell death (Ying, Garnier et al. 2003). It has been suggested that the decrease in pH associated with proton release from hydrolysis of NAD^+ may also contribute to the cell death (Affar, Shah et al. 2002). PARP-1 knockout mice are resistant to these insults, with a decrease in the size of the necrotic area after cerebral artery ligation, reduced myocardial reperfusion injury and enhanced survival after endotoxic shock (reviewed in (Burkle 2000)). Similar results have been reported using chemical inhibition of PARP-1.

PARP-1 is an early target for caspase-3 and -7 in apoptosis, being cleaved at the DEVD motif in the nuclear location sequence (Soldani and Scovassi 2002) and inactivated. The N-terminal p24 fragment retains its DNA binding ability without any catalytic ability acting, in effect, as an inhibitor of base excision repair. There is evidence that the C-terminal p89 fragment can interact with intact PARP-1 and thus blocks intact enzyme homodimerisation which is essential for activity. Thus once the apoptotic destruction of PARP-1 by caspases has commenced there is a rapid inhibition of further DNA repair and the consequent energy consumption. This observation is confirmed in experiments where uncleavable PARP-1 was transfected into PARP-/- cells and apoptosis was delayed (Oliver, de la Rubia et al. 1998).

It would appear that early in apoptosis poly(ADP-ribosylation) contributes to activation of p53 and downstream effectors including the recruitment of AIF from the mitochondria (Conde, Mark et al. 2001; Yu, Wang et al. 2002; Du, Zhang et al. 2003) therefore also being involved in caspase-independent programmed cell death. The caspase-dependent cleavage of PARP-1 during ATP-dependent apoptosis has a role in channelling energy consumption into programmed cell death rather than DNA repair.

In summary PARP-1 activation participates in DNA repair and recovery at low levels of DNA damage and over activation of the same enzyme appears to contribute to cell death in high DNA damage states, the proposed interaction of these two processes is shown diagrammatically in figure 1.6 (taken from (Bernstein, Bernstein et al. 2002)). Both the apparently conflicting roles for PARP-1 in the cell are potentially targets for drug modification in human disease states. These possible clinical uses and the development of PARP-1 inhibitors will be discussed below.

Figure 1.6

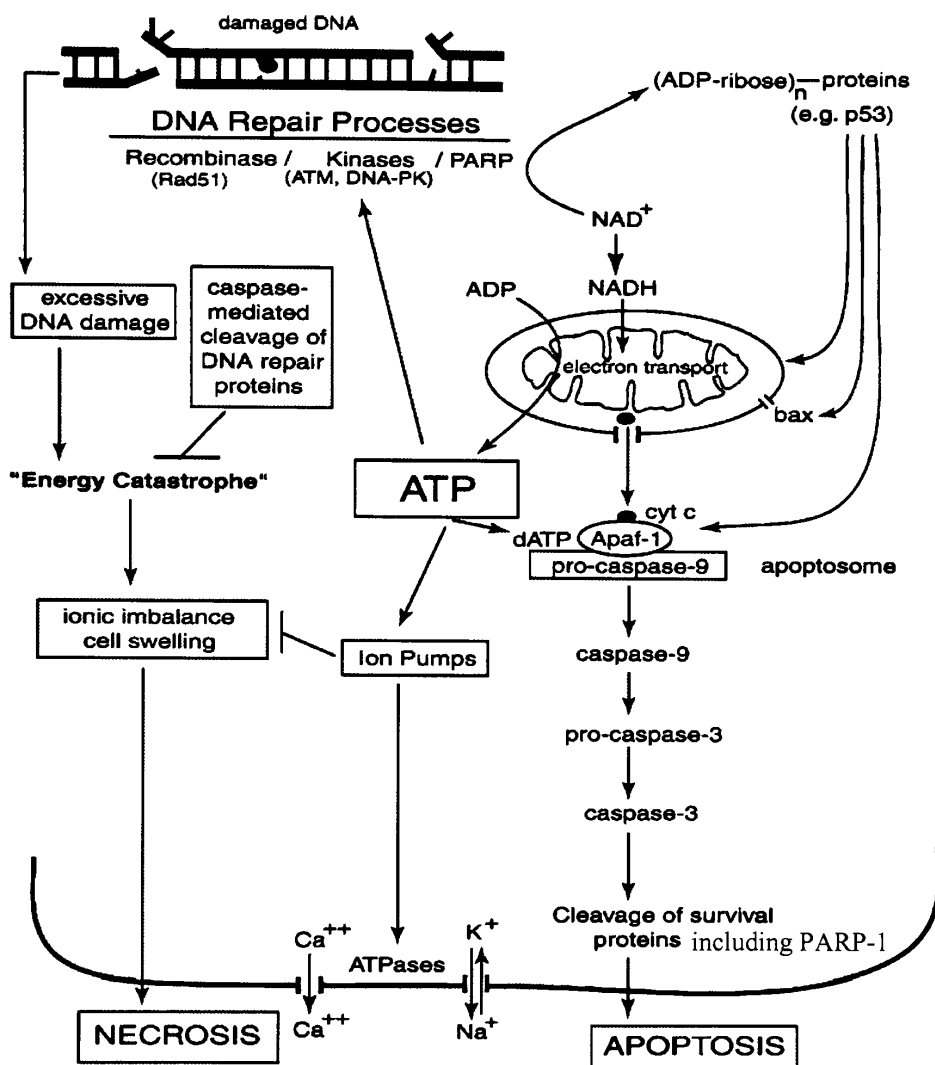


Figure 1.6 Diagrammatic representation of the interaction between ADP-ribosylation, energy use and outcome after excessive DNA damage

1.6 Development of PARP-1 inhibitors

PARP-1 inhibition is an attractive method for studying the significance of this enzyme in biological systems. Many inhibitors have been designed around nicotinamide, which is a by-product of PARP-mediated NAD⁺ cleavage, and is itself a weak PARP-1 inhibitor. The first nicotinamide analogues were the benzamides. Inhibition of PARP by 3-aminobenzamide (3-AB) was reported over two decades ago by Whish with an inhibitory constant (K_i) of $1.8 \pm 0.2 \mu\text{M}$ in L1210 cells (Purnell and Whish 1980). However to inhibit PARP sufficiently to retard DNA repair in intact cells millimolar concentrations of 3-AB are needed. 3-AB is not a specific PARP

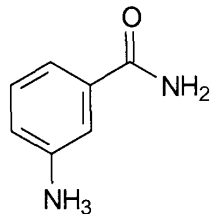
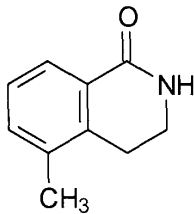
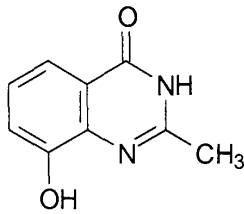
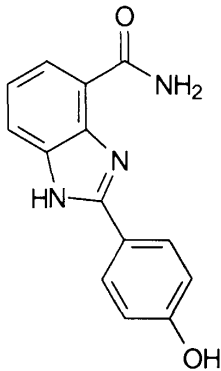
inhibitor, having activity against mono (ADP-ribosyl) transferases and *de novo* purine synthesis, and more specific and potent PARP inhibitors would be required both for study of enzyme activity but also for any potential clinical applications. Considerable effort has been put into finding specific PARP-1 inhibitors (reviewed in (Griffin, Pemberton et al. 1995; Li and Zhang 2001; Southan and Szabo 2003).

The newer more potent PARP inhibitors have been designed based on interaction and inhibition at the NAD⁺ binding site. Extensive studies of structure-activity relationships revealed key desirable features (reviewed in (Griffin, Pemberton et al. 1995). It was proposed that a potent PARP inhibitor should have an unsubstituted aromatic or polyaromatic heterocyclic structure; a carboxamide group restricted to the *anti*-position; at least one amide proton for hydrogen bonding and a non-cleavable bond at the equivalent of the 3'-position of 3-AB. X-ray crystallography of inhibitors in the NAD⁺ binding site has complemented structure activity relationships and allowed the identification of 3 critical hydrogen bonds.

Banasik screened more than 170 compounds available commercially as poly- and mono(ADP-ribose) inhibitors. His group identified several potent inhibitors, e.g. naphthalilides and dihydroxyisoquinolines, all of which have the carbamoyl function incorporated within a ring system (Banasik, Komura et al. 1992).

These advances allowed the second generation of PARP inhibitors to be developed, the bicyclic lactams (PD128763 and NU1025) and benzimidazole-4-carboxamides (NU1085), which showed much greater potency over 3-AB with IC₅₀s in the nanomolar range (reviewed in (Li and Zhang 2001), also figure 1.7).

Figure 1.7

1980	1990	1992	1996
			
3-AB	PD128763	NU1025	NU1085
Km 5,000 nM	85 nM	50 nM	6 nM
Relative potency*	60	100	830

* Fold increase in potency relative to 3-AB

Figure 1.7 Small molecule inhibitors of PARP-1, including the molecule NU1025 and NU1085 identified during the Newcastle PARP inhibitor development programme. Year of discovery given above, relative potency to 3-AB shown.

X-ray crystallography of PD128763, NU1025, naphthalimide and benzamide with PARP-1 showed restriction of rotation of the carboxamide improved binding (Ruf, de Murcia et al. 1998).

Part of the drive to develop potent, specific PARP inhibitors has been based on the observations that inhibition of PARP can potentiate the cytotoxicity of anticancer drugs. Durkacz et al first reported that ADP-ribosylation was involved in DNA excision repair and that inhibition of the enzyme enhanced the cytotoxicity of demethyl sulphate, a DNA alkylating agent, in 1980. At the end of this seminal paper the authors suggested that this “potentiation of cell killing by alkylating agents and PARP inhibitors may be of use in the treatment of human leukaemia” (Durkacz, Omidiji et al. 1980).

There is now considerable academic and commercial interest in the development of PARP inhibitors suitable for use in humans. Interest continues in the field of cancer treatment, where inhibitor use would be envisaged in combination with cytotoxic

agents to enhance the tumour response to chemotherapy or radiotherapy by preventing repair of induced DNA damage. The *in vitro* observations that PARP-1 inhibitors potentiate the cytotoxicity of anti-cancer drugs and ionising radiation, and the fact that *in vivo* PARP-1 knock out mice show increased sensitivity to these agents has stimulated the development of specific PARP-1 inhibitors as potential chemo- and radiosensitisers

However there is expanding interest in other clinical fields consequent on the observation of the protective effects of PARP inhibition or the PARP knockout mutation in cerebral ischaemia, endotoxic shock, inflammatory disorders and reperfusion injury (reviewed in (Tentori, Portarena et al. 2002; Virag and Szabo 2002). The activation of PARP-1 and its putative role in necrotic cell death has led to the development of PARP-1 inhibitors to prevent such activation and decrease resultant cell death. It has been suggested that such agents could be used as a neuroprotective agent after ischaemic stroke and traumatic brain injury, could be cardioprotective after myocardial infarction, and could be used in the treatment of Alzheimer's disease and endotoxic shock (reviewed in (Tentori, Portarena et al. 2002) – see figure 1.8.

Figure 1.8

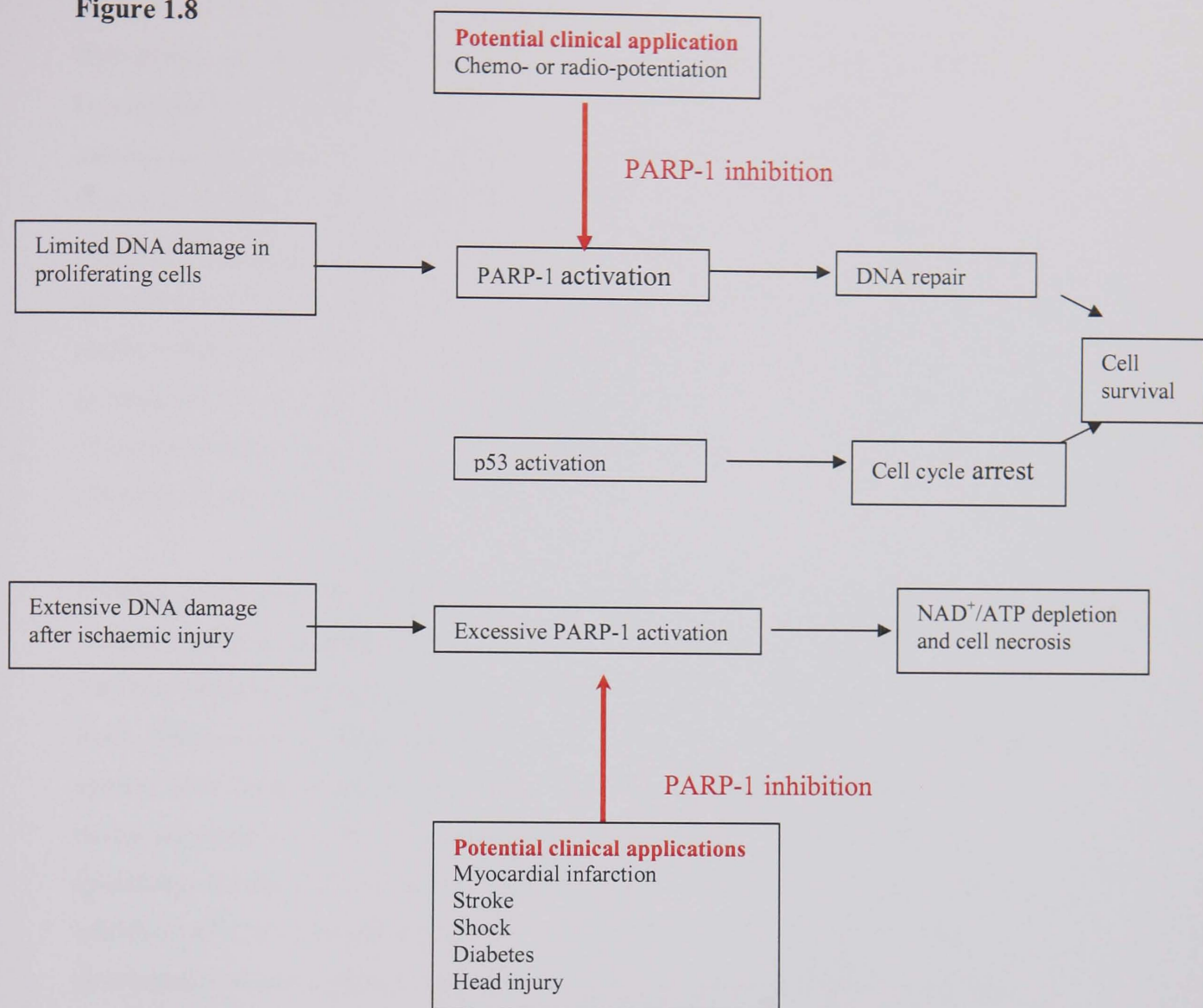


Figure 1.8 PARP activation in apoptotic and necrotic cell death and potential clinical applications of PARP inhibitors

1.7 Development of AG014699

The Medicinal Chemistry Department and Drug Development Group, Cancer Research Unit, University of Newcastle Upon Tyne has identified, using rational drug design, quinazolin-4-[3H]one (e.g. NU1025) and benzimidazole-4-carboxamide (e.g. NU1085) derivatives which are potent inhibitors of PARP-1 (Griffin, Pemberton et al. 1995). NU1025 and NU1085 have been shown to potentiate the cytotoxicity of alkylating agents, bleomycin (a free-radical producing glycopeptide which causes single and double strand breaks) and ionising radiation in a murine leukaemia cell line

(L1210) ((Bowman, White et al. 1998); (Boulton, Pemberton et al. 1995) but not the thymidylate synthase inhibitor nolatrexed or gemcitabine (a nucleoside analogue). Potentiation of camptothecin (a topoisomerase I poison) but not etoposide (a topoisomerase II poison) was reported in the same experimental system (Bowman, Newell et al. 2001). Camptothecin forms both protein-associated and non-protein associated single strand breaks which would bind and activate PARP-1. Etoposide is associated with the formation of protein-associated double strand breaks which would not be a stimulus to PARP-1. The enhancement of both temozolomide and topotecan (a clinically active topoisomerase I poison) cytotoxicity has been confirmed in a panel of human common tumour cell lines independent of p53 status and tissue of origin (Delaney, Wang et al. 2000).

Following the successful development of potent PARP-1 inhibitors in Newcastle a collaboration was established with Agouron Pharmaceuticals (now part of Pfizer GRD) to improve these agents and move them forwards to clinical trials (Canan Koch, Thoresen et al. 2002; Skalitzky, Marakovits et al. 2003) as chemo-potentiating agents. New compounds have been developed using x-ray crystal structure-based design and structure activity relationships to improve both potency and solubility (Skalitzky, Marakovits et al. 2003). Crystallographic analysis of one of the earlier inhibitors (NU1085) bound in the PARP catalytic site (see figure 1.9) led to the development of a new class of inhibitors, the tricyclic lactam indoles (Canan Koch, Thoresen et al. 2002). These compounds are $\geq 1000x$ more potent than 3-AB, $K_i \leq 5$ nm, and potentiate temozolomide and topotecan cytotoxicity at sub-micomolar concentrations. In particular AG14361 showed impressive in vitro activity, had suitable pharmacokinetic properties and was a potent radio- and chemo-sensitiser in vivo (Calabrese, Almassy et al. 2004).

Figure 1.9

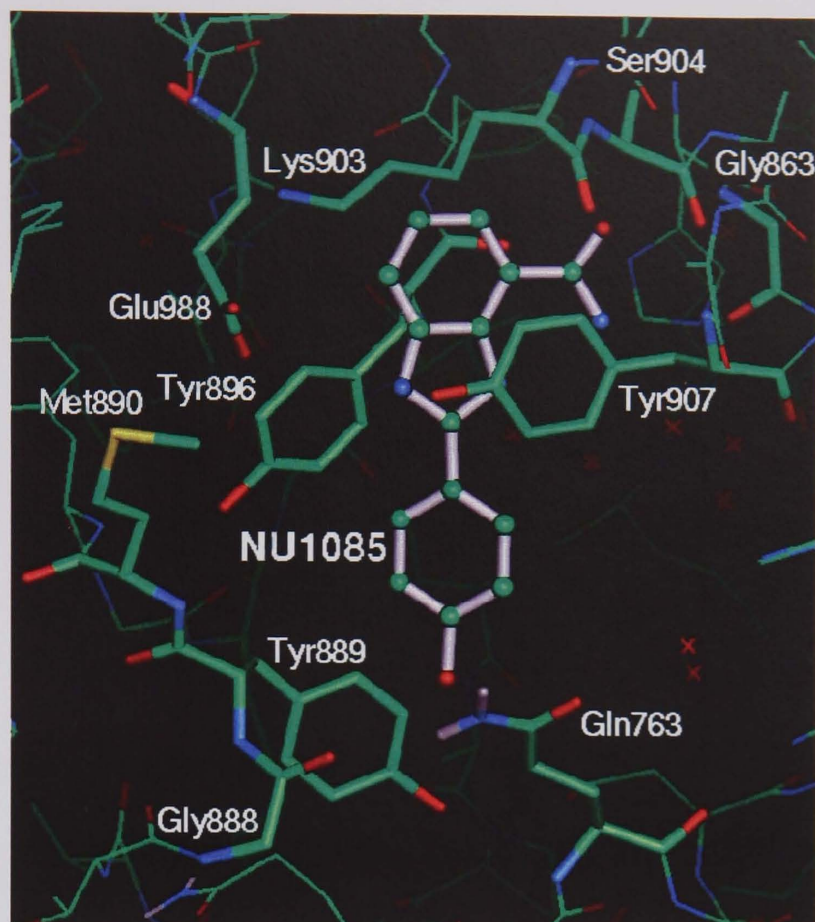


Figure 1.9 Co-crystal structure of NU1085 and NAD⁺ binding site of chicken PARP-1

The clinical candidate, AG014699, and a range of back-up compounds were generated and preclinical evaluation carried out both at Pfizer GRD (formulation and toxicology) and in Newcastle (preclinical efficacy and pharmacodynamics). It was proposed that the PARP-1 inhibitor AG014699 (structure shown in figure 1.10) would enter clinical trials early in 2003.

Figure 1.10

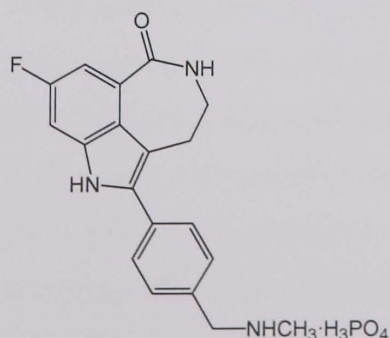


Figure 1.10 Structure of AG014699

A proposal for two phase I combination clinical trials, with temozolomide and irinotecan respectively, was put to the New Agents Committee of Cancer Research UK in 2001. The proposal was approved and these new agent trials will be run through Cancer Research UK's Drug Development Office. The First-in-Human clinical trial of the PARP-1 inhibitor AG014699 will be in combination with temozolomide.

The mechanism of action of temozolomide, its early clinical development and evidence of the interaction with PARP-1 are discussed below, completing the introduction to this thesis. The further preclinical data pertinent to the protocol development for the clinical trial of AG014699 and temozolomide will be discussed in chapter 2.

1.8 Temozolomide

1.8.1 Chemistry and mechanism of action

Temozolomide (CCRG 81045; M&B 39831; NSC 362856; SCH 52365) is an imidazotetrazine. It is one of a family of compounds synthesised by Stevens and colleagues (Stevens, Hichman et al. 1987) which exhibited a broad spectrum of activity against murine tumours. The lead compound, mitozolomide, entered clinical trials but its further development was halted after severe and unpredictable myelosuppression was reported (Blackledge, Roberts et al. 1989). Preclinical studies with temozolomide showed good experimental antitumour activity with lower toxicity which was schedule dependent (Stevens, Hichman et al. 1987). Temozolomide is an orally available drug that is rapidly absorbed with 100% oral bioavailability, peak plasma levels being achieved at 1.2 hours after oral dosing (Danson and Middleton 2001). In the plasma the drug undergoes spontaneous breakdown to the active component, 5-(3-methyl)1-triazen-1-yl-imidazole-4-carboxamide (MTIC) at physiological pH in aqueous solution (Stevens, Hichman et al. 1987). This is in contrast to the original lead drug in this family, dacarbazine, which requires metabolic activation in the liver with demethylation of the parent drug to release MTIC (figure 1.11).

Figure 1.11

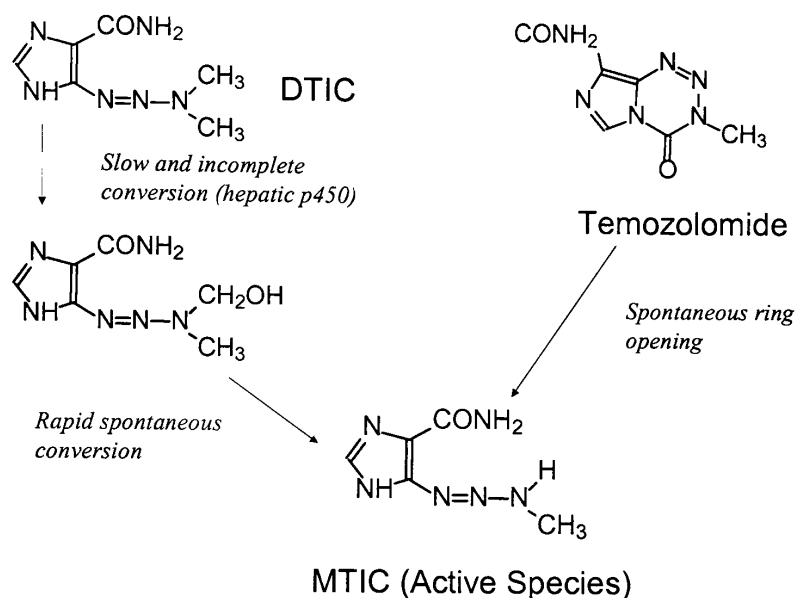


Figure 1.11 Structures of dacarbazine (DTIC) and temozolomide, and the active, DNA methylating species, MTIC

MTIC is unstable and degrades into its methyl diazonium ion, a reactive methylating compound. This acts as a major groove-directed DNA-alkylating agent, preferentially binding to the middle guanine residue of a GGG sequence (Stupp, Gander et al. 2001). Temozolomide generates methyl adducts, the predominate species being N⁷-methylguanine (70%), N³-methyladenine (9.2%) and O⁶-methylguanine (5%) (Newlands, Stevens et al. 1997). It is the O⁶-methylguanine products, which although in the minority, that appear to be responsible for the cytotoxicity of temozolomide (Tentori, Graziani et al. 1995; Hickman and Samson 1999). O⁶-methylguanine is not lethal to cells *per se* but during DNA replication tends to mispair with thymine. This mis-pairing is recognised on the daughter strand by the MMR pathway and the thymine excised. However, unless the original O⁶-methylguanine lesion is repaired by removal of the methyl adduct thymine is likely to be re-inserted. Repetitive futile rounds of mismatch repair causes a state of chronic strand breaks and the MutS branch of MMR signals G2/M cell cycle arrest and the initiation of apoptosis (Karran and Hampson 1996; D'Atri, Tentori et al. 1998; Fink, Aebi et al. 1998).

1.8.2 Repair of temozolomide induced DNA damage

1.8.2.1 N⁷-methylguanine and N³-methyladenine repair

The N-methylpurines formed are promptly repaired by the base excision repair pathway. The modified base is excised by methylpurine glycosylase (MPG) resulting in an abasic site. This initiates the BER repair pathway as discussed in section 1.2.1 with the close involvement of PARP-1 activation in this pathway (see section 1.4). It is thought that unrepaired N⁷-methylguanine lesions are well tolerated, however the N³-methyladenine adduct is mutagenic and cytotoxic if not rapidly repaired (Lawley and Phillips 1996).

1.8.2.2 O⁶-alkylguanine DNA-alkyltransferase and MMR

Repair of O⁶-methylguanine lesions requires the activity of O⁶-alkylguanine-DNA alkyltransferase (OGAT, ATase). ATase is the main component of the Direct Repair Pathway, an efficient mechanism of DNA repair where the altered base is corrected without removal or disruption of the phosphodiester backbone. Overexpression of ATase in mammalian cells confers resistance to DNA alkylating agents (reviewed in (Margison, Koref et al. 2002)), and is a major factor in tumour resistance to alkylating agents. Patients with brain tumours with low-ATase activity demonstrate a higher response rate to DNA alkylating agents, carmustine (Belanich, Pastor et al. 1996) and to temozolomide (Friedman, McLendon et al. 1998); however ATase levels have not been found to be a predictor of response in melanoma patients (Middleton, Lunn et al. 1998) whereas patients with tumours staining positively for MMR proteins were more likely to respond (Friedman, McLendon et al. 1998). The transfer of the methyl group to ATase inactivates the enzyme and enzyme levels in peripheral blood lymphocytes in patients treated with 5 days of temozolomide show a progressive depletion (Lee, Thatcher et al. 1994). It may be that the schedule dependency of temozolomide is related to cumulative depletion. Attempts have been made to exploit this observation by the development of inhibitors of ATase (PaTrin2) which improves the therapeutic index of temozolomide in tumour xenografts (Middleton, Kelly et al. 2000) and is currently in phase II trials.

In the absence of direct repair by ATase the mis-paired thymine is excised by the mismatch repair system but leaving the O⁶-methylguanine in place and therefore subsequent mispairing occurs during repair. It is thought that the repeated attempts to repair this lesion generates double strand breaks and triggers apoptosis (Tentori, Turriziani et al. 1999); figure 1.12 adapted from (Margison, Koref et al. 2002). The hypersensitivity of ATase^{-/-} cells to DNA alkylating agents can be “rescued” by the introduction of MMR deficiency (Karran and Bignami 1992), these double deficient cells will tolerate high levels of O⁶-methylguanine without undergoing apoptosis. MMR mutation in cell lines has been shown to confer resistance to temozolomide, even in the presence of low ATase levels. In MMR proficient cells inhibition of ATase with O⁶-benzylguanine increases sensitivity to temozolomide (Liu, Taverna et al. 1999) but is ineffective in MMR-deficient cells.

Figure 1.12

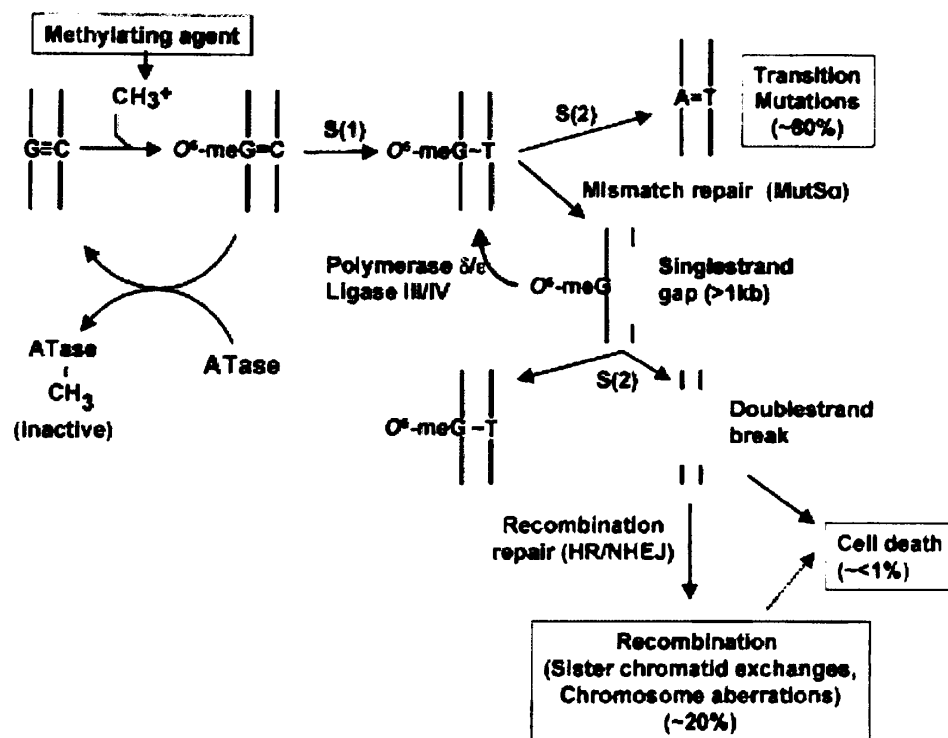


Figure 1.12 Repair of O⁶-methylGuanine either by ATase or the consequences of MMR of the lesion, S(1) and S(2) indicating the first and second rounds of replication following damage.

Tumour cell lines which are deficient in elements of the MMR pathway are resistant to the cytotoxic effects of a number of DNA damaging agents (reviewed in (D'Atri, Tentori et al. 1998). These authors studied MMR proficient and deficient cell lines

and have shown that induction of p53 and signalling for apoptosis following temozolomide treatment involves MMR.

1.8.3 Temozolomide and PARP-1 inhibition

There is an increasing body of evidence that the inhibition of PARP-1 and consequent deficiency in BER will increase the cytotoxicity of temozolomide. Inhibition of BER will cause persistence of strand breaks caused by the more abundant N³-methyladenine lesions in addition to the normally predominant cytotoxic lesion O⁶-methylguanine. 3-methylpurine DNA glycosylase (MPG) catalyses the first step in the repair of N³-methyladenine, subsequent recruitment of the BER complex including activated PARP-1 completing the repair.

Co-administration of potent PARP-1 inhibitors developed in Newcastle enhances the cytotoxicity of temozolomide and the persistence of DNA single strand breaks in L1210 cells (Boulton, Pemberton et al. 1995; Bowman, White et al. 1998), and in a panel of other common tumour cell lines (Delaney, Wang et al. 2000) as discussed above. These data have been confirmed in other studies.

Leukaemic cells resistant to temozolomide due to high ATase levels and MMR deficiency were treated with the combination of temozolomide and NU1025 (Tentori, Turriziani et al. 1999). A three fold reduction in the growth inhibitory IC₅₀ concentration for temozolomide was observed in the presence of the PARP-1 inhibitor and increased rates of apoptosis in the treated group were detected by flow cytometry. More pronounced effects were seen when the temozolomide and NU1025 administration was fractionated (Tentori, Portarena et al. 2001), the authors proposing that this was due to the fact that more extensive DNA damage was introduced. These experiments have been extended into in vivo situations and enhanced the survival of mice bearing cranial lymphomas. The animals were treated with intra-peritoneal temozolomide plus or minus intra-cerebral NU1025. The combination treatment enhanced survival, particularly when the dose was fractionated, temozolomide alone being ineffective (Tentori, Leonetti et al. 2002).

Treatment of glioma cell lines with temozolomide ± 3-AB again demonstrated increased cytotoxicity for the combination, with a reduction in the growth inhibitory IC₅₀ for temozolomide (Tentori, Portarena et al. 2002). This enhancement was more marked in glioma cells known to be deficient in MMR. Me-Lex (MeOSO₂(CH₂)₂-lexitropsin) is a methylating agent which selectively causes N³-methyladenine lesions. These lesions are cytotoxic and repaired by BER. Increased sensitivity of activated human PBLs to Me-Lex is caused by treatment with NU1025 (Tentori, Portarena et al. 2002).

Chemopotential of temozolomide has been demonstrated by the PARP-1 inhibitor CEP-6800 both in tumour xenografts and cell lines. CEP-6800 is a 3-aminomethyl carbazole imide which inhibits both PARP-1 and PARP-2 (Miknyoczki, Jones-Bolin et al. 2003). Potentiation of temozolomide, irinotecan and cisplatin has been observed in their models. Increased DNA damage after temozolomide/PARP inhibitor treatment was demonstrated using a COMET assay over 24 hours following treatment, and PAR accumulation in combination treated xenografts was decreased over control treated animals (temozolomide or irinotecan alone) at 4 hours after dosing. Treatment of U251MG glioblastoma xenografts with a combination of CEP-6800 (30 mg/kg) and temozolomide (34 mg/kg) caused complete regression of the tumours by day 28. Similar potentiation of the activity of temozolomide has subsequently been described in combination with AG14361 (Calabrese, Almassy et al. 2004).

Studies on the combined effect of inhibiting ATase and PARP-1 have been performed in leukaemic cell lines (Tentori, Orlando et al. 1997). Leukaemic cell clones deficient in ATase were transfected to re-express the enzyme. These cells were originally sensitive to temozolomide, re-introduction of ATase increased their resistance, and this effect could be reversed with the ATase inhibitor O⁶-benzylguanine. Combined treatment with temozolomide and a PARP inhibitor increased sensitivity to temozolomide in both the ATase deficient and proficient cells. In cells which are mismatch repair deficient, O⁶-methylguanine lesions are tolerated; inhibition of PARP and thus BER will cause N³-methyladenine to become the predominant cytotoxic lesion.

In a panel of human tumour cell lines temozolomide cytotoxicity was potentiated both by O⁶-benzylguanine and 3-AB treatment in MMR proficient cells, but only by 3-AB in MMR deficient cell lines (Wedge, Porteus et al. 1996). Similarly colon cancer cell lines which were mismatch repair deficient (HCT116) or MMR wild type (SW480) show differential sensitivity to temozolomide, treatment in combination with a PARP inhibitor (PD128763) increased sensitivity to temozolomide in both the proficient and deficient cell lines. Triplet treatment with temozolomide, PD128763 and O⁶-benzylguanine was synergistic in the wild type cells, the addition of the ATase inhibitor having no effect in the MMR deficient cells (Liu, Taverna et al. 1999).

These findings have been reproduced in paired cells lines, both MMR proficient and deficient (Curtin, Wang et al. 2004). The effect of AG14361 on temozolomide-induced growth inhibition was investigated in HCT-Ch3, A2780 and CP70-ch3 (MMR-proficient) and HCT116, CP70 and CP70-ch2 (MMR-deficient) cell lines. AG14361 enhanced temozolomide activity in all the MMR-proficient cell lines, but was more effective in MMR-deficient cells such that temozolomide resistance was overcome. In the same paired cell lines inhibition of ATase by benzylguanine enhanced the cytotoxicity of temozolomide in the MMR-proficient cells only.

The potentiation of temozolomide by PARP inhibitors may be clinically important as loss of mismatch repair occurs frequently in many common sporadic solid tumours (small and non-small cell lung cancer, pancreatic, gastric, colorectal, ovarian, endometrial, cervix and breast cancers) and in the majority of cases of hereditary non-polyposis colon cancer (reviewed in (Tentori, Portarena et al. 2002).

1.8.4 Clinical use of temozolomide

A phase I trial of temozolomide, initially comparing both intravenous and oral schedules, identified the maximum tolerated dose as 200 mg/m²/day for 5 days of a 28 day cycle (Newlands, Blackledge et al. 1992). There was no significant difference in plasma pharmacokinetics between oral and intravenous dosing and the oral route is recommended. Maximum plasma levels were achieved 0.7 hours after dosing. Toxicity included mild nausea compatible with oral dosing and dose dependent

myelosuppression which was dose limiting. Responses were seen in melanoma and malignant glioma encouraging further development. Patients with brain tumours are usually excluded from phase I studies of novel anticancer agents because of concerns relating to informed consent and the lack of penetration of drugs to the brain.

However, the preclinical observations that temozolomide crossed the blood brain barrier in mice justified their inclusion in this trial.

Phase II studies have been conducted in malignant brain tumours (Bower, Newlands et al. 1997; Yung, Prados et al. 1999; Brada, Hoang-Xuan et al. 2001; Harris, Rosenthal et al. 2001) and metastatic melanoma ((Bleehen, Newlands et al. 1995), all using a dose of 200 mg/m²/day for 5 days in a 28 day cycle. Reported response rates of 8% with disease stabilisation in a further 43% of patients with glioblastoma multiforme (GBM) at first relapse (Brada, Hoang-Xuan et al. 2001) and 35% in patients with anaplastic astrocytoma are described. A randomised comparison of dacarbazine and temozolomide in GBM found in favour of the latter with equivalent response rates (5%), but improved median (7.3 v 5.8 months) and progression free survival (21 v 8% at 6 months) for temozolomide. It is in this disease, with its poor prognosis, that temozolomide is licensed and recommended for treatment in the United Kingdom (NICE, 2001; (Dinnes, Cave et al. 2002).

Myelosuppression was the major adverse effect of temozolomide in all the studies in brain tumours. 6-10% of patients developed CTC grade 3 or 4 thrombocytopenia and fewer than 5% developed significant neutropaenia or anaemia (Dinnes, Cave et al. 2002).

Phase II (Bleehen, Newlands et al. 1995) and phase III (Middleton, Grob et al. 2000) studies of temozolomide have been performed in patients with metastatic melanoma. The reported response rate in the phase II study was 24% with a median survival for responders of 14.5 months (compared to 5.5 months overall). Severe myelosuppression was observed in 9% subjects, otherwise toxicity rates were low. The phase III randomised study of temozolomide v DTIC in metastatic malignant melanoma did not show a significant difference in response rate between the two treatment groups (13.5% v 12.1%). Once again the new agent was well tolerated with

CTC grade 3 or thrombocytopenia occurring in 11% of the temozolomide treated group. The nadir occurred late in the 28 day cycles, at 20-21 days post treatment.

Temozolomide is licensed for use in malignant brain tumours in Europe. The equivalence of the phase III trial in melanoma means that its uptake in this disease in Europe has been small although world wide this is a major market for the drug.

There is, therefore, a potential clinical use for PARP inhibitor temozolomide combinations. Potentiation of temozolomide cytotoxicity may improve its efficacy in licensed indications or the change in emphasis of the cytotoxic lesion may alter the range of sensitive human tumours.

1.9 Summary

The introduction to this thesis has attempted to cover the background to the experimental work described herein. A brief summary of the proposed mechanisms of DNA damage repair, in particular base excision repair, is given to explain the rationale for the development of PARP-1 inhibitors as possible chemo- or radio-potentiating agents. The development of the tricyclic lactam indoles is summarised. A novel PARP-1 inhibitor in this class, AG014699, entered clinical trials in combination with temozolomide in 2003.

The main points covered in the chapter are listed below

1. The action of many chemotherapeutic agents used in the treatment of human tumours can be compromised by a variety of mechanisms, including DNA repair.
2. Temozolomide is a DNA methylating agent in clinical use. The predominant DNA lesions formed by temozolomide, O⁶-methylguanine, N³-methyladenine and N⁷-methyladenine are repaired by ATase, MMR (O⁶) and BER (N³ and N⁷) respectively.
3. PARP-1 is an enzyme involved in BER and p53 mediated responses to DNA damage.

4. Potent inhibitors of PARP-1 have been developed, leading to a clinical candidate, AG014699, which is $\geq 1000x$ more potent than the early inhibitors.
5. Tumour xenograft and cell line studies show that the antitumour activity and cytotoxicity of temozolomide is enhanced by co-administration of a PARP-1 inhibitor.

The next chapter will discuss the preclinical evaluation of AG014699 and related compounds in relation to the protocol design and development for the phase I study in humans. Chapters 3-5 describe the laboratory experimental methods used and the experiments undertaken to validate a suitable pharmacodynamic assay for use in the clinical trial. Chapter 6 summarises a phase II study of temozolomide alone in patients with malignant melanoma which provides clinical data to validate the laboratory assays.

Chapter 2

Protocol development of Phase I clinical protocol for first-in-human use of a PARP-1 inhibitor in combination with a cytotoxic agent

2.1 Introduction

The role of PARP-1 in base excision repair and its potential in combination with temozolomide has been discussed in chapter 1. As part of the Northern Institute for Cancer Research Drug Development programme potent novel PARP-1 inhibitors have been developed. One of these, AG014699, has been identified as the potential clinical candidate and has moved forwards into a First-in-Human clinical trial. The phase I clinical trial is based in the United Kingdom with Newcastle as the coordinating centre. The other participating investigators and centres are Professor Harris and Dr Middleton in Oxford and Professor Johnson and Dr Wilson in Belfast.

The initial proposal which was considered and accepted by the New Agents Committee (NAC) of Cancer Research UK (formerly Cancer Research Campaign) comprised two trials with AG014447, one in combination with irinotecan, a topoisomerase I inhibitor, and one with temozolomide. It is this latter trial that is critical to the work described in this thesis, the trial with irinotecan is planned for a later phase of the clinical development. The nomenclature of the compound for clinical use was subsequently changed, AG014699 is the phosphate salt of the parent compound AG014447 (8-Fluoro-2-(4-methylaminomethyl-phenyl)-1,3,4,5-tetrahydro-azepino[5,4,3-cd]indol-6-1). During the clinical trial the drug is referred to and prescribed as AG014699, however the compound measured in pharmacokinetic studies in AG014447.

The initial proposal to the New Agents Committee proposed the clinical development of AG14361. At a late stage of the preclinical planning stage AG014447/AG014699 was discovered. This agent is more potent and more water soluble and was finalised as the first clinical candidate. The late change in trial agent means that some of the early pharmacodynamic assay development was done using AG14361 as the drug reference. All final validation has been done using AG014699. The chemical structure of AG014699 is shown in figure 1.10, this is a yellow solid, molecular weight of 421.36. The compound is water soluble, and is stable for at least 30 days either in the solid form or in solution in 5% dextrose (Pfizer, unpublished observations). Crystallographic analysis of AG014447 bound to the inhibited target enzyme revealed that the drug binds to the active site of PARP-1, forming 3 hydrogen

bonds. The K_i , determined using ^{32}P -NAD⁺ incorporation into polymer by purified full-length human PARP, is 1.4 nM (unpublished Agouron/Pfizer data). AG014699 inhibits oligonucleotide-stimulated PARP-1 activity measured using a [^{32}P] NAD⁺ incorporation assay in permeabilised SW620 cells (IC_{50} = 24 nM). Analysis of the time course of inhibition after exposure to 0.4 mM AG014699 showed >60% inhibition of PARP-1 up to 2 hours post-treatment confirming its tight binding and/or cellular retention (Suzanne Kyle, personal communication).

A large part of this MD project has involved authorship of the first draft of the phase I clinical trial protocol, and subsequent modifications and review in collaboration with colleagues from the other centres involved, Cancer Research UK and Pfizer. The toxicology summary of the protocol (section 1.2.4) was written by Professor Herbie Newell and Sections 7.1.2.1 and 5.1, the pharmacokinetic processing of and pharmaceutical information on AG014699 was written by Dr Poe Hsyu of Pfizer GRD. The approved protocol is currently recruiting patients into part 1 of the trial.

In this chapter of the thesis the salient preclinical studies will be discussed and the protocol design assessed in detail.

2.2 Preclinical efficacy study

During the preclinical assessment of AG014699 a number of critical efficacy studies were carried out in Newcastle. The design and results of these are summarised below as these were instrumental in decisions made during the development of the phase I trial protocol. The practical work for this efficacy study was performed by Chris Calabrese, Suzanne Kyle, Huw Thomas and Mike Batey.

There were two arms to the studies: an efficacy arm and a PK/PD arm.

2.2.1 Efficacy

Groups of 5 CD-1 nude mice were inoculated subcutaneously with 1×10^7 SW620 colon cancer cells. The implanted tumours were allowed to develop; when they were palpable (approx 4x4 mm, ~day 10 after inoculation) treatment was started. The

groups of animals were treated with oral temozolomide ± an intra-peritoneal injection of PARP inhibitor for 5 days, control animals received normal saline or AG14361 only. The animals were then maintained under standard conditions and monitored for toxicity and tumour size. Animals displaying distress due to side effects of treatment or tumour burden were sacrificed. The end point of the study was defined as 100 days and all remaining animals sacrificed at this point.

An initial study using two doses of temozolomide ± AG14361, the first potential clinical candidate, demonstrated in SW620 xenografts marked potentiation of the cytotoxicity of temozolomide (Calabrese, Almassy et al. 2004), see figure 2.1. Temozolomide was dosed at 68 mg/kg which is equivalent to the recommended adult human dose, and 136 mg/kg. The doses of AG014361 used were 5 mg/kg and 15 mg/kg. It can be seen that temozolomide caused tumour growth delay in these xenografts, but this is markedly potentiated by 5 mg/kg AG14361. The higher dose of AG14361 (15 mg/kg) in combination with standard dose temozolomide (68 mg/kg) caused cures in this tumour xenograft.

Figure 2.1

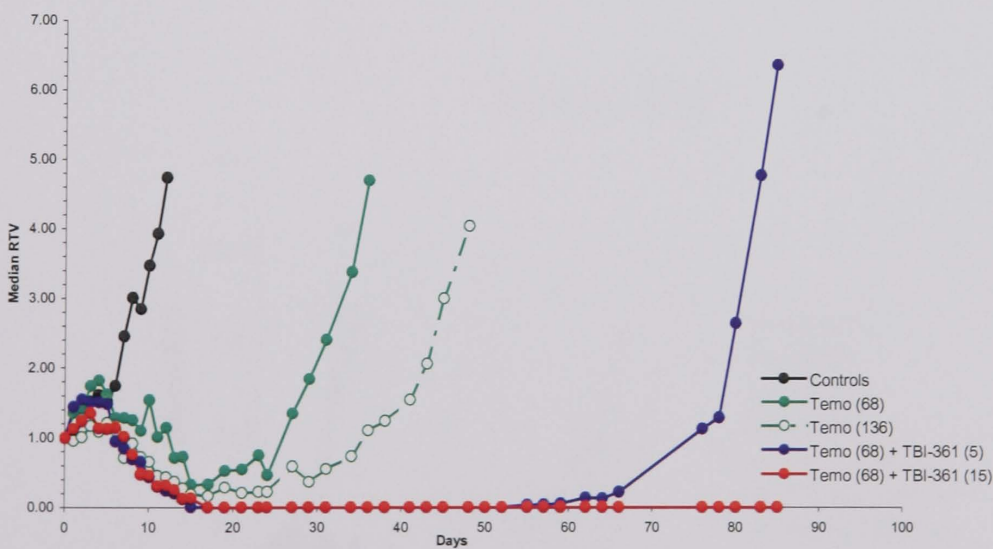


Figure 2.1 Relative tumour volume (RTV) against time for the different treatment groups documented in the figure legend. Temo = temozolomide, TBI-361 = AG014361. Median RTV in groups of 5 mice.

When the new clinical candidate AG014699 was identified as the agent which would be taken first into clinical trials the experiment described above was repeated using this new inhibitor. Groups of 5 mice were again treated for 5 days with control vehicle, temozolomide alone at a dose of 68 mg/kg and 136 mg/kg of temozolomide in combination with 0.1 mg/kg, 1 mg/kg or 10 mg/kg AG014699. An additional group of animals was treated with 10 mg/kg AG014699 alone to establish whether this dose was toxic and/or efficacious as a single agent and as a control for cannulation effects.

The results are shown in figure 2.2; temozolomide alone delayed tumour growth by about 22 days (time to RTV4 in treatment group – time to RTV4 in control) whereas AG014699 alone at the highest dose used had no effect on tumour growth compared to control. Treatment with the combination of temozolomide 68 mg/kg with AG014699 0.1 mg/kg caused a modest potentiation of the response to temozolomide. A ten-fold increase in dose of inhibitor to 1 mg/kg caused xenograft cures, as had been demonstrated previously with 15 mg/kg AG14361. However, increasing the dose of PARP-1 inhibitor by another ten-fold in combination with temozolomide was toxic and all animals had to be sacrificed. This dose of AG014699 alone was not toxic.

Figure 2.2

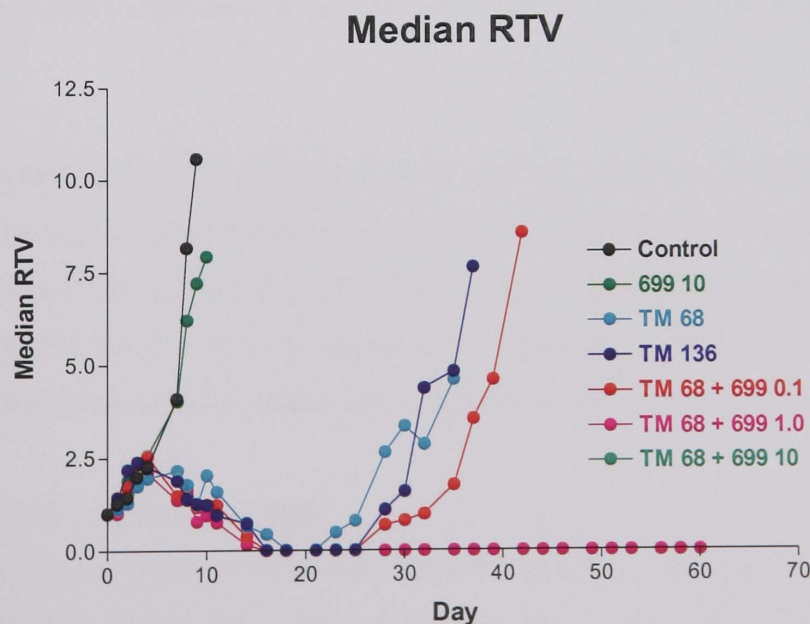


Figure 2.2 Median RTV against time from treatment in groups of 5 nude mice bearing SW620 colon cancer xenografts. Treatment of each group shown in figure legend.

2.2.2 PK and PD

In the second phase of this pre-clinical efficacy study similar groups of nude mice were established but the animals sacrificed at intervals after treatment and blood and tumour samples taken for pharmacokinetic and pharmacodynamic assessment. Groups of 5 animals were implanted with 1×10^7 SW620 colorectal cancer cells. Treatment was started when the tumours were larger than in the efficacy study to aid sampling. No tumour was allowed to grow to greater than 10 mm diameter to avoid problems with tumour necrosis causing inhomogeneity. Treatment with temozolomide \pm AG014699 was started approximately 15 days after implantation when the tumours had reached 7 x 7 mm. The same combinations and doses of treatment were used, although animals received a single dose only prior to sacrifice. Samples were taken at 0.5, 6 and 24 hours.

Animals were sacrificed by cervical dislocation and blood withdrawn immediately by cardiac puncture for pharmacokinetic analysis. Whole blood was centrifuged to obtain plasma and the concentration of AG014447 (the parent compound present in the plasma) measured by HPLC. The tumour xenografts were removed and snap frozen in liquid nitrogen prior to homogenisation and measurement of AG014447 concentration and PARP activity by [32 P] NAD⁺ incorporation (assay described in chapter 3).

Having confirmed the efficacy of AG014699 in potentiating temozolomide this PK/PD study had a critical influence on two aspects of the phase I trial design; the definition of a PARP inhibitory dose (PID) and the recommended starting dose of AG014699. The basis of these decisions will be discussed further below (section 2.4 and 2.5), the relevant PK/PD results are summarised below.

2.2.2.1 PK/PD at efficacious dose

Plasma and tumour levels of AG014447 were measured in 5 animals at each time point after dosing. The times points chosen were 30 minutes, 6 hours and 24 hours after intra-peritoneal injection of 1 mg/kg AG014699. The selection of the times was based on previous preclinical evaluation of the pattern of PARP inhibition with

similar inhibitors (Calabrese, Almassy et al. 2004) and also the clinical use of temozolomide. The 30 minute time point was chosen to give a peak plasma level. The 6 hour time point coincides with a time at which temozolomide would have formed the maximum number of strand breaks (Danson and Middleton 2001), and therefore demonstration of PARP inhibition at this time would provide support for the proposal that PARP inhibition, and thus inhibition of BER, would be instrumental in the potentiation of the cytotoxic drug. In clinical use temozolomide is given every 24 hours for 5 days and it would be envisaged that the PARP inhibitor would be given on a similar schedule. The 24 hour time point gives an estimate of the AG014699 retention and PARP activity immediately prior to the planned re-dosing time.

The pharmacodynamic and pharmacokinetic results for animals dosed with 1 mg/kg AG014699 is summarised in figure 2.3. This is the dose which maximally potentiated temozolomide in SW620 xenografts. Plasma levels of AG014447 (yellow bars) were between 110-120 ng/ml 30 minutes after injection falling rapidly to <10 ng/ml at 6 hours and were undetectable at 24 hours. AG014447 levels in tumour (red bars) were undetectable at 30 minutes, around 50 ng/g tissue at 6 hours with evidence of retention in the tumour at 24 hours. This confirms the published data on AG14361 (Calabrese, Almassy et al. 2004).

PARP activity (blue bars), expressed as a percentage of the mean activity measured in matched control tumours, was assessed by measuring the incorporation of [³²P] NAD⁺ into acid precipitated material. This assay is published (Boulton, Pemberton et al. 1995; Calabrese, Almassy et al. 2004) and discussed in detail in chapter 4. Significant (>50%) inhibition of PARP activity was observed in tumours at 30 minutes, despite the drug levels being below the limit of detection at this time. At 6 hours the activity was 50% inhibited with a return towards baseline by 24 hours. The relevance of all these results to the PARP phase I combination study will be discussed below.

Figure 2.3

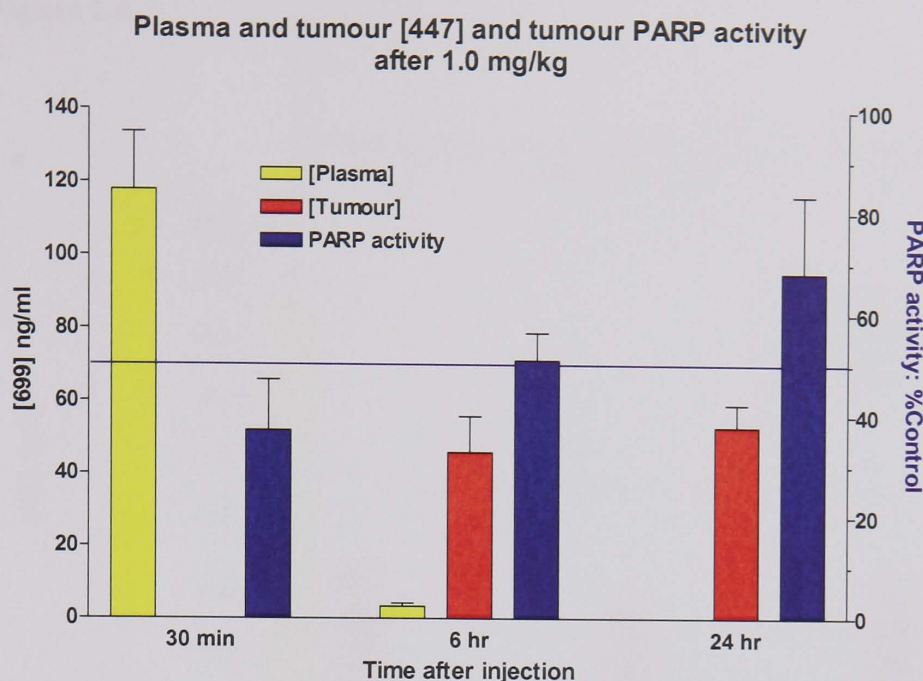


Figure 2.3 Plasma and tumour AG014447 levels (mean \pm SD, n=5) left y axis 30 minutes, 6 and 24 hours after 1 mg/kg AG014699 i.p , tumour PARP activity as % control right y-axis (mean \pm SD, n=5).

2.2.2.2 PK/PD at toxic dose

An identical experiment was performed dosing animals with 10 mg/kg AG014699, the dose of inhibitor which potentiated the toxicity of temozolomide to such an extent that animals had to be sacrificed after 5 days dosing.

The results are shown graphically in figure 2.4. Plasma levels of AG014447 30 minutes after dosing were approximately 10-fold those seen in the previous experiment (1500-2000 ng/ml cf 110-120 ng/ml), and had fallen to ~ 50 ng/ml by 6 hours. Drug was still detectable in the plasma at 24 hours (1.5 ng/ml). Tumour drug levels were also higher (\approx 200 ng/g tissue) and did not show a significant decline over the 24 hours. PARP activity in the tumours was less than 10% of control values at both 30 minutes and 6 hours after dosing; significant PARP inhibition (\sim 80%) was still found at 24 hours, the point at which re-dosing would occur during treatment. The plasma levels of AG014447, the degree of PARP inhibition and level of toxicity observed were all instrumental in the defining of the starting dose of AG014699 in human trials and the definition of PK endpoints (see section 2.5).

Figure 2.4

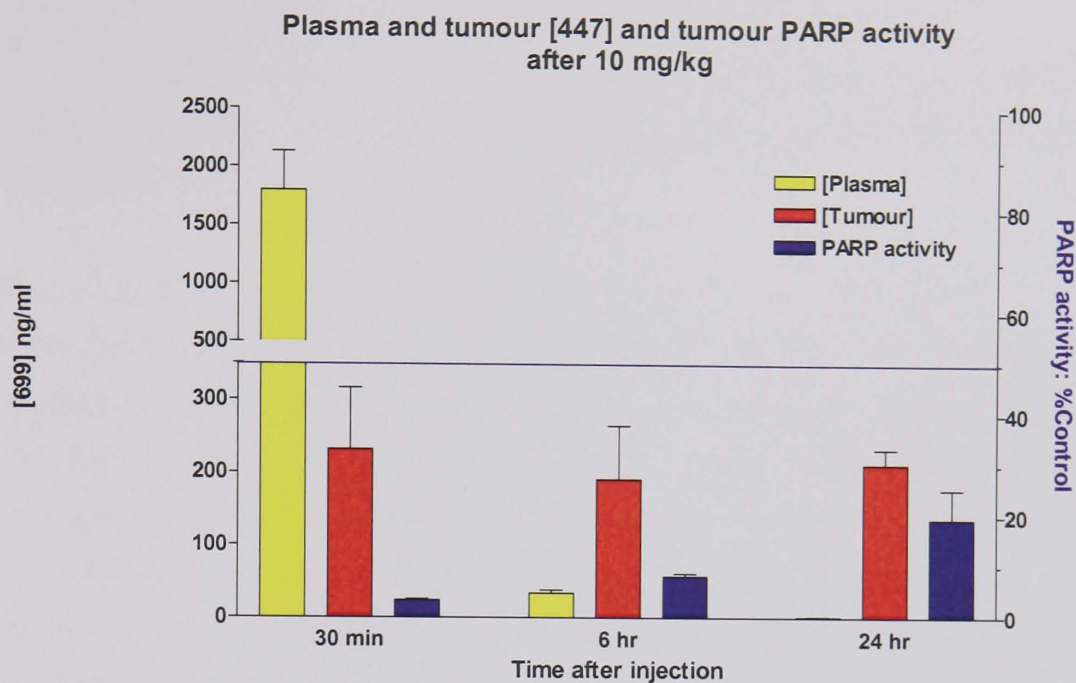


Figure 2.4 Plasma and tumour AG014447 levels (mean \pm SD, n=5) left y axis 30 minutes, 6 and 24 hours after 1 mg/kg AG014699 i.p , tumour PARP activity as % control right y-axis (mean \pm SD, n=5).

2.3 Protocol development

2.3.1 Summary of protocol design

Any novel anti-cancer agent must be registered with one of the regulatory authorities before it can enter into standard clinical treatment. Before registration is permitted a programme of preclinical drug toxicity assessment and rigorous clinical trials must take place. Preclinical repeated-dose toxicity studies of a defined duration, depending on the proposed length of treatment of patients, are required in one rodent and one non-rodent species by US and European regulations (Farrell, Leighton et al. 2003). These studies should use similar schedules and duration to those planned in the Early Clinical Trial. The results from the toxicity studies are used to predict possible toxicity and to define starting dose.

The trial outline proposed and approved in the NAC application was a phase I combination study of AG014699 with temozolomide in patients with advanced solid malignancies. Development of anti-cancer drugs, which may have serious and life threatening toxicities, involves the treatment of patients rather than healthy volunteers. This places a burden of careful study design on researchers to minimise the chance of serious toxicity whilst avoiding treating large numbers of patients at a sub-therapeutic dose.

Phase I clinical trials aim to determine the toxicity profile of new drugs or combinations and establish acceptable doses for subsequent studies. It is hoped that preliminary evidence of activity will also be seen, however the chances of this are small given the disparate and resistant tumour types enrolled. The overall response rate in phase I anticancer drug trials is reported as 4-6% (reviewed in Horng, Emanuel et al. 2002). The specifics of trial design will vary between trials, depending on whether the trial is a single agent phase I, a cytotoxic combination study or involves one of the biological targeted therapies; however the general principles in study design are similar. The starting dose is defined from the results of preclinical toxicity studies. Cohorts of between 1-3 patients are treated at each dose level and toxicity assessed, if no significant toxicity is observed the dose is increased by a previously defined factor and a new cohort of patients recruited. When toxicity is observed the cohort is expanded and subsequent dose escalation may be in smaller increments. In combination studies the individual drugs may be escalated alternately or in sequence. The maximum tolerated dose is thus defined. A variety of dose escalation schemes exist including standard and modified Fibonacci, continued reassessment (O'Quigley, Pepe et al. 1990), accelerated titration (Simon, Freidlin et al. 1997), and pharmacologically guided dosing. All the schemes aim to minimise the numbers of patients treated at low ineffective doses whilst safely defining dose limiting toxicity (Rubinstein and Simon 2003).

The initial proposal for the first in human study of AG014699 is summarised in the protocol concept sheet below (figure 2.5) which was submitted as part of the early negotiations over trial set-up before my involvement with the project. This is the working template from which the protocol evolved and illustrates the starting point from which the protocol was written. A number of changes have been made and these

changes and the rationale for the starting dose and primary endpoint definitions are discussed below.

Figure 2.5

Protocol Concept Sheet

Phase I / Pharmacokinetic / Pharmacodynamic Study of PARP Inhibitor (AG014447)
in combination with temozolomide

Primary Objectives	To determine a PARP-inhibitory dose of AG014447 using PK and PD endpoints for PARP inhibition. To determine the MTD of temozolomide in combination with this PARP-inhibitory dose
Secondary Objectives	To evaluate the single-agent and combination pharmacokinetics of AG014447 To document any responses in melanoma patients included in the study.
Study Design	Single-Agent AG014447 days 1-5. Combination AG014447 + temozolomide day 15-19. PK studies at all dose levels. Part 1: Open to all patients. Continues until PK studies indicate potentially PARP-inhibitory levels. Part 2: Melanoma patients only, obligatory post-treatment biopsy for measurement of PARP inhibition.
Drugs	Time 0 minutes: AG014447 by 30 minute iv infusion Time 60 minutes: Temozolomide orally.
Dose Escalation	AG014447. Starting dose determined from preclinical toxicology / PK / PD studies. Final dose determined by clinical PK/PD studies. Escalation in 50% dose increments. Temozolomide: Starting dose 100, 126, 159, 200 mg/m ² (50% of starting and geometric increments). 3 patients per dose level. ≥3 week follow up on all patients before escalation
Inclusion Criteria	Part 1: Patients ≥ 18 years of age with advanced cancer for which no satisfactory treatment exists, PS 0-2, Standard anticancer Phase 1 Lab tests Part 2: As Part 1, but also must have malignant melanoma with at least two lesions and consent to post-treatment biopsy.
Exclusion Criteria	Brain metastasis Serious intercurrent disease
Statistical Design	Consider use of 2-drug modified continual reassessment method
Pharmacodynamic correlates	PARP activity in leucocytes PARP activity in tumour biopsies (Part 2) PARP protein level in biopsies (Part 2)
Pharmacokinetics	Both agents
Toxicity Evaluation	History and physical examination before each dose Full blood count, biochemistry, liver function and toxicity assessments weekly
Efficacy Evaluation	Responses in assessable patients using RECIST criteria. Apoptosis measurements in biopsies

Following a prolonged period of drafting and discussion of the trial design the final format of the agreed clinical trial is summarised as follows. Treatment under part 1 of the protocol commenced in June 2003.

The First-in-Human trial is an open-label, non-randomised, dose escalation phase I combination study in two parts, escalating first the dose of AG014699 then that of temozolomide. A Modified Fibonacci scheme is being used to increase the dose of the inhibitor, with the subsequent dose escalation of temozolomide being based upon the clinical use of temozolomide, the available tablet sizes and thus increasing towards the established maximum tolerated dose of temozolomide alone in equal increments. The dosing strategy including the proposal for test “single agent” dose is discussed in the following sections.

2.3.2 Dosing plan for the two parts of the study

Part 1 – Fixed dose temozolomide, escalating dose of AG014699

Patients with advanced solid malignancies of any type for whom no standard therapy exists and who are of a reasonable performance status, physically and on blood indices, are being recruited to this part of the study. Patients receive one half the standard dose of temozolomide throughout this part of the trial, i.e. 100mg/m². The PARP-1 inhibitor is given by intravenous infusion one hour before temozolomide dosing. Treatment started at a low, safe dose of AG014699 with cohorts of 3 patients. Dose escalation of AG014699 has been initially been by dose doubling. If any grade 2 toxicity is seen according to Common Toxicity Criteria (CTC version 3.0), subsequent dose increments will be smaller (30% or less), a modified Fibonacci dose escalation. This part of the trial will be complete when a PARP-1 inhibitory dose (PID) of AG014699 is reached, and not on the basis of observed toxicity unless this is severe and unexpected. The basis of this decision is discussed further below. Pharmacokinetic and pharmacodynamic samples are being taken on the first cycle in every patient.

Part 2 – Fixed dose AG014699, escalating dose of temozolomide

Patients with advanced metastatic malignant melanoma will be recruited to part 2 of the trial. These patients will be asked to have a biopsy of a melanoma lesion before

and after dosing with the combination so that the degree of DNA damage (strand break number) can be assessed and also tumour AG014699 pharmacokinetics and pharmacodynamics can be measured. The starting doses of this part will be Temozolomide 100 mg/m² and the PARP-1 inhibitory dose of AG014699. The dose of AG014699 will be fixed throughout this stage of the study and the dose of temozolomide escalated until dose-limiting toxicity is seen, a lower dose level will then be investigated to define the maximum tolerated dose of the combination. It is envisaged that the doses of temozolomide investigated would be 100 mg/m², 125 mg/m², 150 mg/m², 175 mg/m² and up to 200 mg/m² depending on toxicity observed. Pharmacokinetic and pharmacodynamic samples will once again be taken on the first cycle in every patient. A maximum tolerated dose (MTD) will be established and this cohort of patients expanded to at least 6 to further evaluate toxicity and allow some indication of response.

2.3.3 Single agent dosing with AG014699 prior to cycle 1

In the initial protocol concept it was proposed that patients would receive 5 daily doses of AG014699 on days 1-5 of cycle one, with treatment with the combination starting on day 15 of this cycle and the total length of the first cycle being six weeks. All subsequent cycles would be four weeks in length, without this single agent treatment.

The reason for this schedule was to obtain single agent PARP-1 inhibitor PK data and to look for potential toxicity of the novel agent. A PARP-1 inhibitor would not be expected to be active against cancer cells on its own; the rationale for its action depends on enhancing DNA damage caused by other agents. It would be ethically difficult to carry out a dose-finding trial of the single agent alone in a population of patients with limited life-expectancy in whom quality of life is paramount, given that administration would be of no therapeutic benefit.

During the process of writing the phase I trial protocol the specific plan for 5 test doses was discussed further and amended for a number of reasons. There was concern over the delay before patients received combination therapy as the 5 day test dosing then one week wash out period meant that there was a two week delay from

entry into the trial and receipt of temozolomide and AG014699. Preclinical toxicology studies did not observe significant toxicity with AG014699 alone at doses predicted for clinical use apart from some local irritation at the injection sites in smaller animal species, all toxicity appeared to be related to exacerbation of the side effects of temozolomide in the combination studies. It was felt that a more appropriate design would be for patients to receive one single agent AG014699 dose, then PK and PD data in humans could be obtained and an assessment made for any possible unexpected single agent toxicity.

The final study design involves patients receiving a single dose of AG014699 seven days (range 11-6 days) prior to starting the combination therapy on cycle one only. This dosing day is designated “day -7” (or -6 etc) allowing cycle one of combination treatment to start on day 1 and all cycles therefore being 28 days long with re-treatment on day 29. In the event of any dose limiting toxicity being observed, defined in the protocol in section 2.2.2.1, the cohort of patients would be expanded to six. This expanded cohort of patients will receive 5 single doses of AG014699 on days -14 to -10 of their first cycle to enable assessment of whether the observed toxicity is due to the novel agent or the combination with temozolomide. The minimum of 6 days between single agent treatment and starting combination is sufficient to allow processing of the PK samples and issuing of the results from the CRO (Contract Research Organisation) before combination dosing. PD assessment of the degree of PARP inhibition is also possible in this time frame. This allows investigators the possibility of discussing any unexpected handling of the drug before embarking on the combination, a fact which may be particularly important once toxicity has been observed in other patients in the cohort.

2.3.4 Study objectives and endpoints

The primary and secondary objectives of the study as proposed in the protocol concept sheet were expanded during the protocol development and the additional endpoints are listed below. It proved necessary to define clinical study endpoints for both part 1 and part 2 of the trial. The definition in the protocol is given below and the rationale for completion of part 1 of the study based on PD endpoints discussed in section 2.4

Additional Primary Objectives:

- to determine and establish the toxicity profile of the above combination and to identify the dose limiting toxicity (DLT)
- to select doses of AG014699 and temozolomide for combination use in phase II evaluation

Additional Secondary Objectives:

- to investigate pharmacokinetics of temozolomide when given in combination with AG014699 and possible interactions

Clinical study end points:**Part 1**

A primary endpoint of the trial is to establish a PARP inhibitory dose (PID) of AG014699 in adult patients using pharmacokinetic and pharmacodynamic parameters measured in patients' blood. Development and validation of the PD assay was ongoing during protocol drafting. Whilst it was acknowledged that, ideally, PD data would be used to define PID an alternative PK endpoint was also defined in the protocol. In the absence of significant toxicity, the primary PK end point will be the dose that results in a plasma concentration of AG014699 that exceeds by a factor of 10 the level that maximally potentiated the antitumour activity of temozolomide at 6 hours in mice (ie, $10 \times 10 \text{ ng/mL} = 100 \text{ ng/mL}$). If pharmacodynamic data suggest a plateau in inhibition at a concentration lower than this, escalation may be stopped. If toxicity is observed, clinical effects will be used to guide dosing.

Part 2

The endpoint in part 2 will be dose limiting toxicity (DLT) of the combination of temozolomide and AG014699, based on drug-related adverse events graded according to the NCI Common Toxicity Criteria (CTC) Version 3.0, occurring during the first cycle of treatment. DLT will have been reached when 2 patients at a given dose level (with up to 6 treated at that level) have experienced drug-related DLT. The maximum tolerated dose (MTD) will be defined as a dose below that eliciting DLT. (Standard definitions for dose limiting toxicity in phase I trials).

2.4 Preclinical toxicology and starting dose

Before entering patient trials investigational cancer drugs are subject to pre-clinical toxicology studies. These are aimed at screening for unexpected adverse toxicity and also projecting a human starting dose. Classically, two toxicology studies would be performed, one in a rodent species and one in non-rodents (Farrell, Leighton et al. 2003). The rodent study identifies a dose in mg/m^2 which produces severe toxicity in 10% of animals (STD_{10} or LD_{10}). The second study should confirm that this dose does not cause severe toxicity in the non-rodent species. The starting dose for a phase I study in humans would normally be one-tenth of this LD_{10} or one-third of the toxic dose level (TDL) in the larger animal species (reviewed in Mahmood 2003). An alternative approach when estimating starting doses in a combination study is to define the MTD of the combination and use one-tenth of the MTD in the most sensitive species as the starting dose in the human study. The aim in all situations is to start at a safe dose of a novel agent or combination but to minimise the potential for starting at an inappropriately low dose and hence avoid treating large numbers of patients with ineffective doses.

Single agent toxicity studies of AG014699 were performed in rats and beagle dogs. Doses of 5, 15 and 75 $\text{mg}/\text{kg}/\text{day}$ for 5 days were given to groups of 20 male and female rats (32, 97 and 484 mg/m^2 respectively). At doses over 15 $\text{mg}/\text{kg}/\text{day}$ bone marrow hypocellularity was observed with a most marked decrease in erythroid precursors. Minimal to moderate myocardial degeneration was observed in rats treated at the highest dose of AG014699, similar lesions were observed in dogs at 50 mg/kg in acute and multi-dose range finding studies. The concern about potential cardiac toxicity led to the definitive single agent study being repeated in beagle dogs utilising dose of 15, 25 and 40 $\text{mg}/\text{kg}/\text{day}$ for 5 days. The cardiac lesions were not reproducible in this definitive study although ECG abnormalities were observed. Animals developed a persistent sinus tachycardia or an atrioventricular nodal rhythm. AG014699 was acutely emetogenic in dogs at doses over 15 $\text{mg}/\text{kg}/\text{day}$.

These single agent toxicity studies used doses of AG014699 significantly above the starting dose predicted from the combination studies. It was felt that it was unlikely that combination dosing in humans would reach the equivalent doses and that toxicity

from AG014699 alone was not likely. However, in response to the suggestion of potential cardiac toxicity a new exclusion criterion of “patients with active or unstable cardiac disease or myocardial infarction within 6 months, and patients with left ventricular ejection fraction below the institutional limit of normal, determined by multiple gated acquisition (MUGA) scan or echocardiogram” was introduced. All patients will have an Echocardiogram or MUGA scan prior to entry and this will be repeated after 4 cycle of treatment. All patients will also have serial ECGs before and after the test dose and during treatment on cycle 1 of the combination. The ECG will be repeated and compared to baseline before the beginning of each subsequent treatment cycle.

Pre-clinical pharmacokinetic studies in mice, rats, dogs and monkeys indicated that AG014699 had a moderate to rapid clearance and a large volume of distribution. The half-life ranged from 2.1 to 5.2 hours in the species studied. Combination pharmacokinetic studies with temozolomide did not demonstrate a significant pharmacokinetic interaction. Studies of elimination of radiolabelled [¹⁴C] AG014699 in bile-duct cannulated rats documented 49%, 31% and 17% recovery from urine, bile and faeces respectively, with a mean cumulative recovery of 98%. The short half-life and rapid clearance of AG014699 support the decision to dose daily immediately prior to temozolomide. Temozolomide is very rapidly absorbed, reaching peak plasma concentration at 1.2 hours after dosing (Newlands, Stevens et al. 1997; Danson and Middleton 2001). In a phase I combination trial of an established drug (temozolomide) and a novel agent which will be used for the first time in humans it was felt that temozolomide should be given after AG014699. The main rationale for this was that if unexpected, unpredictable acute toxicity was observed with the novel agent management of this would not be complicated by prior administration of a cytotoxic drug.

The proposed starting dose of AG014699 in combination with temozolomide was determined by analysis of the animal toxicity and pharmacokinetics in mice, rats, and dogs. These pre-clinical toxicology studies were performed by CTBR (Quebec, Canada) on behalf of Pfizer GRD. An initial range finding study in rats was performed where groups of 10 male animals were dosed with temozolomide 15 mg/kg/day for 5 days in combination with a range of AG014699 doses from 0.02 to

2.1 mg/kg/day. Assuming a weight of 200 g (Body surface area, BSA 0.031 m²) these doses were equivalent to 100 mg/m² temozolomide, the proposed starting dose in the human trial, and up to 13.5 mg/m² AG014699. No clinical toxicity or lethality was observed at the highest dose in this range finding experiment.

An AG014699 + temozolomide combination toxicity study was undertaken, evaluating low- mid- and high-dose AG014699 + Temo. The same dose of temozolomide (15 mg/kg/day x 5 days) was used as above. Low-dose AG014699 was set at the non-toxic 2.1 mg/kg/day dose of AG014699 used in the range finding study. The mid- and high-dose combinations were based on the same dose of temozolomide and a half-log escalation of the AG014699 dose. Two groups of 10 male and 10 female animals were treated for 5 days, one group being sacrificed on day 6 and one on day 29. The doses investigated are summarised in table 2.1.

Table 2.1

Treatment	Temozolomide		AG014699	
	mg/kg/day	mg/m ² /day	mg/kg/day	mg/m ² /day
Vehicle control	15	97	0	0
Temo only	15	97	0	0
Low-dose + temo	15	97	2.1	13.5
Mid-dose + temo	15	97	6.6	42.5
High-dose + temo	15	97	21	135.5

The toxicity observed in these animal studies was essentially a potentiation of the expected toxicity of temozolomide, with reduction in blood indices, reduced food consumption and loss of body mass and gastrointestinal side effects. These were more marked in the high-dose AG014699 group with lethality in 3/20 animals soon after completion of treatment. The MTD from this study was felt to be the mid-dose of AG014699, 42.5 mg/m². The starting dose based on one-tenth of the MTD of AG014699 given in combination with temozolomide in rats would be 4 mg/m².

However, experiments performed in the drug development laboratory in Newcastle in parallel to the preclinical toxicology carried out by Pfizer internal operatives, have shown that the equivalent of 3 mg/m² in mice produced significant PARP-1 inhibition and potentiation of the antitumour activity of temozolomide. Full toxicology studies could not be performed in this species because of problems related to tail vein injection sites. The small volumes of drug required for treatment of mice meant that infusions of AG014699 were acidic and hypertonic and caused tail vein necrosis. This problem was not observed in the larger animal species. After prolonged discussion with Pfizer collaborators it was decided to opt for a lower starting dose. This was partly for safety reasons since potentiation of activity could also mean potentiation of toxicity and the concern was that starting at 4 mg/m² might risk significant toxicity at the first dose level. A ten-fold increase in the dose of AG014699 from the curative dose (1 mg/kg, 3 mg/m²) to 10 mg/kg (equivalent to 30 mg/m²) in combination with temozolomide was so toxic that the animals had to be killed. The same dose of the individual drugs was not toxic (figure 2.4).

In addition, it was felt that there was a danger that no gradation in PARP-1 inhibition between escalations of AG014699 would be observed if the starting dose caused significant PARP-1 inhibition. This would then introduce the question as to whether we should reduce the inhibitor, and also might mean that the PARP inhibitory dose (PID) was defined at an excessive dose of AG014699. This could have future implications for the use of the drug and drug costs if it were subsequently proven that a similar level of inhibition could be achieved with a lower dose.

After discussion of all the pre-clinical toxicity data and comparison of doses with those used in the mouse efficacy study the starting dose of AG014699 was set at 1 mg/m², one fortieth of the MTD of the combination in rats, with infusion one hour before the administration of temozolomide.

2.5 Definition of pharmacodynamic endpoints

The primary endpoint of part 1 of the first in human PARP inhibitor trial is to determine a PARP inhibitory dose of AG014699 using pharmacokinetic (PK) and

pharmacodynamic end points for PARP inhibition. It would be hoped to define this dose using a measure of PARP inhibition in the patient's peripheral blood lymphocytes (PBLs) rather than relying on pharmacokinetic data and extrapolation from animal PD and efficacy studies. The major laboratory work undertaken during this MD project has been development and evaluation of PARP activity assays which can be used to measure the degree of PARP inhibition achieved in patients. This work is described in chapters 4 and 5.

AG014699 has been designed to act as a potentiator of cytotoxic agents and therefore the dosing strategy will be different in a phase I trial compared to that undertaken with a new cytotoxic drug. Classically, in phase I trials the dose of the new agent is escalated until toxicity is seen. For AG014699 to be effective the dose needs to cause inhibition of the PARP-1 enzyme in human cells. Preclinical toxicology data has shown that in the animal species tested there was no significant toxicity associated with dosing with AG014699 alone unless doses far higher than those needed to inhibit PARP-1 and potentiate temozolomide were given. The most likely potential cause of toxicity in part 1 of the study is therefore an increase in the toxic effects of temozolomide.

The decision to complete this phase of the study will be based on achieving a PARP-1 inhibitory dose of AG014699, i.e. a proof of principal that the action of AG014699 is indeed inhibition of PARP-1. A PARP-1 inhibitory dose has been defined in the protocol as that dose at which PARP-1 activity in peripheral blood lymphocytes is reduced to 50% of baseline and there is a plateau in the degree of inhibition achieved between 2 PARP escalations. This definition is based on the SW620 xenograft efficacy experiment described above (figure 2.3). At a dose of AG014699 which significantly potentiated temozolomide, PARP-1 was inhibited by approximately 50% in the tumours at 6 hours after dosing. It was felt that at least this degree of inhibition should be achieved in humans before it could be said that AG014699 was being given at adequate doses. The 6-hour time point also coincides with the point of maximum strand breaks after temozolomide and therefore PARP-1 inhibition at this time is important. 50% inhibition was felt to be a minimum requirement; if a greater degree of inhibition can be achieved in the absence of toxicity this would be accepted. The

aim of this part of the study would be to obtain the maximum non-toxic inhibition which is sustained over the period when temozolomide is causing DNA strand breaks.

Should it prove difficult to define a suitable dose of AG014699 using the proposed pharmacodynamic endpoint a pharmacokinetic primary endpoint has been defined in the protocol so that escalation can be stopped and part 1 of the trial concluded. The rationale for defining a “fall back” position is two fold. The protocol was written during development of the PD assays and it was accepted that it might not be possible to validate a suitable PD assay and an alternative strategy was needed. Even with a suitable assay it was felt that if doses such as these were being reached without demonstration of significant PARP-1 inhibition it would suggest that AG014699 was not sufficiently potent and an alternative clinical candidate should be explored rather than continued escalation.

Part I of the trial involves escalation of the starting dose of 1 mg/m^2 using a modified Fibonacci scheme. It was initially proposed to the NAC that a continual reassessment method would be used. This method was described by O’Quigley (O’Quigley, Pepe et al. 1990) and aims to base dose escalation by prediction of toxicity using data from all patients previously treated and not to base escalation decisions on the preceding cohort only. The aim is to more accurately predict and avoid severe toxicity and reduce the number of patients treated at a low, potentially ineffective dose. Following extensive discussion it was decided that for the first part of the study a more classical phase I trial design, with escalation of AG014699 in combination with a fixed dose of temozolomide would be used. The aim of this part of the study was to demonstrate that AG014699 could be safely administered to patients and that PARP-1 was inhibited by the drug. In preclinical studies AG014699 potentiated the toxicities associated with temozolomide administration. For this reason in the first part of the trial it was decided to fix the dose of temozolomide at 100 mg/m^2 (half the normal adult dose) until significant PARP inhibition is achieved. Toxicity will only be seen if AG014699 has an unexpected toxicity on its own in humans or if it successfully potentiates half-dose temozolomide to cause significant myelosuppression.

2.6 Precursor study rationale and links with PARP inhibitor study

Critical to the successful conduct of the phase I PARP inhibitor/temozolomide combination protocol discussed above was the development of a pharmacodynamic assay that could measure PARP-1 activity and hence the degree of PARP inhibition in both human tumour biopsies and also in human peripheral blood lymphocytes (PBLs) as a surrogate for target tissue inhibition. The methodology, development and validation of two such assays is described in chapters 3, 4 and 5. In addition, a precursor study was proposed prior to the phase I study to provide supporting data for the First-in-Human PARP inhibition combination study. This precursor study is described in detail in chapter 6 and the results presented therein, the rationale for it is summarised below.

The major justification for this precursor study was to provide control data for the effect of temozolomide alone on the endpoints to be measured in the First-in-Human study so that it could be ascertained which effects were due to the addition of AG014699 rather than temozolomide alone. The proposed precursor study would treat 12 patients with advanced malignant melanoma with full dose temozolomide (200 mg/m²/day for 5 days every 4 weeks) and on the first cycle blood and tumour biopsy samples would be taken for analysis of PARP activity and DNA damage. The proposal had a number of potential benefits for the first in human trial.

1. It provided additional validation for the proposed pharmacodynamic assay
2. There are no data in the literature on the effect of cytotoxic agents, in particular temozolomide, on PARP activity. Although treatment would not be expected to affect PARP activity, this is not proven.
3. It was proposed that the COMET assay will be used during the precursor study to evaluate the number of strand breaks produced by standard doses of temozolomide in PBL and tumour samples. This would allow direct comparison with the number of breaks caused by temozolomide in combination with the PARP inhibitor and provide control data to support

the proof of principle that PARP-1 inhibition potentiated the action of temozolomide by causing DNA damage to persist following the inhibition of BER.

4. Analysis of changes in ATase levels and N⁷-methyl adenine and N³-methyl guanine formation after temozolomide would again provide control data to be used in analysis of any similar results from the combination study.
5. The conduct of a precursor study in the same three clinical centres prior to embarking on a First-in-Human study with complex sampling and processing schedules has the advantage of allowing any operational “hiccups” be identified prior to the main study.

2.7 Conclusion

This chapter describes the key preclinical experiments and toxicology which were critical to the design of the first in-human phase I study of AG014699 and temozolomide. This protocol was submitted to the northern MREC (multi-centre research ethics committee) in January 2003 and approved with minor alterations to the patient information sheets and consent forms only. Enrollment into the study commenced in June 2003 in Newcastle, Oxford and Belfast, with the validated pharmacodynamic assay being performed in Newcastle within NICR.

Chapter 3

Laboratory Methods

The materials used and standard laboratory techniques are described below. For the pharmacodynamic assays developed during this MD thesis the final assay protocol only is described in this methods section. Any variation/evolution of the assay technique is given in the appropriate section.

3.1 Materials

3.1.1 General laboratory chemicals

All chemicals were obtained from Sigma (Poole, Dorset, UK) unless stated otherwise. Dulbecco's phosphate buffer saline was prepared from tablets produced by Gibco (Paisley, UK). Sucrose, sodium hydroxide and potassium chloride were supplied by BDH (Lutterworth, UK) and digitonin by Boehringer Mannheim (Roche Diagnostics, Lewes, UK). In addition a BCA protein assay kit (Pierce, Perbio Science, Rockford, IL, USA) containing BCA albumin standard, BCA protein assay reagent A and BCA protein assay reagent B was used for protein concentration determination. Milk powder was obtained from Marvel Premier Brands UK Ltd (Spalding, UK), and ECL Western Blot Detection kits from Amersham (Little Chalfont, UK). AG014699 and AG14361 were supplied by Pfizer GRD (La Jolla, USA).

3.1.2 Tissue culture reagents

Cells were maintained in RPMI 1640 medium (Sigma) supplemented with 10% foetal calf serum (Invitrogen, Glasgow, UK) and 1 U/ml Penicillin-streptomycin solution (Sigma), in a Hereus incubator (Fischer Scientific, Manchester, UK) maintained at 37°C in a humidified atmosphere of 5% CO₂ in air. Cell handling was performed under sterile conditions in a Class II tissue culture cabinet. Sterile tissue culture plasticware was obtained through Fischer Scientific (Manchester, UK). L1210 cells used were routinely cultured in NICR, originally obtained from ATCC (American Type Culture Collection, Manassas, VA).

3.1.3 Clinical supplies

Nycomed[®] Lymphoprep was obtained from Axis-Shield (Oslo, Norway) and EDTA and Lithium heparin pre-prepared blood collection tubes from BD Vacutainer (Plymouth, UK).

3.1.4 Radiochemicals

[³²P] NAD⁺ was supplied by Amersham (370 MBq/ml, 10 mCi/ml) and Wallac Optiphase HiSafe2 by Perkin Elmer (Loughborough, UK)

3.1.5 Antibodies

The 10H mouse monoclonal primary antibody was generously supplied by Professor Alexander Bürkle, the Goat anti-mouse secondary antibody (HRP-conjugated) was obtained from DAKO (Ely, UK).

3.1.6 Other reagents

Oligonucleotide was initially synthesised by Dr J Lunec, (NICR), subsequent supplies were obtained from Invitrogen. Purified PAR polymer was obtained from BIOMOL Research Lab (Plymouth Meeting, PA, USA).

3.2 Tissue culture and preparation of Quality Control samples

3.2.1 Methods

All experiments to establish and validate a suitable quality control (QC) standard for the pharmacodynamic assays were performed using the murine leukaemia cell line L1210. This cell line grows reliably in tissue culture under standard conditions with a cell doubling time of 10-12 hours and has been used extensively in the investigation of the cellular effect of PARP inhibitors. Cells were grown as a suspension to a density of approximately 6×10^5 /ml at harvesting to ensure they were in the exponential growth phase. Allowing the cell density in the suspension to increase causes some cells to enter G₀. During experiments to establish and validate the assays cells were grown in a total volume of 50-100 ml, when bulk preparation of QC samples for frozen storage was required cells were grown in a final volume of up to 500 ml.

Whenever fresh L1210 standards were required on the day of assay cell density was counted using a haemocytometer and sufficient medium harvested to obtain the required number of cells. The cell suspension was spun at room temperature at 1500 rpm for 10

minutes to obtain a cell pellet. The pellet was resuspended in 20 ml phosphate buffered saline (PBS), and re-centrifuged as above at 4°C to obtain a washed cell pellet. This was stored on ice prior to use for up to one hour.

3.2.2 Preparation of QC samples for the [³²P]NAD⁺ incorporation PARP activity assay

QC standards for freezing were prepared as follows. The cell suspension was cultured in large flasks so multiple aliquots of contemporaneous cells could be obtained. After counting the suspension at harvesting appropriate volumes to obtain approximately 12×10^6 cells were separately centrifuged as above. The pellets obtained were resuspended in 1 ml of RPMI culture medium supplemented with 10% foetal calf serum and 10% DMSO and transferred to a screw capped cryotube (Nunc, Roskilde, Denmark) for storage and frozen at -80°C. Samples were labelled with the approximate cell number, date of storage and laboratory book reference so that the length of storage of any given QC samples could always be ascertained. When required for assay an aliquot was defrosted as rapidly as possible, transferred to a 30 ml Universal container and 20 ml ice cold PBS added. After mixing the sample was centrifuged at 1500 rpm for 5 minutes at 4°C, this wash being repeated before the pellet was held on ice for up to one hour prior to performing the assay.

3.2.3 Preparation of QC samples for immunoblot assay

QC samples for the immunoblot assay were harvested from exponentially growing L1210 cells (cell density $\sim 6 \times 10^5$ /ml as discussed above). The cell suspension was aliquoted such that 1×10^6 cells were obtained in each individual sample, the medium spun off as above and the sample resuspended in 1 ml of medium plus 10% DMSO and 10% foetal calf serum. These samples were placed in cryovials and frozen at -80°C. Similar documentation of the samples with date, number of cell and lab book reference ensured tracking of the sample use. When required for assay an aliquot was defrosted as rapidly as possible, transferred to a 30 ml Universal container and 20 ml ice cold PBS added. After mixing the sample was centrifuged at 1500 rpm for 5 minutes at 4°C, this wash being repeated before the pellet was held on ice for up to one hour prior to performing the assay.

3.3 Lymphopreparation of human PBMCs

All procedures were carried out wearing a suitable laboratory coat and protective gloves. All needles were disposed of into an appropriate clinical waste container, any solutions requiring disposal were diluted with excess bleach solution prior to washing away with excess water.

A 5 ml whole blood sample was collected into a pre-prepared Lithium Heparin or EDTA blood tube and mixed gently to ensure anticoagulation. The sampled blood was held on ice and processed as soon as practical, usually within minutes of collection. The blood was diluted 1:1 with PBS and then layered over 8-10 ml of lymphoprep in a 30 ml disposable Universal tube. The lymphopreparation was carried out at room temperature in order to maximise the peripheral blood mononuclear cell harvest through the Ficoll gradient.

Care was taken to avoid any mixing of the blood and lymphoprep prior to centrifugation. The samples were centrifuged at 800xG for 15 minutes in a swing-out rotor refrigerated centrifuge at 16°C. The centrifuge brake was taken off to avoid disturbance of the PBMC layer during the deceleration process.

The leukocyte band, visible at the interface between plasma and the lymphoprep, was harvested with a glass Pasteur pipette and put into a fresh 30 ml Universal tube. 20 ml ice-cold PBS was added to the lymphocyte suspension and the cells pelleted by centrifugation at 4°C. A second identical wash was performed to obtain a PBMC pellet free of Lymphoprep.

When the cells were required for an immediate assay the cell pellet was held on ice for up to one hour prior to assay. PBMCs prepared for storage were resuspended in 500 µl of pre-chilled RPMI plus 10% foetal calf serum + 10% DMSO. This aliquot was transferred to a labelled screw capped Eppendorf tube and frozen. Samples were stored at -80°C for up to 15 weeks.

3.4 Preparation of tissue/tumour homogenates

3.4.1 Collection and storage of tumour samples

Patients with metastatic malignant melanoma who had biopsiable disease were eligible for the TemoCOMET clinical trial described later in this thesis. The trial was approved by The Local Ethics Research Committee (LREC) and informed consent obtained from all patients before any trial specific procedures were performed. Small biopsies were obtained under local anaesthesia from metastatic lesions in these consenting patients, before and at one time point after receiving a dose of temozolomide.

The biopsies were collected from the operating theatre in a sterile container and placed immediately on ice. Within 30 minutes they were snap frozen in liquid nitrogen and stored at -80°C until homogenised for analysis

During the development of both the $[^{32}\text{P}]\text{NAD}^+$ incorporation and immunoblot PARP assay mouse liver was used as a surrogate tissue to establish the assay technique and to validate some elements of the process. Livers were obtained from control/untreated mice sacrificed as part of other on-going research in the Drug Development Laboratory, maintained on ice until snap freezing in liquid nitrogen and storing as described above.

3.4.2 Homogenisation of Tissue

All samples were prepared in an isotonic buffer made as described in section 3.5.1 below. For the $[^{32}\text{P}]\text{NAD}^+$ incorporation assay only 25 μl of 100 mM dithiothreitol (DTT) was added to each 1 ml isotonic buffer (final concentration = 2.5 mM) immediately prior to use.

Frozen tumour or liver was defrosted on ice and the wet weight documented. For weights over 100 mg the tissue was homogenised using a Pro 2000 (Pro Scientific Inc, Monroe, CT, USA) in 3 volumes (1 mg \approx 1 μl solution) of isotonic buffer, giving a

homogenate with an overall dilution of 1 in 4). Where smaller samples had been obtained they were homogenised in 99 or 999 volumes, giving final dilutions of 1 in 100 and 1 in 1000 respectively.

The homogenate was kept on ice throughout the process, homogenisation was performed in 10 second bursts to prevent undue warming of the sample. Unless for assay on the day of homogenisation samples the homogenates were re-frozen to -80°C and stored at this temperature until use. Prior to assay the samples were further diluted with isotonic buffer where necessary to a final dilution of 1 in 40 ($[^{32}\text{P}] \text{NAD}^+$ incorporation assay) or 1 in 1000 (immunoblot assay).

3.5 $[^{32}\text{P}]\text{NAD}^+$ incorporation PARP activity assay in Peripheral blood lymphocytes (PBLs)

3.5.1 Stock solution preparation and storage

Stock solutions were prepared and stored for up to 3 months for the following reagents:

Isotonic buffer (7 mM Hepes, 26 mM KCl, 0.1 mM dextran, 0.4 mM EGTA, 0.5 mM MgCl_2 , 45 mM sucrose dissolved in 200 ml distilled water, pH adjusted to 7.8) was stored at 4°C and supplemented with 25 $\mu\text{l/ml}$ 100 mM DTT stock immediately prior to use (final concentration = 2.5 mM).

DTT 100 mM stock (154 mg in 10 ml distilled water) was stored at -20°C in 500 μl aliquots and defrosted when required.

Digitonin stock solution (0.15 mg/ml in water) for cell permeabilisation was stored at 4°C for up to 3 months.

Oligonucleotide was prepared from pellets of a palindromic sequence (CGGAATTCCG) synthesised by Dr J Lunec, Molecular Biology, NICR were stored at -20°C . Stock oligonucleotide solution was prepared by dissolving the pellet in 500 μl of 10 mM Tris/EDTA (pH to 7.8) and pipetting vigorously to ensure fully dissolved. The solution was heated to 60°C in a water bath and cooled at 1°C per minute to ensure correct reannealing. 9.5 ml Tris/EDTA buffer was added once cool to obtain 10 ml stock. A dilution of 1/50 of the DNA solution was made and the optical density read at 260 nm. 1 OD unit is equivalent to a concentration of 50 μg DNA/ml,

hence the concentration of the stock solution was calculated. The stock solution was diluted with further Tris/EDTA buffer to a final concentration of 200 µg/ml. 500 µl aliquots were stored at -20°C in screw top microtubes and thawed prior to the assay procedure.

10% TCA/NaPPi solution and **1% TCA/NaPPi** solution were prepared and could be stored at room temperature until used as “stop” and washing solutions respectively at the latter stages of the assay. These solutions were stable for 3 months under these storage conditions.

NAD⁺ stock 600 µM was prepared fresh on the day of assay. Aliquots of 4.5 mg NAD⁺ were stored at -20°C under anhydrous conditions and an aliquot was dissolved in 1 ml of distilled water on the day of use. 10 µl of the NAD⁺ solution was made up to 1 ml and the optical density measured at 260 nm. The molar extinction coefficient of NAD⁺ is 18, thus the molarity of the stock solution was calculated using the equation $\{(OD \text{ reading} \times 100)/18\}$. An appropriate dilution was made to obtain 4 ml of 600 µM stock. 3-5 µl of [³²P] NAD⁺ were added to this immediately prior to reaction.

3.5.2 Assay procedure

The principle of this assay involves the measurement of incorporation into acid precipitable matter of ³²P ADP-ribose from a [³²P] NAD⁺ substrate by PARP-1, which has been maximally stimulated by a blunt ended oligonucleotide. Although there is a family of PARP enzymes which also could incorporate ³²P ADP-ribose into polymers PARP-2 is the only other PARP known to be activated by DNA breaks. PARP-2 is not stimulated by blunt ended DNA double strand ends (G. de Murcia, personal communication) and so this assay is specific for PARP-1. The majority of the [³²P] NAD⁺ incorporated into protein during the reaction will be as poly(ADPribose) and thus gives an indirect measure of enzyme activity when maximally stimulated in the presence of oligonucleotide, or basal activity in its absence.

[³²P] NAD⁺ incorporation PARP activity assays were performed using either human peripheral blood lymphocytes or mouse L1210 cells. Any frozen cell preparation was defrosted rapidly at room temperature and washed twice in ice cold PBS, as described above, so that the freezing medium containing DMSO was removed.

The prepared cell pellets were resuspended in 0.15 mg/ml digitonin stock to a density of 3×10^7 cells per ml for 5 minutes to permeabilise the cells. 9 volumes of ice-cold isotonic buffer were added and the sample stored on ice until assayed. No samples were held on ice for longer than one hour before assay incubation.

A 10 μ l sample of each cell suspension was diluted 1:1 with Trypan Blue and the number of permeabilised cells per ml counted on a haemocytometer for each suspension. This accurate counting allowed correction of results obtained to counts per million cells and allowed comparison between samples. Use of Trypan blue also allows the extent of cell permeabilisation by digitonin to be assessed, this should be >90% with the above method.

The assay was performed in a water bath warmed to 26°C and set to agitate at 70 oscillations per minute. The reaction tubes were set up as in the table below (table 3.1) and allowed to come up to temperature before addition of the cell samples. In addition, the cell suspensions were warmed in the water bath for 7 minutes prior to reaction to ensure the process occurred at 26°C.

Table 3.1

Reagent	T0	+ oligo	- oligo	Final concentration
Oligonucleotide (200 μ g/ml)	5 μ l	5 μ l		2.5 μ g/ml
[³² P] 600 μ M NAD ⁺ stock	50 μ l	50 μ l	50 μ l	75 μ M
Water	45 μ l	45 μ l	50 μ l	
Running total	100 μl	100 μl	100 μl	
Cell suspension ($\approx 3 \times 10^7$ /ml)	300 μ l	300 μ l	300 μ l	$\approx 10^6$ cells/tube
Reaction Total	400 μl	400 μl	400 μl	

Each cell suspension was assayed in triplicate for the T0, + and – oligonucleotide samples. 2 ml ice cold 10% TCA + 10% NaPPI was added to the T0 tubes prior to addition of permeabilised cells to correct for non-specific binding of radio-label to the

filter. Oligonucleotide is omitted in one set of samples to measure basal PARP activity in comparison to total stimutable activity. The permeabilised cell suspension was vortexed briefly and the reaction started by adding 300 μl (approx. 1×10^6 cells) of this to each reaction tube. After exactly 6 minutes the enzymatic reaction was stopped by adding 2 ml of ice cold 10% TCA + 10% NaPPi and vortexing. The tubes were then kept on ice for at least one hour prior to filtration to allow precipitation of cellular macromolecules including poly(ADP-ribosylated) proteins..

Following precipitation on ice samples were filtered through a Millipore-12 funnel manifold (Bedford, Mass, USA) attached to a vacuum. The glass microfibre filters (Whatman Int Ltd, Maidstone, UK) were soaked in 10% TCA + 10% NaPPi and placed rough side up on the filtration apparatus and the contents of individual assay tubes vortexed, then added to an individual funnel on the filtration apparatus. Each tube was washed 2x with 4 ml 1% TCA + 1% NaPPi, and washings added to the funnel after vortexing. The filters were aspirated with gentle suction, and 4 further 4 ml washes of 1% TCA + 1% NaPPi drawn through each filter. Following air drying of the filter papers they were added to individual scintillation vials, 10 ml scintillant was added to each vial and the vials prepared in racks for counting. Triplicate standard vials were set up of scintillant plus 5 μl of ^{32}P 600 μM NAD^+ . This adds 3000 pmoles of NAD^+ to the standard vial and allows calculation of DPM per pmol NAD^+ . Vials were counted on a Wallac β -counter (Perkin Elmer Life Sciences, Loughborough, UK) for 2 minutes and results displayed as “disintegrations per minute” (DPM).

DPM for each sample + or – oligo were corrected by background (T0) subtraction. The values DPM per pmol NAD^+ calculated from the standard vials allowed conversion to pmol NAD^+ per assay tube. The number of permeabilised cells added to each reaction tube was calculated from the number of Trypan Blue-staining cells per ml of cell suspension. From these reference values it was possible to express the mean experimental values in terms of pMol NAD^+ per million cells incorporated into polymer following maximal PARP-1 activation.

3.6 [³²P] NAD⁺ incorporation PARP activity assay in Tumour/Tissue Homogenate

3.6.1 Stock Solutions and Storage

The stock solutions used to perform a [³²P] NAD⁺ incorporation PARP activity assay in homogenised tissue are the same as those described above in section 3.5.1

3.6.2 Assay procedure

The stored tissue or tumour homogenate (section 3.4.2) was defrosted on ice and a further dilution made with isotonic buffer to obtain an overall 1 in 40 dilution. The assay was performed in a water bath warmed to 26°C and set to agitate at 70 oscillations per minute. The reaction tubes were set up as in the table below (table 3.2) and allowed to come up to temperature before addition of the homogenate. In addition, the homogenates were warmed in the water bath for 7 minutes prior to reaction to ensure the process occurred at 26°C.

Table 3.2

Reagent	T0	Reaction	Final concentration
³² P 600 µM NAD ⁺ stock	50 µl	50 µl	75 µM
Water	50 µl	50 µl	
Running total	100 µl	100 µl	
Homogenate (1 in 40)	300 µl	300 µl	
Reaction Total	400 µl	400 µl	

It is not necessary to add oligonucleotide to these reactions as homogenisation introduces sufficient DNA strand breaks to maximally stimulate PARP (S. Kyle, personal communication). Each homogenate was assayed in triplicate for the T0 and reaction samples. 2 ml ice cold 10% TCA + 10% NaPPi was added to the T0 tubes prior to addition of homogenate to correct for non-specific binding of radio-label to the filter.

The homogenate was vortexed briefly and the reaction started by adding 300 μ l to each reaction tube. After exactly 6 minutes the enzymatic reaction was stopped by adding 2 ml of ice cold 10% TCA + 10% NaPPi and vortexing. The tube was then kept on ice for at least one hour prior to filtration to allow protein precipitation.

Following at least 1-hour cooling on ice samples were filtered through a Millipore filtration manifold and the radioactivity determined and converted to pmol NAD^+ by reference to ^{32}P NAD^+ standards as described in section 3.5.2.

During the cooling phase the remaining homogenate was centrifuged at 800 xG for 5 minutes at 4°C. The supernatant was withdrawn and a Pierce protein assay performed. The supernatant could be stored frozen at -20°C and the protein assay performed at a later date without compromising accuracy. The protein assay was performed as per the Pierce protocol. Bovine serum albumin standards were set up over the range 1.2 mg/ml - 0.2 mg/ml from a 2 mg/ml stock. 1 in 5 and 1 in 10 dilutions of the reacted homogenate were made. 10 μ l of these unknown sample dilutions were loaded in quadruplicate onto a 96-well micro-titre plate, incubated in 200 μ l of the freshly mixed BCA protein reaction mix (1 volume reagent B with 20 volumes reagent A) at 37°C for 30 minutes. The protein concentration in the homogenate was read using a Titertek Multiscan MCC/340 plate reader (Thermo Life Sciences, Basingstoke, UK). The protein concentration in the homogenate was calculated from the mean concentrations for both the 1 in 5 and 1 in 10 dilutions. All further dilutions and standards were made up in isotonic buffer without DTT added. Addition of DTT interferes with the protein assay.

The amount of protein added to the reaction tubes was calculated from the protein concentrations measured above. From these reference values it was possible to express the mean experimental values in terms of pmol NAD^+ per mg protein incorporated into polymer by maximal PARP-1 (and PARP-2) activation.

3.7 Immunoblot assay for measuring PAR formation as a measure of PARP-1 activity in peripheral blood lymphocytes and cell suspensions

The principle of this assay depends on the specific binding of a mouse monoclonal antibody to the ADP-ribose polymer, a secondary anti-mouse antibody coupled to horse radish peroxidase (HRP) amplifies the signal which is detected when luminol in the ECL reagent is broken down by the HRP to give off light. The light emission, which is proportional to the amount of antigen (PAR), is measured by chemiluminescence detection.

3.7.1 Stock Solutions

Stock solutions were prepared and stored for up to 3 months for the following reagents:

10 mM Tris/EDTA was prepared by adding 0.121 g Tris and 0.292 g EDTA to 90 ml distilled water. This was buffered to pH 7.8 with 1M NaOH and the volume made up to 100 ml. The solution was transferred to a labelled bottle and stored at room temperature.

Isotonic buffer was prepared as in section 3.5.1. The solution was labelled as per the Standard Operating Procedure and stored at 4°C for 3 months at most. DTT was not added to the isotonic buffer prior to use.

Reaction buffer was also made in advance by adding 1.12 g Tris.HCl (100 mM) and 2.4 g MgCl₂ (120 mM) to 90 ml of distilled water. This was again buffered to pH 7.8 with 1 M NaOH and made up to a 100 ml final volume with distilled water. This solution was stored at 4°C and was considered stable for up to 3 months.

7 mM NAD⁺ stock solution was made up fresh on the day of experiment. Solid NAD⁺ was stored desiccated in pre-weighed aliquots at -20°C. 500 µl of distilled water was added to an aliquot of approximately 2.5 mg NAD⁺. The concentration was calculated from the optical density as described in section 3.5.1 and the stock diluted with distilled water to obtain a 7 mM solution.

Stop solution for the assay was prepared from AG014699 stock solution stored in -20°C freezer as 10 mM stock in DMSO. This stock was diluted 1 in 800 in PBS to provide a final concentration of 12.5 µM AG014699 by adding 25 µl stock to 20 ml PBS on the day of reaction. This solution was kept on ice until used.

Oligonucleotide pellets of a palindromic sequence (CGGAATTCCG) were obtained directly from Invitrogen and stored in -20°C freezer. A Stock solution of $200\ \mu\text{g/ml}$ was prepared from the oligonucleotide pellets as described in section 3.5.1.

Digitonin ($0.15\ \text{mg/ml}$) was prepared as in section 3.5.1.

PBS-MT was made by adding $5\ \text{g}$ milk powder and $50\ \mu\text{l}$ Tween 20 to $100\ \text{ml}$ PBS. This solution can be stored overnight at 4°C . PBS-T was similarly prepared by adding $50\ \mu\text{l}$ Tween 20 to $100\ \text{ml}$ PBS

10% TCA/2% NaPPi solution was prepared from $100\ \text{g}$ TCA and $20\ \text{g}$ NaPPi dissolved in $900\ \text{ml}$ distilled water. After stirring to dissolve all crystals the final volume was made up to $1000\ \text{ml}$ with distilled water. This solution is stable for 3 months at room temperature.

3.7.2 Preparation of PAR standards

Purified PAR was supplied by BIOMOL Research Laboratories as a branched and linear polymer, average chain length 25 ADP-ribose monomers (range 3-300). It is supplied as $100\ \mu\text{l}$ of a $10\ \mu\text{g/ml}$ solution. $1\ \mu\text{g}$ is equivalent to $2000\ \text{pmol}$ ADP-ribose monomer. The polymer must be stored frozen at -80°C , and repeated freeze-thaw cycles avoided.

On receipt of the PAR polymer it was placed at 4°C until aliquoting on the day of receipt, if the stock needed to be left overnight before aliquoting it was placed in a -80°C freezer. The supplied stock was stored as $4\ \mu\text{l}$ aliquots in Eppendorf tubes. These were kept frozen at -80°C and defrosted at room temperature on the day of reaction. The aliquoted sample was diluted 1 in 80 with sterile water (adding $316\ \mu\text{l}$ water) to give a new stock solution with $25\ \text{pmol}$ of ADP-ribose monomer per $100\ \mu\text{l}$ of solution. This solution was serially diluted according to the table (table 3.3) below in Eppendorf tubes, providing enough standard for two blots. $100\ \mu\text{l}$ of each dilution was added to $300\ \mu\text{l}$ PBS and the total volume ($400\ \mu\text{l}$) loaded into an individual well completing one row of the manifold to provide a standard curve, range 0-25 pmol monomer.

Table 3.3

Final concentration	Volume of preceding dilution	Volume of sterile water
25 pmol	Undiluted stock	
5 pmol	50 μ l	200 μ l
1 pmol	50 μ l	200 μ l
0.2 pmol	50 μ l	200 μ l
0.04 pmol	50 μ l	200 μ l
0 pmol	0 μ l	250 μ l

3.7.3 Assay Procedure

PARP activity was assessed and the immunoblot assay validated using both human peripheral blood lymphocytes and mouse L1210 cells. The method below describes the assay as finally validated. Any variation to the procedure which was used during individual experiments whilst the assay was being developed will be described in the relevant results sections in this thesis.

Any frozen cell preparation was defrosted rapidly at room temperature and washed twice in ice cold PBS, as described above, so that the freezing medium containing DMSO was removed. The prepared cell pellets for assay were resuspended in 0.15 mg/ml digitonin stock to a density of approximately $1-2 \times 10^6$ cells per ml for 5 minutes to permeabilise the cells. 9 volumes of ice-cold isotonic buffer were added and the sample stored on ice until assayed. A 6 μ l aliquot of the cell suspension was withdrawn after vortexing, mixed with an equal volume of Trypan Blue and the cell density counted using a haemocytometer. The cell suspension was diluted if necessary with isotonic buffer to achieve appropriate cell density for reaction (2.44×10^5 /ml, (range $2-10 \times 10^5$ /ml)).

No samples were held on ice for longer than one hour before assay incubation. The assay was performed in a water bath warmed to 26°C and set to agitate at 70 oscillations per minute. The reaction tubes were set up as described in the table below (table 3.4), note the volume of reaction buffer to be added to make a final reaction volume of 100 μ l was calculated knowing the cell suspension volume containing the required cell number.

However reaction buffer was added **before** the cell suspension. Once prepared the tubes were allowed to come up to temperature before addition of the cell samples. In addition, the cell suspensions were warmed in the water bath for 7 minutes prior to reaction to ensure the process occurred at 26°C.

L1210 QC samples were analysed with each batch of clinical samples to provide quality control. These were prepared as described in section 3.2.3, and prior to each assay one aliquot defrosted and permeabilised for assay as above. Triplicate samples were reacted and analysed. These cells have greater stimutable PARP activity so between 5,000-10,000 were loaded to ensure a reading within the limits of the standard curve.

Table 3.4

Reagent	+ oligo	Final concentration
Oligonucleotide	5 µl	10 µg/ml
7 mM NAD ⁺	5 µl	350 µM
Running total	10 µl	
Cell suspension	40-60 µl	
Reaction buffer	To make volume to 100 µl	
Reaction Total	100 µl	
Stop Solution	400 µl	10 µM
Final volume	500 µl	

Each sample was assayed in triplicate. The permeabilised cell suspension was vortexed briefly and the reaction started by adding the appropriate volume as calculated above to give 10,000-20,000 PBMCs or 5,000-10,000 L1210 cells to each reaction tube. The permeabilised cell suspension was replaced on ice. The reaction was stopped exactly 6 minutes after addition of cells by adding 400 µl of ice cold 12.5 µM AG014699 (final concentration 10 µM) and vortexing. The vortexed tube was placed on ice and completed reaction loaded onto the blotting membrane within 1 hour. Each cell suspension being analysed for PARP-1 activity was recounted using a haemocytometer and the cell density in the reaction mixture calculated. Control (T0) cell samples (for cell specific background), were prepared in triplicate for each patient or L1210 QC sample. A volume of unreacted cells (from the remaining diluted cell

suspension) identical to that used in the reaction mixture was added to 400 μ l PBS. This preparation was loaded onto the blot alongside the reaction specimen to give an estimate of the endogenous PAR levels within the cells.

A specific 6x4 array 24-well manifold has been designed which attaches to the base plate of a standard 96-well dot-blot manifold (BRL, Life Technologies Inc, Gaithersburg, MD). This allows loading of a larger volume of reaction solution, with approximately 1 cm diameter wells.

Hybond N membrane (Amersham, Little Chalfont, UK) and filter paper (Whatmann, Maidstone, UK) were soaked in PBS and the dot blot manifold set up with the membrane lying on two layers of filter paper. The PAR standards were loaded across the top row of the 6 wells. Each reaction mixture was vortexed and loaded into wells alongside the appropriate T0 samples. The manifold was aspirated with gentle suction, and washed with 400 μ l 10% TCA 2% sodium pyrophosphate, re-aspirated, then a further wash with 800 μ l 70% ethanol performed.

The membrane was trimmed, marked in the top right hand corner and rinsed twice in PBS before blocking for 1 hour with PBS-MT. Overnight incubation with the primary antibody (diluted 1 in 500 in PBS-MT) at 4°C was followed by 2 washes in PBS-T and then incubation in secondary antibody (1 in 1000 in PBS-MT) for 1 hour at room temperature. The incubated membrane was washed frequently with PBS over the course of one hour then exposed for one minute with ECL reaction solution.

The exposed membrane was placed on the tray within the Fuji LAS3000 UV Illuminator (Raytek, Sheffield, UK) and the chemiluminescence during a 5 minute exposure measured using the imaging software (Fuji LAS Image version 1.1, Raytek). The acquired image was analysed using Aida Image Analyser, version 3.28.001, and results expressed in LAU/mm². Three background areas on the exposed blot were measured and the mean of the background signal from the membrane subtracted from all results. The PAR polymer standard curve was analysed using a one site binding non-linear regression model and unknowns read off the standard curve so generated. Results were then expressed in terms of number of cells loaded and standardised to a given number of cells (usually 20,000).

3.8 Immunoblot assay for measuring PAR formation as a measure of PARP activity in homogenised tumour/tissue

3.8.1 Stock solutions

The stock solutions used to perform an immunoblot PARP activity assay in homogenised tissue are the same as those described above in section 3.7.1

3.8.2 Assay Procedure

Where quality control (QC) standards were required L1210 mouse cells were used. These cells were grown, stored and prepared for assay as described above (section 3.2) and the assay reaction and blot loading performed as described in section 3.7.2.

PAR standards were prepared and used in an identical way to that described in section 3.7.2. The assay procedure described below is that validated for use in the PARPi clinical trial. Once again any deviations from the assay procedure for an individual experiment will be described in the relevant section of the results.

Homogenised tumour or normal tissue was either used fresh (within 1 hour of homogenisation, being held on ice during this period) or defrosted on ice if stored at -80°C as described in section 3.4.2. A further dilution was made with isotonic buffer to obtain an overall 1 in 1000 dilution. The assay was performed in a water bath warmed to 26°C and set to agitate at 70 oscillations per minute. The reaction tubes were set up as in the table below (table 3.5) and allowed to come up to temperature before addition of the homogenate. In addition, the homogenates were warmed in the water bath for 7 minutes prior to reaction to ensure the process occurred at 26°C.

Table 3.5

Reagent	Reaction tube	Final concentration
7 mM NAD ⁺	5 µl	350 µM
Reaction buffer	45 µl	

Running total	50 µl	
Homogenate	50 µl	I in 2,000
Reaction Total	100 µl	
12.5 µM 699	400 µl	10 µM
Final volume	500 µl	

Each sample was assayed in triplicate. The homogenate was vortexed briefly and 50 µl added to each reaction tube to start the reaction. The remaining homogenate was replaced on ice. The reaction was stopped exactly 6 minutes after addition of homogenate by adding 400 µl of ice cold 12.5 µM AG014699 (final concentration 10 µM) and vortexing. The reaction tube was placed on ice and entire contents loaded onto the blotting membrane within 1 hour of reaction. Control (T0) cell samples (for cell specific background), were prepared in triplicate for each patient or QC sample. An identical volume (50 µl) of homogenate (from the remaining 1 in 1000 dilution of homogenate) was added to 400 µl PBS. This was loaded onto the blot alongside the reaction specimen. The same manifold, membrane and procedure used to assess PARP activity in lymphocytes was used for this experiment. PAR standards and QC samples were made up and loaded as described in sections 3.7.2 and 3.7.3

After loading of all samples the remaining 1 in 1000 tissue/tumour homogenate was centrifuged at 800 xG for 5 minutes at 4°C to remove any particulate matter that might interfere with the Pierce protein assay. The supernatant was withdrawn and a Pierce protein assay performed as per the Pierce protocol. If the protein assay was deferred the supernatant was stored frozen at -20°C. At least 200 µl of supernatant was stored so that a repeat assay could be performed if necessary. Bovine serum albumin standards were set up over the range 0.250 mg/ml- 0 mg/ml from a 2 mg/ml stock. A lower standard curve was required and the assay run according to the “enhanced” protocol because of the high dilution of the homogenate necessary to ensure that the assay fell within the immunoblot polymer validated standard curve. 25 µl of these unknown supernatants were loaded in quadruplicate onto a 96-well micro-titre plate, incubated in 200 µl of the freshly mixed BCA protein reaction mix (1 volume reagent B with 20 volumes reagent A) at 37°C for 30 minutes. The protein concentration in the homogenate was read using a Titertek Multiscan MCC/340 plate reader.

The chemiluminescence measured was analysed as described in section 3.7.3, the results were expressed in terms of pmol PAR formed per mg protein loaded.

3.9 Statistical analyses

All clinical results are analysed using descriptive statistics. All other statistical analyses have been performed using the standard statistical analyses with the Graph pad Prism Version 3.03.

Chapter 4

Validation of [³²P] NAD⁺ incorporation assay for PARP activity in clinical samples

4.1 Introduction

Pivotal to the design of the First-in-Human trial of a PARP inhibitor was establishment and validation of a robust laboratory assay which measured the relative activity of human PARP-1 before and after treatment with the inhibitor so that a comparison of the degree of inhibition achieved could be made. The decision to move from part 1 (AG014699 escalation) to part 2 (temozolomide escalation) is dependent on achieving a PID (in the absence of toxicity).

An assay for PARP-1 activity in permeabilised cells has been developed in the Drug Development Laboratory, Cancer Research Unit, University of Newcastle and published in peer reviewed literature (Boulton, Pemberton et al. 1995). The principle of the assay relies on the fact that PARP-1 is constitutively expressed in cells and is stimulated by addition of blunt ended oligonucleotide (Grube, Kupper et al. 1991). The assay measures incorporation of [³²P] ADP ribose into acid-precipitable ADP-ribosylated cellular proteins in a given number of cells provided with a [³²P] NAD⁺ substrate by radiochemical scintillography. The degree of PARP-1 inhibition can be determined on post-treatment samples by reference to pre-treatment controls.

This [³²P]NAD⁺ incorporation radiolabel PARP-1 activity assay has been described using established tumour cell lines as a permeabilised cell suspension and also homogenised human tumour xenografts (Calabrese, Almassy et al. 2004), but its use with human peripheral blood lymphocytes had not been investigated or validated. In the context of a clinical trial in human subjects it is possible to take multiple blood samples but practically more difficult to obtain repeated tumour tissue samples. It is therefore essential for the design of part 1 of the trial to document the degree and duration of PARP-1 inhibition achieved at the different doses of AG014699 in blood cells.

In addition to the adaptation of the assay for use with a new cell preparation, it was necessary to establish a reliable standard cell sample that could be run with every clinical trial assay to provide quality control and establish individual test run acceptance criteria for the assay. Assays used in clinical trials must comply with ICH

GCP guidelines, and should also be validated to as close to ICH GLP guidelines as is practical in an academic laboratory.

In the last two decades there has been the emergence of quantitative macromolecule-detecting technologies which allow pharmacodynamic endpoints to be used far more widely in clinical trials. Use of the data generated by these assays for drug registration with the regulatory authorities has brought to the forefront the difficulty of minimising the variability of biological assays and of validating them for regulatory purposes. International Workshops were held in 1990 and 2000, sponsored by the American Association of Pharmaceutical Scientists (AAPS), to address these issues and summary reports issued for guidance (Shah, Midha et al. 1992; Miller, Bowsher et al. 2001). In addition, the U.S Food and Drug Administration (FDA) has issued a guidance document (2001) and Handbooks of ICH Good Clinical Practice and ICH Good Laboratory Practice provide further advice (1996).

Validation of a pharmacodynamic (PD) bioassay is accepted to be a difficult issue (Shah, Midha et al. 1992; 2001; Miller, Bowsher et al. 2001), given the intrinsic variability of biological samples. Additionally the difficulty of obtaining multiple samples from a patient/human population means that much of the assay development and validation needs to be performed using surrogate biological preparations. Shah and colleagues suggest that when attempting to establish and validate a PD assay that the pharmacodynamic effect should be related to the actual therapeutic endpoint of the activity of the drug. The workshop report (1990) suggests 3 phases of bioanalytical method validation which are shown in table 4.1. Not all the steps in pre-study evaluation will be applicable to a given assay but the model provides a useful guide for examining an assay for use in a clinical trial.

Table 4.1

Phase of bioanalytical method validation	
1 – Bioanalytical Method Establishment	
2 – Pre-study Validation	a) Specificity b) Calibration Model c) Precision, accuracy, recovery d) Quality Control samples e) Stability f) Acceptance Criteria
3 – In-study Validation	

This chapter describes the pre-study validation of an existing bioanalytical method, including establishing a human blood cell preparation technique which provided cells suitable for use in the radiolabel PARP activity assay. The ability to measure PARP inhibition with a potent PARP inhibitor (AG14361) was evaluated in these cells. In addition, quality control (QC) standards were established to be run with each individual assay so that acceptance criteria could be defined as well as enabling inter-assay comparison. The sample handling and storage conditions were investigated to establish whether frozen storage of samples produced any deterioration in the activity of the PARP-1 enzyme or any loss of inhibition. Similar experiments were performed to validate use of the assay to measure PARP activity in frozen homogenised tumour samples.

4.2 Measurement of PARP activity in human peripheral blood lymphocytes

4.2.1 Lymphopreparation and permeabilisation

4.2.1.1 Lymphopreparation

Separation of the different blood cell populations from whole blood was performed by centrifugation through a liquid gradient. Prepared gradients are available commercially and different cell populations can be separated. Nycomed Lymphoprep

was used for all experiments to separate mononuclear cells from erythrocytes, platelets and polymorphonuclear cells. The [^{32}P] NAD^+ incorporation PARP activity assay was performed using peripheral blood lymphocytes only (PBLs) and the method used described in chapter 3 section 3.3.

LymphoprepTM (Ficoll-Isopaque) is a commercially produced sterile solution containing 9.1% (w/v) sodium diatrizoate and 5.7% (w/v) polysaccharide. It has a density of 1.077 ± 0.001 g/ml and an osmolality of 280 ± 15 mOsm. The solution allows one step centrifugation to separate mononuclear blood cells from erythrocytes and granulocytes (neutrophils) and was first described by Bøyum (Boyum 1968). The solution aggregates the erythrocytes, increasing their sedimentation rate and with appropriate centrifugation conditions a layer of mononuclear white blood cells (PBLs) collects at the interface between the diluted plasma, and the ficoll-isopaque.

When designing an assay that would be used on serial blood samples taken from a patient consideration needs to be given to the total volume of blood that can safely be withdrawn without adversely affecting the patient's well being. It was decided therefore that any assay developed could not depend on impractically large numbers of cells being available to produce reliable results. Clinical trial sample analysis would be performed on the cells harvested from 5 ml of whole blood.

The normal range for total white blood count in human blood is $4-11 \times 10^9$ per litre. Approximately 70% of these cells will be neutrophils, and 20% PBLs. Lymphopreparation of 5 ml blood typically gives a total harvest of $5.6 \pm 3.5 \times 10^6$ cells (mean \pm SD of 26 samples prepared over 2 days from healthy volunteers), an estimated extraction of 75% of the available cells.

The possibility of increasing the cell harvest by including polymorphomononuclear cells was investigated. There were some concerns over this since it is reported in the literature that some highly differentiated tissues do not express PARP-1, namely gastrointestinal epithelial cells, neutrophils and epidermal cells (Chatterjee and Berger 1998), and stable cell populations do show lower enzyme levels than rapidly dividing cells (Prof A Bürkle, personal communication). A consistent finding over repeated assessment of PBLs in parallel with L1210 control cells was that the mature blood

cells have lower inducible PARP-1 activity than an immortalised cell line. It was decided to investigate whether inclusion of polymorphs would alter the measured PARP-1 activity in nucleated blood cells.

Separation of both PBLs and granulocytes can be achieved using Polymorphprep™ Axis-Shield (Oslo, Norway), a solution of 13.8% (w/v) sodium diatrizoate and 8.0% (w/v) Dextran 500. It has a density of 1.113 ± 0.001 g/ml and an osmolality of 445 ± 15 mOsm. This solution is more hypertonic than “Lymphoprep”, causing shrinkage and faster sedimentation of erythrocytes. Two lymphocyte bands are formed and polymorphonuclear cells can be harvested along with PBLs. The number of cells harvested from 5 ml whole blood by this method was greatly improved, an average of 26×10^6 cells were obtained allowing loading of the required one million cells. However, as would be predicted from the published data this led to even lower levels of PARP-1 activity / 10^6 cells being measured in the permeabilised white cells, since the additional cells had low or negligible PARP-1 activity. The measured value was 10.3 ± 0.9 pmol NAD^+ incorporated per million cells, 8% of the matched L1210 control value compared to approximately 30 pmol NAD^+ (24%) incorporated per million cells for pure PBL samples (see table 4.2). The absolute counts were low meaning that there was greater potential for noise in the system as there was a less clear differentiation between background (T0) samples and the reaction scintillation counts. This is presumably due to the dilution of the signal from polymer in cells expressing PARP-1 because of the high proportion of cells without enzyme activity. It was concluded that PBLs only would be used to develop the assay. This decision meant that the number of PBLs harvested from the 5 ml sample of blood could be a limiting factor in assay development.

4.2.1.2 Permeabilisation

To ensure the most accurate measure of maximum stimulatable PARP-1 activity in clinical samples it was felt important that cell handling times were kept to a minimum so that the potential for loss of activity was reduced or, indeed, any inhibition of the enzyme was not lost. Cells can be permeabilised by 30-minute ice-cold hypotonic shock (Boulton et al 1995) or by a 5-minute exposure to 0.15 mg/ml digitonin (Calabrese et al, 2004) prior to transfer to isotonic buffer. Digitonin permeabilisation would reduce cell handling time and therefore potentially be the preferred method.

To ensure both assays gave comparable data L1210 cells and PBLs were assayed by both methods.

L1201 cells were cultured and harvested as described in section 3.2, permeabilised either with hypotonic buffer (9nM Hepes pH 7.8, 4.5% Dextran, 4.5 mM MgCl₂, and 5 mM DTT) for 30 minutes or with digitonin (0.15 mg/ml water) for 5 minutes, or with both hypotonic and digitonin solutions for 30 minutes. After the permeabilisation time 9 volumes of isotonic buffer was added. The cells permeabilised with digitonin alone were held on ice until those prepared by hypotonic shock were available and all cell preparations assayed simultaneously. The results are shown in figure 4.1, PARP activity is expressed in terms of the radioactivity (DPM) per million cells. The data shown is the mean and standard deviation of triplicate samples, and this preliminary experiment suggested that there was no difference between the two permeabilisation techniques. (These experiments were performed with the able assistance of Suzanne Kyle)

Figure 4.1

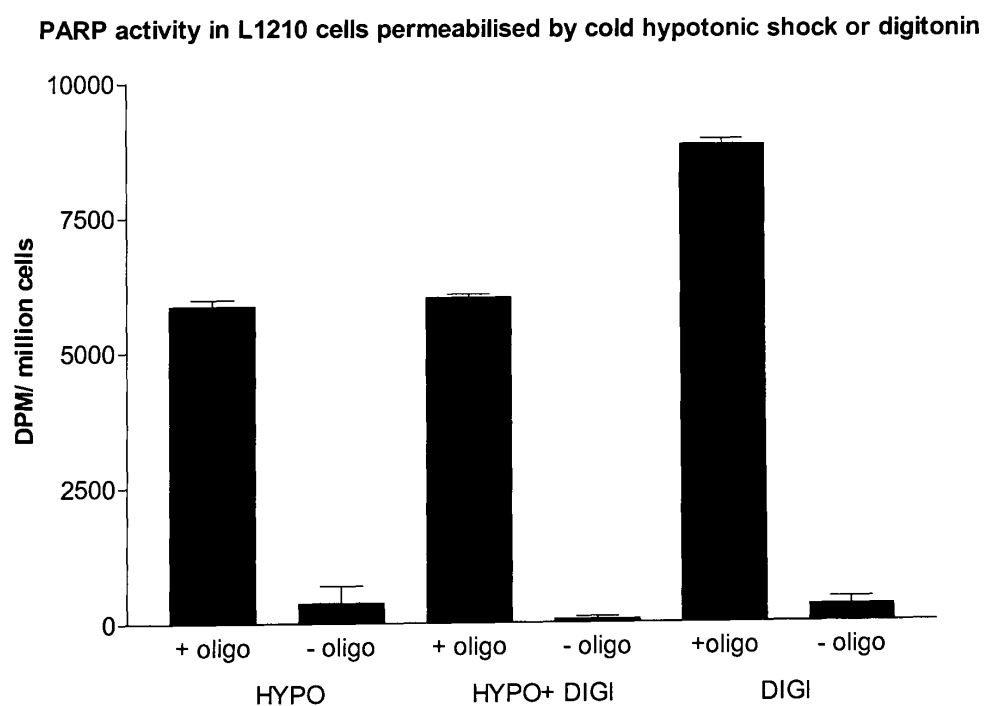


Figure 4.1 DPM for triplicate samples of L1210 cells permeabilised either with hypotonic buffer (HYPO), digitonin (DIGI) or both (HYPO + DIGI) with (+oligo) and without (- oligo) stimulation with oligonucleotide. Mean +SD, n=3

Further investigation of the affects of the two permeabilisation techniques was performed using both L1210 cells and human PBLs. Following permeabilisation 6 μ l aliquots of the cell suspension were stained with 6 μ l Trypan Blue and not only the cell density in the preparation but also the percentage of cells which were permeabilised was assessed using light microscopy and a haemocytometer. Both permeabilisation techniques consistently produced >95% permeabilisation of the cells.

Summary data from repeated assays on different days is shown in table 4.2, demonstrating that there is no significant difference between the maximally stimulated PARP-1 activity following permeabilisation by hypotonic shock or digitonin in either L1210 cells (p= 0.91) or human PBLs (p=0.90). The degree of PARP-1 activity is expressed in terms of pmol NAD⁺ incorporated into polymer per million permeabilised cells in the reaction time.

Table 4.2

	PARP activity (pmol NAD/10⁶ cells/6 min)	
	Hypotonic shock	Digitonin
L1210	121 \pm 73 (4)	124 \pm 48 (16)
PBLs	34 \pm 10 (2)	31 \pm 13 (8)

Data are mean \pm SD with the number of assays given in parenthesis. (p values calculated using Students T test, unpaired, 2-tailed).

In order to determine if the permeabilisation technique affected the measurement of PARP inhibition fresh PBLs were obtained from whole blood in a healthy volunteer by lymphopreparation, the washed cells being resuspended in isotonic buffer and separated into 2 portions. One sample of cells was exposed to 0.4 μ M AG14361 prior to permeabilisation. AG14361 is a potent PARP-1 inhibitor and PARP-1 activity is suppressed to <10% normal with this concentration (Calabrese, Almassy et al. 2004). The inhibited and control PBL suspensions were then again divided into 2 aliquots, the cells pelleted by centrifugation and separate aliquots permeabilised either by hypotonic shock or with digitonin. The results are shown in figure 4.2. Mean and

standard error of triplicate samples is given, results again expressed as pmol NAD⁺ incorporated per million cells. There was no evidence that use of digitonin rather than hypotonic shock affected the result, and the presence of the PARP-1 inhibitor meant that PARP activity was undetectable in either preparation. Further data from repeated experiments on different days comparing the two permeabilisation techniques is summarised in table 4.2 as discussed above.

Figure 4.2

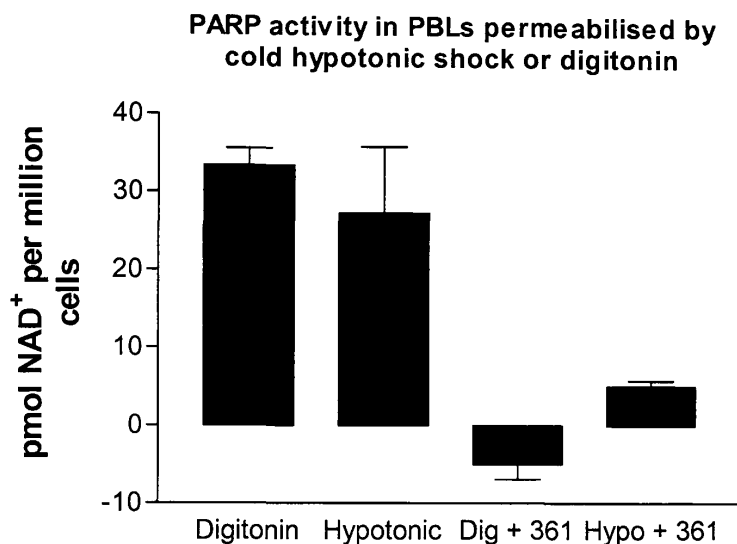


Figure 4.2 PARP activity in PBLs measured with 2 different permeabilisation techniques. Mean + SEM, n=3.

On the basis of these combined results it was decided that changing permeabilisation technique to the shorter exposure to digitonin would not affect the result of the assay. Digitonin permeabilisation had the advantage of shortening the cell handling time before determination of PARP activity hence reducing the potential deterioration of the enzyme with time in isolated cell preparations. It also decreased the risk of cumulative DNA damage due to cell handling.

All subsequent experiments and the validation of the assay have used the digitonin permeabilisation technique.

4.2.2 Demonstration of PARP inhibition in human PBLs

The clinical trial primary endpoint in part 1 of the temozolomide/PARPi trial is the demonstration of PARP inhibition in PBLs from patients treated with AG014699. It was necessary to demonstrate that PARP-1 could be inhibited in these cells and that this inhibition could be measured prior to embarking on full validation of the proposed assay.

To this end whole blood from healthy volunteers was incubated with varying concentrations of AG014699 at 37°C for 20 minutes. In parallel, PBLs from healthy volunteer blood were prepared first and then exposed to the drug as a cell suspension in tissue culture medium. AG014699 was dissolved and diluted in DMSO to 100x the final concentration so that the final concentration of DMSO in any incubation did not exceed 1%. Following an incubation period of 20 minutes the drug was removed by washing and the cells prepared, permeabilised and assayed for PARP activity. The results are shown in figure 4.3, data are from triplicate samples giving mean and SEM. Inhibition of the PARP-1 activity was observed when whole blood was incubated in a known concentration of AG014699 prior to lymphopreparation (the most similar situation to that to be experienced in patients) and also when the inhibitor was added to a suspension of washed isolated PBLs. In both cases the inhibitor was washed off before permeabilisation, indicating that the inhibitor can permeate the PBL cell membrane.

Figure 4.3

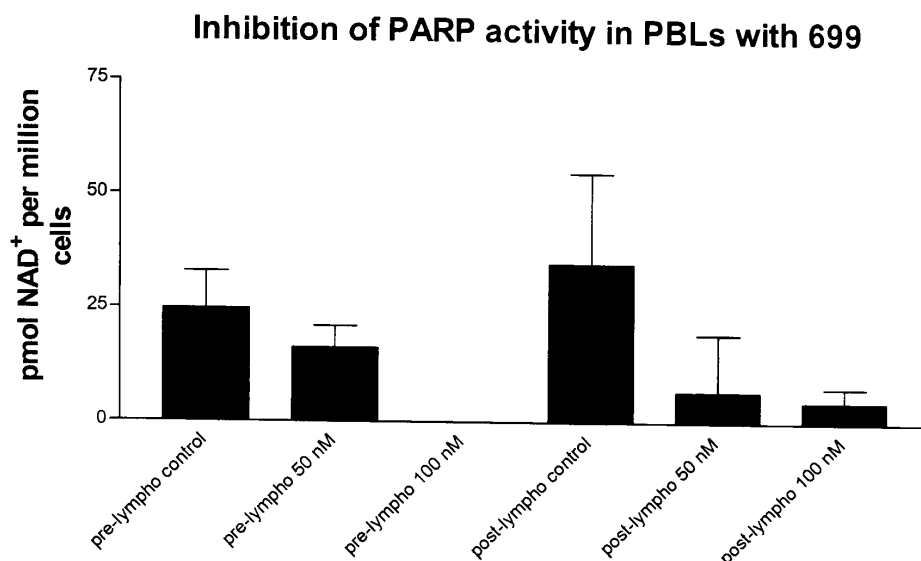


Figure 4.3 Inhibition of PARP-1 in PBLs. Mean +SEM, n=3. prelympho = incubation with inhibitor prior to lymphopreparation, post-lympho = incubation with inhibitor after preparation of PBLs. 50 and 100 nM refer to the concentration of AG014699.

4.3 Establishment of quality control samples

The aim of this project was to establish a validated pharmacodynamic assay for use in an early clinical trial. As discussed in the introduction to this chapter identification of the standard biological matrix which can act as a quality control for each assay containing unknown samples is a critical step in any such validation (Shah, Midha et al. 1992; Miller, Bowsher et al. 2001). In practical terms it was also important that validation of the assay could be carried out using a surrogate but validated cell type rather than repeatedly drawing blood from the healthy volunteer population.

It was decided to assess the mouse leukaemia cell line (L1210) for QC function. PARP-1 activity in fresh exponentially growing L1210 cells, permeabilised with digitonin, was measured as described above. Summary data from serial experiments carried out on separate days is given in table 4.3. PARP activity is expressed as pmol NAD⁺ incorporated per million cells. The number of repeated assays on separate days using freshly prepared [³²P] NAD⁺ stock is shown in column 2. The range of values obtained is shown in column 4. The result for each individual assay is the mean of triplicate or quadruplicate samples.

Table 4.3

	n	pmol NAD⁺/10⁶ cells (mean ± SD)	CV (%)	Range
Fresh L1210	20	124 ± 51	41.4	50-200
Fresh PBLs	10	32 ± 12	37.3	16-55
		% Control		
PBL as % L1210 control	5	25 ± 8	32.6	18-37

Comparison of the maximal PARP-1 activity obtained from repeated PBL samples is also shown in table 4.3. The PBL result is also expressed as a percentage of the matched L1210 control assayed on the same day. This confirms the reports that maximal PARP-1 activity is lower in this “mature” cell population when compared to immortalised cells, the results being in the range of 20-30% the mean L1210 value. When a linear regression analysis was performed on 6 pairs of matched PBL and L1210 samples, assayed in parallel $r^2 = 0.89$ suggesting that a significant relationship exists between the values and it is justified to use L1210 cells as a QC comparator for the PBL result.

4.4 Validation of sample storage and handling techniques

The preliminary experiments reported above demonstrated that PARP activity and inhibition of PARP-1 could be measured in human PBLs. However during the course of the clinical trial patient samples will be obtained over a period of 12 days on cycle 1 of treatment for pharmacodynamic assessment. It is planned that sample will be taken on day -7 when the PARP-1 inhibitor is given alone and on days 1 and 4 when given with temozolomide. Samples will be taken prior to treatment, at the end of the infusion (T0), 4-6 hours post infusion, and at 24 hours. Immediate assay of each of

these samples would not be practical and would also mean that any inter-assay variation could affect comparison of results within one patient.

In addition, performing the study at three Cancer Research UK centres means that storage and shipping of sample to Newcastle for PARP-1 assays is necessary. Therefore, lymphocytes prepared at the other centres will need to be frozen and shipped to the laboratory. It was essential to establish that the PARP enzyme activity is stable with freezing over time. In addition it was necessary to establish that the level of PARP inhibition in the fresh samples did not deteriorate with freezing and storing at -80°C for prolonged periods so that there could be confidence that the PARP-1 activity measured in patient samples after storage was a true reflection of the inhibition of PARP-1 activity in PBLs at the time of sampling.

Initial experiments to investigate the effects of storage were performed with L1210 cells. These cells gave reproducible PARP activity results and it was planned to use them as QC samples. Use as QC samples would be simplified if frozen aliquots of these cells could be used in serial assays; therefore it was necessary to confirm enzyme stability after freezing in these cells. In addition, the initial experiments to investigate the preservation of PARP-1 inhibition with freezing were performed using L1210 cells because of the difficulty of obtaining large numbers of PBLs.

4.4.1 PARP-1 activity in fresh versus frozen L1210 cells

L1210 cells were grown in 200 ml of medium as described in the methods (section 3.2). The cells were harvested in the exponential growth phase, washed and counted. One sample of cells was analysed fresh on the day of harvesting and multiple aliquots were frozen in medium + 10% DMSO. The original cell culture was maintained in a healthy growth phase in the incubator for the duration of the experiment. At regular intervals one of the frozen samples was rapidly thawed, washed in buffer and assayed according to the standard operating procedure. At the same time a sample of freshly harvested cells from the growing stock was also analysed so that results could be expressed in terms of a fresh enzyme control assayed in the same sample run.

The results are presented in figure 4.4 and table 4.4. Figure 4.4 shows the mean PARP-1 activity measured in triplicate defrosted samples expressed as a percentage of the mean activity from triplicate samples of the matched fresh sample. It demonstrates that the enzyme activity is stable with storage in this manner. These paired samples were stored over a range of 1 to 15 weeks with no evidence of deterioration in maximally stimulated enzyme activity.

Figure 4.4

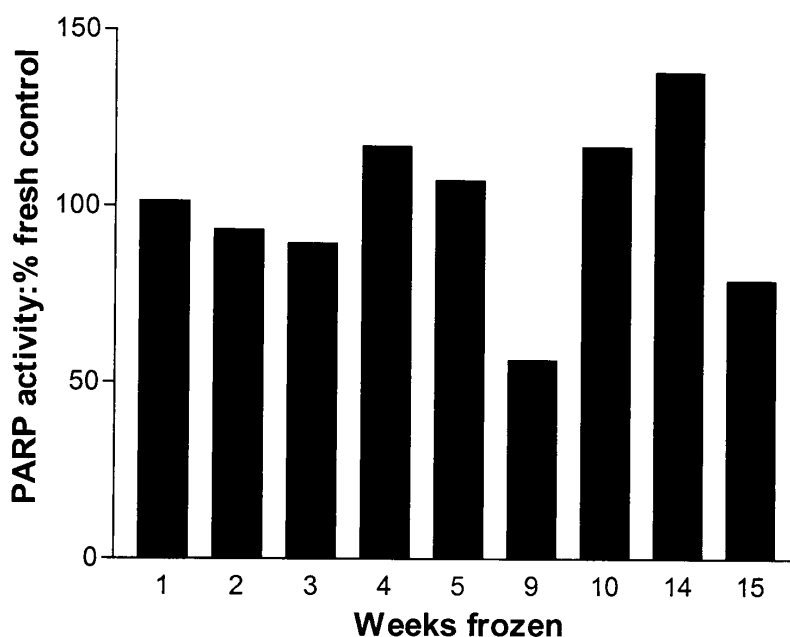


Figure 4.4 Data from paired L1210 cell samples, fresh and frozen assayed in triplicate on the same day. Results displayed as control data expressed as a percentage of the fresh control value assayed on that day

Repeated assays of frozen L1210 cells gave a mean PARP activity of 119 ± 52 pmol $\text{NAD}^+ / 10^6$ cells (mean \pm SD, $n=12$ with a range of 40-185, CV(%) 43).

Although there is considerable variation between individual assays the mean (and standard deviation) PARP-1 activity of frozen samples was very similar to that obtained with fresh samples. For all clinical trial assays batched frozen L1210 cells are used and one sample run as QC with every clinical assay. This allows comparison to be made between assays by comparing the relative values with respect to the QC results. To ensure that there is consistency between batches of L1210 QC cells

samples were prepared in bulk batches and stored in the designated -80°C freezer. A new batch is prepared once there are 6 samples only available and at least 2 assays run using the old and new batch of QC samples in parallel so direct comparison between assays remains possible. The projected recruitment time for the PARPi trial means that banking sufficient QC samples to cover the entire 2 year period would mean that samples would be used outwith the time frame assessed above for stability of the PARP enzyme with freezing.

4.4.2 Preservation of PARP-1 inhibition with frozen storage

Although the PARP-1 enzyme function when maximally stimulated with oligonucleotide is preserved with frozen storage for up to 3 months it was also necessary to establish whether there was a deterioration in the degree of inhibition when the inhibited cells were stored for a period prior to analysis.

Exponentially growing L1210 cells (6×10^5 cells/ml, total volume 250 ml) were exposed to either $0.4 \mu\text{M}$ AG014361 (20 μl of $40 \mu\text{M}$ stock AG014361 in DMSO diluted in 1980 μl medium, final DMSO concentration 1%) or in medium plus 1% DMSO (control samples) for 20 minutes at 37°C , the cells were pelleted out of this solution by centrifugation, washed in PBS and one aliquot assayed for PARP activity. The rest of the samples were frozen in aliquots of 15×10^6 cells for subsequent tandem assay of inhibited/control cells.

Paired samples were defrosted and analysed over a 14 week period. The results are shown in figure 4.5. Data are expressed as the % of PARP-1 inhibition demonstrated in the frozen sample compared to its own control sample which had been frozen for the same length of time. Values for PARP-1 activity are derived from triplicate samples. There was no evidence of a loss of the degree of inhibition of the enzyme over this period of storage.

Figure 4.5

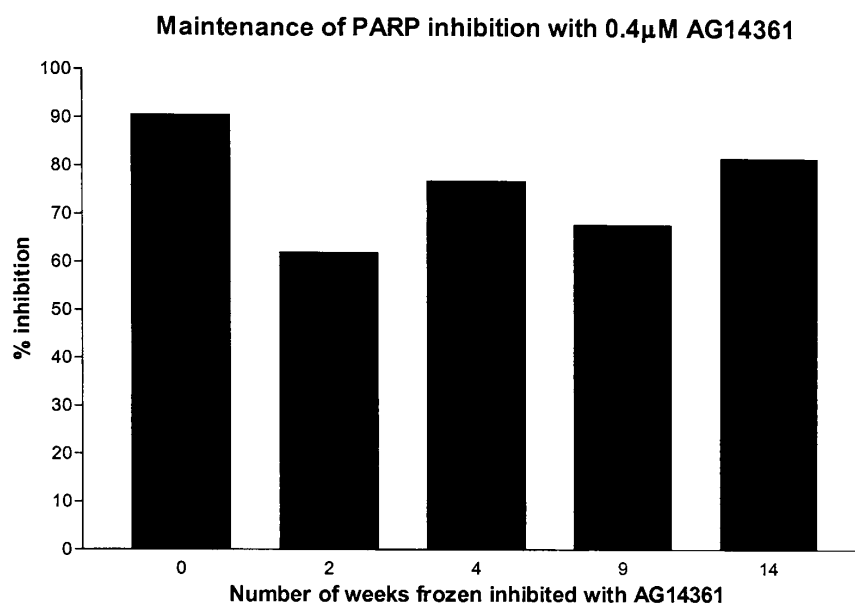


Figure 4.5 Preservation of inhibition with frozen storage. Mean of triplicate samples expressed as % matched uninhibited control

The same experimental design was used to set up a series of L1210 cell samples inhibited with different concentrations (10 nM, 50 nM, 100 nM) of AG014699, the clinical trial candidate. These samples were frozen and serially analysed as described above. The practical work for this experiment was ably performed by Suzanne Kyle. The results are shown in figure 4.6 once again there was no evidence in a deterioration of the degree of inhibition with time.

Figure 4.6

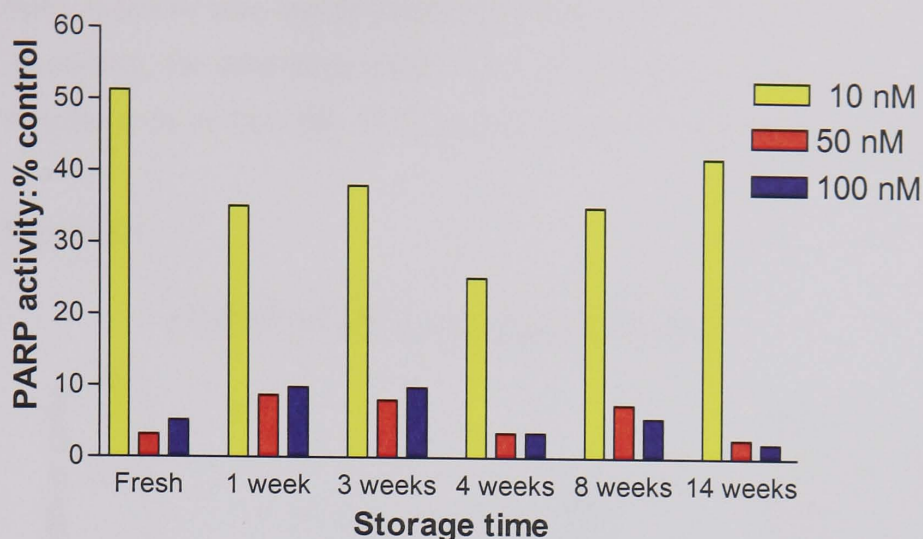


Figure 4.6 Graph showing the degree of PARP-1 inhibition caused by a given concentration of AG014699. Data are expressed as a percentage of the control (DMSO incubation only prior to freezing) L1210 samples assayed on the same day, PARP-1 activity being measured in pmol NAD⁺ incorporated per million cells.

4.4.3 Comparison of frozen storage temperature

In the experiment described above stored samples had been frozen by placing in a freezer maintained at -80°C. It is more common in clinical facilities to have -20°C storage available, particularly because of the constraints of space and the requirement for more sophisticated monitoring and back-up facilities if -80°C storage is used.

An experiment was designed to assess what storage temperature was necessary for the integrity of the clinical samples. L1210 cells were grown in tissue culture in the usual manner. The harvested cells were divided into 4 portions. These were incubated in medium containing 10 nM, 50 nM, 100 nM AG014699 or 1% DMSO as a control for 20 minutes. The inhibitor solution was washed off and the sample divided into 3. One aliquot was processed for immediate radiolabel PARP assay, and the others resuspended in medium + 10% DMSO for freezing. One of these was placed in the -80°C freezer as previously and the other in the -20°C freezer.

The two frozen samples were defrosted and analysed after 10 days at this temperature. The results are shown below in figure 4.7 and figure 4.8. Figure 4.7 shows the data

expressed as mean and SD of triplicate values in pmol NAD⁺ incorporated per million cells. It can be seen that freezing and storage at -20°C does not preserve the samples adequately, the standard deviation in the results is much larger than with fresh samples or those frozen at -80°C and the degree of inhibition has not been preserved.

Figure 4.7

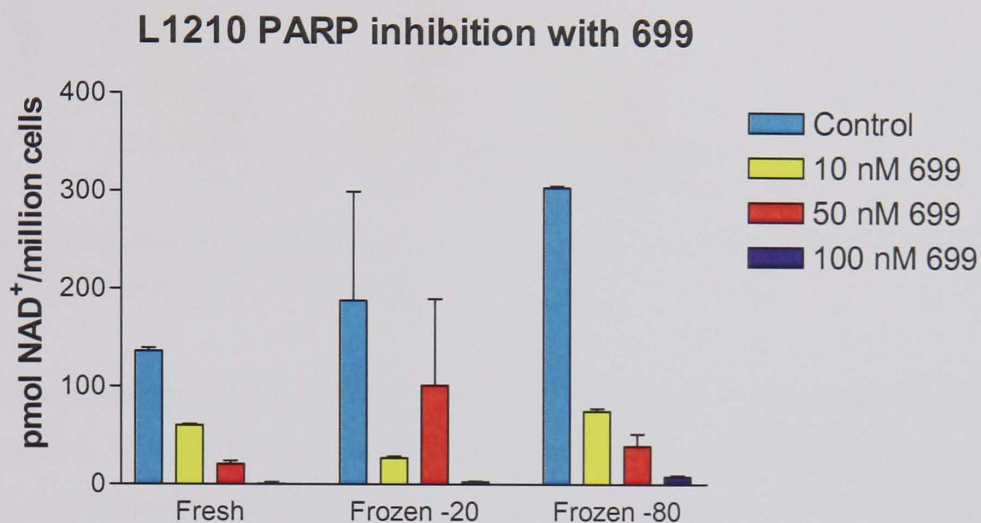


Figure 4.7 Comparison of the preservation of PARP inhibition at different storage temperatures. Mean + SD, n=3.

When the means from the above data with the inhibited samples is expressed as a percentage of their own control value comparison can be made between the assays on the fresh cells performed 10 days earlier with those of the frozen samples. The pattern of inhibition measured is very similar in the fresh and -80°C frozen samples but more variable when frozen at -20°C (figure 4.8).

Figure 4.8

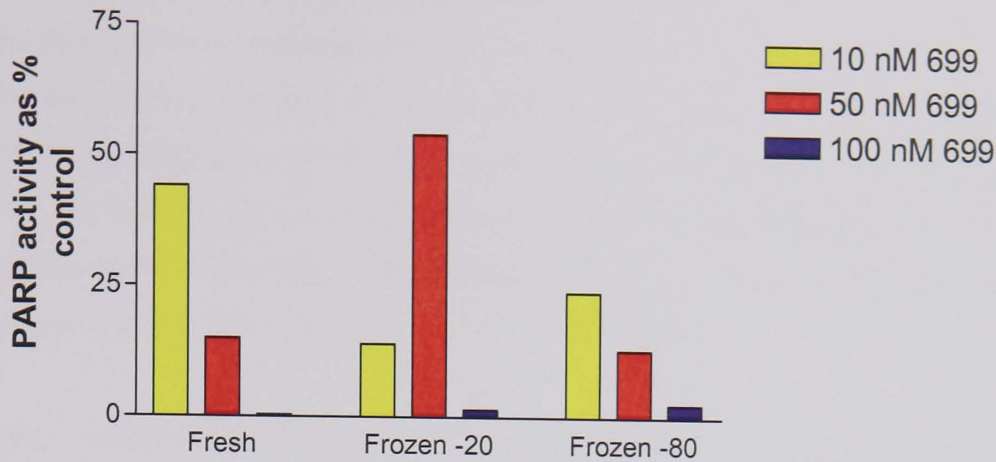


Figure 4.8 Comparison of effect of storage temperatures on inhibition of PARP-1. Mean data from figure 4.7 expressed as % own control value

It was concluded that freezing and storing at -20°C did not adequately preserve the samples. Despite the resource implications it was recommended that samples should be placed directly into storage at -80°C , and kept at this temperature until transfer to the analysis site.

4.4.4 Enzyme stability in PBLs

The feasibility of freezing prepared PBLs for a period of days, then defrosting and measuring PARP activity was investigated in the following manner. Blood from a healthy volunteer was drawn, PBLs harvested and one aliquot assayed and the other frozen in medium + 10% DMSO at -80°C for one week. At the point of thawing further blood was obtained from the same volunteer and from an additional source. The two fresh samples were analysed at the same time as the thawed sample and the appropriate L1210 control cells. Three measurements were obtained from the same individual and assayed in triplicate; fresh week 1 = $8.7 \text{ pmol NAD}^+ / 10^6 \text{ cells}$, fresh week 2 = $16.0 \text{ pmol NAD}^+ / 10^6$ and frozen week 2 $12.7 \text{ pmol NAD}^+ / 10^6$. These data demonstrated the inherent variability of a biological assay, and emphasises the difficulty of comparing between assays. However expressing the measured PARP-1 activity in PBLs in terms of the QC sample run in the same assay appeared to suggest that there had not been a significant deterioration in the PBL enzyme function over 1 week of storage (values of 14%, 14% and 11% of matched QC sample respectively).

The practicalities of the clinical trial necessitate frozen storage of blood samples, therefore further experiments were carried out to establish the stability of the PARP-1 enzyme with more prolonged storage and also the stability of enzyme inhibition. These experiments were carried out using L1210 cells and are described in sections 4.4.1-4.4.3 above, partly to strengthen the validity of using these as the QC samples but also because of the practical problems in obtaining large volumes of blood to prepare multiple frozen aliquots of PBLs from one source.

4.4.5 Temporal fluctuation in PBL PARP activity

The experiments described above had shown that PARP-1 activity can be measured in human PBLs using the radiolabel PARP activity assay and that this assay might be adaptable for use as a clinical trial pharmacodynamic assay. During the clinical study blood samples are withdrawn from the patient for PD assay over a 24 hour period on three separate days, initially on the test dosing day where AG014699 is given alone, then on days 1 and 4 of the combination treatment to determine the degree of PARP inhibition achieved and any cumulative inhibition. All the samples from a 24 period are analysed together so that results can be expressed using the baseline sample as the control.

For this strategy to be appropriate it was necessary to establish whether there was a temporal variation in PBL PARP-1 activity. 5 ml whole blood samples were withdrawn from a group of healthy volunteers at T0 and either 4 or 24 hours later to correspond with the patient sampling times. PBLs were obtained by lymphopreparation and frozen in medium + 10% DMSO. The samples were subsequently defrosted and all analysed in one assay run so that comparison of the absolute values was possible.

All the data obtained were close to the mean PARP activity measured in human PBLs and within the range given in table 4.3 (see figure 4.9).

Figure 4.9

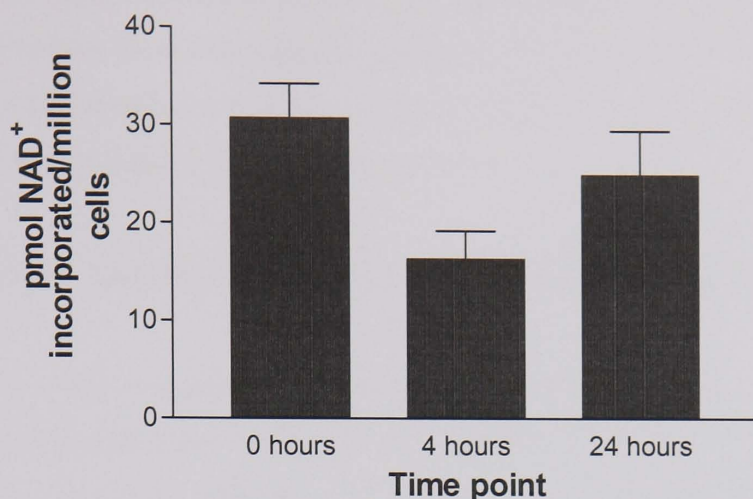


Figure 4.9 Mean + SD over paired PBL samples. N= 15 for baseline, n=7 at 4 hours, n=8 at 24 hours.

For a closer evaluation of temporal variation only the data from samples where there was an adequate ($>1 \times 10^6/\text{ml}$) harvest of PBLs was considered. There was no evidence for a variation with sampling time in the value obtained for maximally stimulated PARP activity in human PBLs in normal volunteers (figure 4.10, mean and standard deviation of triplicate measurements).

Figure 4.10

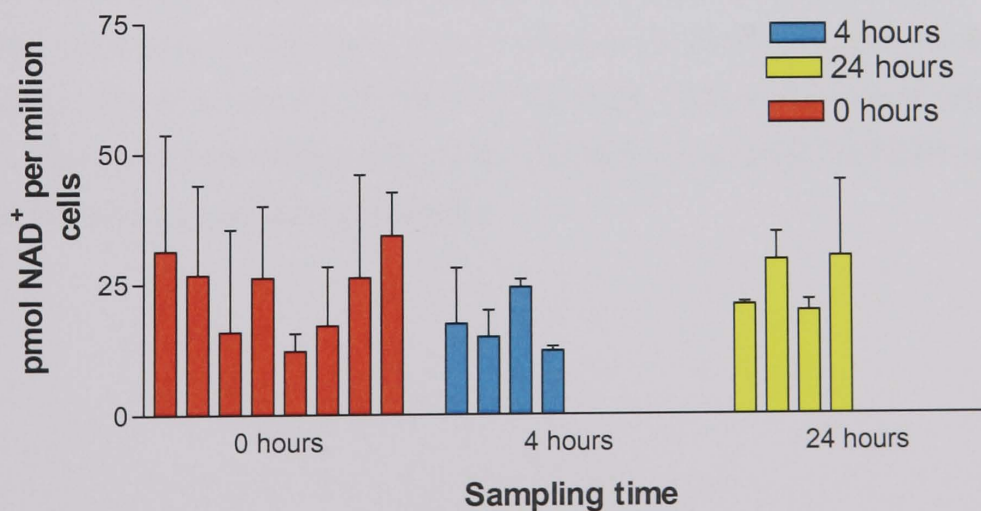


Figure 4.10 Individual results from human PBL assay, mean + SD of triplicate measurements

The results of this experiment did not suggest there was a clear variation in the maximally stimulated PARP-1 activity in human PBLs over a 24 hour period. However there was a great variation in the number of PBLs separated from the 5 ml blood samples, in subjects where few cells were obtained this led to an unacceptably large standard deviation in the results.

4.4.6 Assessment of enzyme integrity after transportation of samples

The First-in-Human trial is based at three clinical centres; all the PARP-1 activity pharmacodynamic assays are being performed in the NICR, Newcastle. PBL samples obtained in the different clinical centres will be transported overnight on dry ice (solid CO₂, sublimation point at -78.5°C) to the NICR for analysis. It was therefore important to establish whether treatment of the samples in such a manner would cause deterioration in the samples.

L1210 cells were grown to a suitable cell density in suspension. Cells were harvested, washed and frozen in medium + 10% DMSO at -80°C . A sample of the freshly growing cells was passaged and allowed to continue to divide for one further day. After freezing two aliquots of the stored QC samples were packaged as for transport in a polystyrene container filled with solid CO₂, left overnight on the bench top to mimic the transport conditions of the samples. These samples were analysed in parallel with a fresh L1210 sample and one which had remained in storage at -80°C . Results are shown in table 4.4, PARP-1 activity being expressed in terms of pmol NAD⁺ incorporated per million cells; mean, standard deviation and coefficient of variation (%) from quadruplicate samples.

Table 4.4

	pmol NAD⁺/10⁶ cells (mean±SD)	CV (%)
Frozen L1210	54 ± 13	24.1
Fresh L1210	84 ± 13	15.2
Transport condition L1210 (1)	79 ± 26	32.7
Transport condition L1210 (2)	67 ± 4	6.5

There was no a significant deterioration in the measured PARP-1 activity with the planned transport conditions. The samples will be considered adequately stored if they arrive at the receiving centre still frozen and with solid CO₂ in contact with the vials, maintaining the temperature below -20°C.

4.5 Assay validation for use with human tumour samples

Tumour biopsies from patients with metastatic malignant melanoma will be taken during the second part of the study and PARP-1 activity and inhibition will be assessed in these samples. The published [³²P] NAD⁺ incorporation PARP-1 assay is already established to be able to measure PARP activity in tissue homogenates. Therefore, in terms of validating the assay for the clinical trial the issues to resolved were confirmation that freezing and storage of the tissue did not affect the measured PARP activity, validation of the change to the assay methodology (omission of oligonucleotide) and demonstration that PARP inhibition with AG014699 could be measured in tissue homogenates.

There is great practical and ethical difficulty in obtaining multiple samples from a patient/human population. This paucity of samples is a particular problem when small tissue biopsies are being analysed. Therefore, of necessity, assay development and validation work must be done using surrogate tissues. All experiments have

either been carried out using homogenised mouse liver as a readily available tissue, and because in patients the liver is a common site of metastatic disease and hence a potential source of samples or using human tumour xenografts in nude mice. The close homology of PARP-1 between species makes this an acceptable manoeuvre.

4.5.1 Confirmation of activation in the absence of added oligonucleotide

When PARP-1 activity is measured in permeabilised cells a blunt-ended oligonucleotide is added to the reaction to maximally stimulate PARP-1 by providing multiple blunt ended strand breaks. Mechanical homogenisation of tumour samples or visceral tissue to dissociate the cells causes sufficient DNA breakage to maximally stimulate PARP-1 (M. Batey, MSc thesis). Maintaining the sample on ice during and after homogenisation prevents polymer formation utilising endogenous NAD^+ on these introduced DNA strand breaks.

Whether addition of oligonucleotide was required to ensure maximal stimulation of PARP-1 was investigated by incubating samples from the same homogenised liver sample in the presence or absence of 5 μl oligonucleotide. The results are expressed in terms of NAD^+ incorporated per mg protein added, mean and standard deviation of quadruplicate samples. Addition of oligonucleotide to these preparations (figure 4.11) did not further enhance the measured PARP activity and is, therefore, unnecessary.

Figure 4.11

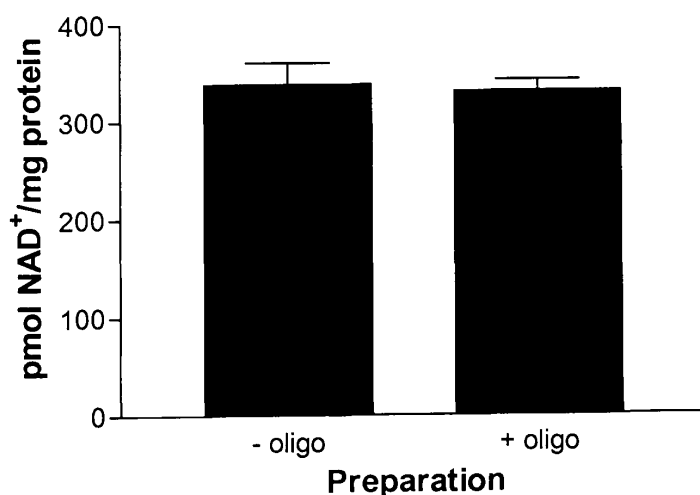


Figure 4.11 Effect of adding oligonucleotide to homogenised tissue. Mean + SD, n=3. PARP activity expressed as pmol NAD^+ incorporated per mg protein

4.5.2 Affect of freezing and storage of tissue samples

During part 2 of the clinical trial small tumour samples will be obtained from patients under local anaesthesia and snap frozen in liquid nitrogen immediately after biopsy with no further processing at this stage. Samples will be stored at -80°C . They will be transferred to the assay laboratory frozen from the clinical centres. It has been shown above that PARP-1 enzyme activity and inhibition is preserved with freezing in cell preparations. As part of the assay validation process it was necessary to demonstrate that snap freezing and storage of tissue over time does not cause deterioration in enzyme function.

Each liver was divided into 2, one portion processed immediately and the other snap frozen for 1-8 weeks at -80°C prior the homogenisation and assay as described in sections 3.4.2 and 3.6. The PARP activity (pmol/mg protein) was compared. These paired data are shown in figure 4.12 (mean and standard deviation of triplicate results), there was not a significant deterioration in the samples with freezing and storage. This means that snap freezing of tumour biopsies, with subsequent frozen transport to the laboratory is feasible in the clinical setting.

Figure 4.12

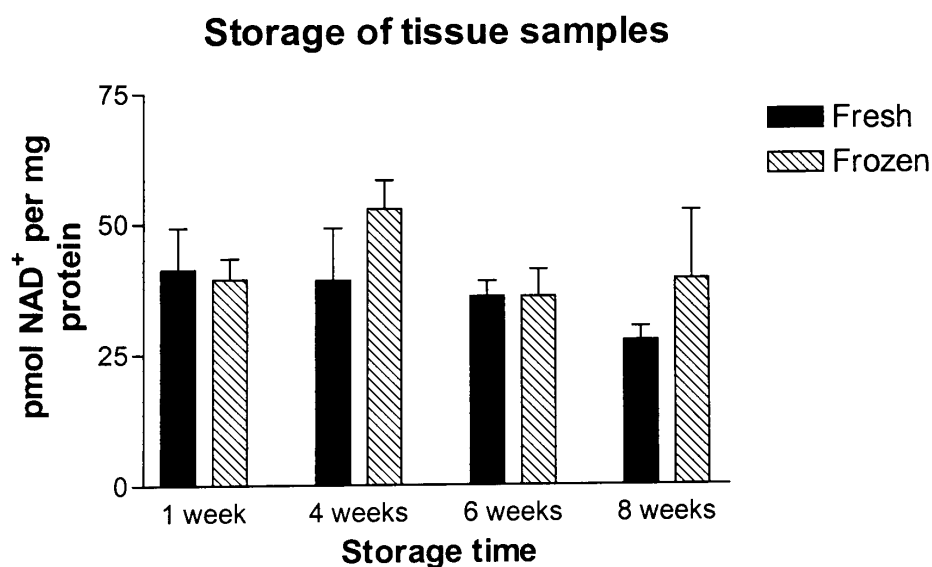


Figure 4.12 Stored tissue results (mean + standard deviation) paired with freshly analysed sample of same liver. No significant deterioration with storage time

4.5.3 PARP inhibition with AG014699 in tissue

PARP-1 inhibition by AG014699, the clinical candidate, has been demonstrated in cell culture suspensions (L1210 cells) and in isolated human PBLs in the sections above. During the preclinical development and evaluation of the proposed clinical candidate nude mice bearing human tumour xenografts (SW620 human colon cancer cell tumours) were treated with a single intra-peritoneal dose of AG014699 dissolved in sterile water. The dosages used were 0.1 mg/kg, 1 mg/kg and 10 mg/kg. Vehicle was injected as a control. The mice were sacrificed 30 minutes later and the tumours removed and snap frozen.

These samples were subsequently homogenised and assayed as described in section 3.7. The results are shown in figure 4.13 confirming that inhibition of PARP-1 within the tumour can be demonstrated and that the degree of inhibition can be measured with the described assay. The practical work for this experiment was performed by Suzanne Kyle.

Figure 4.13

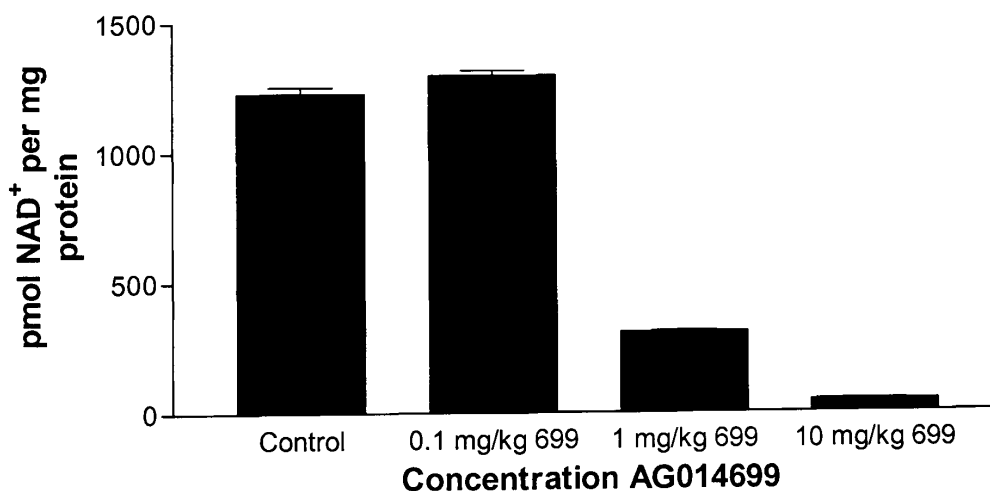


Figure 4.13 Demonstration of inhibition of tumour PARP-1 Data derived from the mean of three tumours analysed in triplicate, mean and standard deviation shown.

In summary, it was demonstrated that the assay could be adapted for use with frozen homogenised tissue and that enzyme inhibition could be demonstrated. This PARP

activity assay can therefore be used to measure the degree of PARP inhibition achieved in the clinical trial tumour samples.

4.6 Intra-assay validity

As part of the validation procedure the intra-assay precision was investigated. This was done to establish two facts, did analysis of the same sample give the same result when done at the beginning and the end of the assay and what were the lower limits for cell numbers analysed for accurate PARP activity determination?

L1210 cells were harvested and permeabilised for the assay in the standard way. A cell suspension density of 3×10^6 cells per ml was obtained. This solution was serially diluted with isotonic buffer to obtain samples such that 0.75×10^6 , 0.66×10^6 , 0.5×10^6 , 0.33×10^6 cells would be added to the reaction tube rather than the protocol stipulated 1×10^6 . Six replicates of these suspensions were analysed in one assay run.

The results are summarised in table 4.5. As the cell number added to the reaction tubes decreases the variation in the replicates increases, demonstrated by the increase in observed standard deviation. This increase was also observed when analysing PBL samples. Their intrinsically lower PARP activity meant that any additional variation due to low cell numbers might compromise detection of PARP inhibition by AG014699. For the purposes of assay validation it is felt that the range of values for added cells over which the assay is reliable is $0.6-1.0 \times 10^6$.

Table 4.5

Cell density	pmol NAD ⁺ incorporated	pmol NAD ⁺ /10 ⁶ cells
1.0	135 ± 10	135 ± 10
0.75	108 ± 5	144 ± 6
0.66	85 ± 7	144 ± 10
0.5	63 ± 20	127 ± 41
0.33	45 ± 4	138 ± 11

4.7 Discussion

The work described above explains the steps taken to develop and then validate a pharmacodynamic assay for potential use during the PARPi trial. These data were also used to produce a full validation report for use of the radiolabel PARP activity assay with human PBLs and a supplementary validation report for its use with tumour samples. These validation reports have been reviewed and accepted by the Quality Control section of Cancer Research UK and by Pfizer GRD.

Most published material on method validation and ICH guidelines (1996) refer to the validation of analytical procedures, largely based around chromatographic methods. For these procedures it is clearly possible to be much more precise than when validating a bio-assay. The ICH guidelines list five key characteristics of an assay which need to be demonstrated and defined; specificity, linearity, range, accuracy and precision. FDA Guidance (2001) defines the fundamental parameters for bioanalytical validation as being accuracy, precision, selectivity, sensitivity, reproducibility and stability.

The principles to be used for establishing a valid method are defined in the 1990 AAPS International Workshop report (Shah, Midha et al. 1992) as being

- a) Production of a specific detailed description and protocol of the method (Standard Operating Procedure)
- b) Investigation of each step in the method to determine the extent that external variables may affect the estimation of the result
- c) Validation of the method for the intended use
- d) Wherever possible validation should be performed using the same biological matrix as the intended samples
- e) Within and between run accuracy should be demonstrated to allow accuracy and precision to be assessed
- f) For assays where a standard curve is included the range of the curve, relationship between response and concentration and lower limit of quantification must be defined

The conference report acknowledges the difficulty of applying all these principles to a biological assay and states that “the pharmacodynamic effect measured for bioequivalence studies should be related to the actual pharmacologic (therapeutic) end point of the activity of the drug”.

Therefore, when validating an assay based on a biological system such as enzyme activity it is acknowledged to be much more difficult to produce detailed and exact validation of data. Huber (Huber 1998) states that compound analysis a precision of better than 1% relative standard deviation is easily achieved whereas for biological samples the precision is likely to be between 10-16%.

The pharmacodynamic effect which is measured by the [³²P] NAD⁺ incorporation PARP activity assay is the number of pmol NAD⁺ incorporated into acid precipitable macromolecules by PARP-1 in the 6 minute reaction period. Addition of the permeabilised cells to a plentiful supply of the enzyme substrate (NAD⁺) and a powerful enzyme activator (oligonucleotide) means that NAD⁺ incorporation into poly(ADP-ribose) is the major reaction product that can be precipitated by TCA. The assay has been designed to assess inhibition of PARP-1 activity by AG014699 by measuring a reduction in the ability to form this reaction product. It would seem, therefore, that the radiolabel assay does fulfil this validation requirement.

Detailed Standard Operating Procedures have been produced for both the assay using PBLs as the experimental matrix and that using homogenised tumours. Validation has focused on the intended clinical use of the assay and wherever practical the method has been validated using the biological matrix of the intended unknown samples. The influence of external factors on the validity of assay results has been investigated by studying the effects of storage and transport of the samples on both enzyme activity but also the maintenance of inhibition.

The steps taken to address intra and inter assay variability whilst adapting the PARP activity assay for use for analysis of clinical trial samples have included the definition of quality control samples to be run with each assay. Within the SOP QC acceptance limits for an assay are defined based on the multiple replicates analysed. This provides confidence that a given assay run has produced valid readings for the

unknown values if the QC samples lie in the expected range (118.9 ± 51.6 pmol NAD⁺ per million cells).

Throughout the development and validation of this PARP-1 assay for use in the clinical trial it became apparent that the low cell recovery from whole blood compromised the assay results. Studies on intra-assay reproducibility described above using L1210 cells, which have higher basal levels of PARP-1 activity than PBLs, showed the assay was less robust and variability increased as cell numbers were reduced. This problem would be expected to be more marked when analysing cells with a lower basal enzyme activity. It has been shown that inclusion of polymorphonuclear cells would not improve the situation.

One option to increase the number of cells it is possible to add to each reaction tube is to decrease the number of replicates within an assay, but there was concern over reducing this to fewer than 3. During the clinical trial blood will be taken from patients for pharmacokinetic analysis of AG014699 and temozolomide, and for two pharmacodynamic assays, the PARP activity assay and also COMET analysis for DNA strand breaks. Increasing the volume of blood drawn from the patient would obviously increase the absolute number of cells harvested but could significantly impact on the patient's wellbeing. This was, therefore, not considered an option to improve assay reproducibility.

Another option would be to omit the “- oligo” triplicate set of reaction tubes, thus reducing by 33% the number of cells needed. The “-oligo” samples give a measure of background PARP-1 activity in the permeabilised cell population, however decisions in the trial will be made based on the degree of inhibition measured when PARP-1 is maximally stimulated. Omission of these replicates would still leave a requirement for a minimum of 3.6×10^6 cells to perform the assay, leaving no scope for assay repetition if the QC indicated an invalid run. A poor cell harvest would make obtaining a reliable result difficult. Patients recruited into phase I anticancer drug trials have failed standard therapy for their tumour and many have had significant previous cytotoxic treatment and have low bone marrow reserve and blood counts at

the bottom of the normal range. The possibility of the low PBL harvest is greater in the phase I trial population than when drawing blood samples from healthy volunteers.

Therefore despite the successful and accepted validation of the [^{32}P] NAD^+ incorporation PARP activity assay there remained significant concerns that in clinical practice it might prove less robust. Chapter 5 describes the work undertaken to set up and validate an alternative assay based upon an immunological method using far fewer cells.

Chapter 5

Development and Validation of Immunoblot PARP activity assay

5.1 Introduction

The extensive scientific interest in and diverse potential clinical uses of PARP-1 inhibitors (discussed in chapter 1) means a number of authors have described assays which attempt to measure PARP-1 activity or inhibition. Earlier assays relied upon radio-labelled substrate (Aboul-Ela, Jacobson et al. 1988; Boulton, Pemberton et al. 1995) or purification of poly(ADP-ribose) by complex chromatography (reviewed in (Shah, Poirier et al. 1995). De Murcia's group reported an ELISA based screening assay (Decker, Miranda et al. 1999) and more recently a non-radioactive biotinylated NAD assay has been described (Brown and Marala 2002) which is suitable for use with high-throughput screening (HTS) of PARP inhibitors. Dillon and colleagues reported a $^3\text{H-NAD}^+$ FlashPlate scintillation proximity assay which again can be used for HTS since it can be adapted for use with a 384-well plate format (Dillon, Smith et al. 2003).

The development of monoclonal antibodies has produced a widely used tool in both scientific research and clinical practice, with a multitude of commercially available products and assays. The rapid emergence over the previous decade of quantitative macromolecule detecting assays, including immunoassays, was identified in the 2000 AAPS Validation Workshop, and the issues surrounding their validation included as a key goal in the conference (Miller, Bowsher et al. 2001).

The possibility of using a monoclonal antibody against poly(ADP-ribose) (PAR) to detect polymer formation and thus enzyme activity with Western Blotting was first described in 1995 (Shah, Kaufmann et al. 1995). Whilst exploring potential alternative PARP activity assays which would allow smaller biological samples advice and help was sought from Professor Alex Bürkle. His laboratory studies PARP-1 and its relationship to ageing. In 1999 they published a report of a "quantitative nonisotopic immuno-dot-blot method" which allows assessment of cellular poly(ADP-ribosylation) capacity (Pfeiffer, Brabeck et al. 1999). This assay exposed permeabilised cells to oligonucleotide and a reaction buffer containing NAD^+ . The formation of PAR under these circumstances was stopped after the fixed

period by the addition of an excess of ice-cold 3-aminobenzamide. The permeabilised cells were then blotted onto a nitrocellulose membrane, fixed and exposed to a primary monoclonal antibody which binds to PAR. An HRP-conjugated secondary antibody was used to detect the bound primary and the chemiluminescence signal detected and quantified. Pfeiffer et al reported that intensity of the chemiluminescent signal was a function of the cell number loaded and that PARP-1 inhibition with 3-aminobenzamide could be demonstrated.

The primary antibody used in the assay described above in the 10H anti-PAR antibody was generated by Dr M Miwa from a mouse hybridoma cell line (Kawamitsu, Hoshino et al. 1984). The antibody binds to a linear structure of the ADP-ribose polymer which is greater than 15-20 ADP-ribose monomers in length, ethanol precipitation of antibody-bound polymer suggested that 10H binds to almost all molecular sizes of polymer generated from rat liver PARP (Kawamitsu, Hoshino et al. 1984). Antibody binding to polymer is inhibited by 20% by the presence of excess monomer suggesting some cross-reaction with the monomer subunit. Species cross-reactivity is reported for human, mouse, rat, bovine and monkey poly(ADP-ribose) (Shah, Kaufmann et al. 1995). These authors also report a “simple activity-Western blot technique” which can detect polymerase activity in cultured cells by virtue of detection of the reaction product. The 10H antibody is commercially available from Alexis Biochemicals at >95% purity but in all the experiments reported below has been generously supplied by Professor A Bürkle. In the early experiments much advice and assistance was given by Professor Bürkle, his colleague Dr Pfeiffer and by Dr Paul Jowsey (NICR).

It was decided that the quantitative immuno-dot-blot method might be a suitable assay for modification and validation as an alternative pharmacodynamic assay in the clinical PARP inhibitor trial. The published method demonstrated linear chemiluminescence detection for up to 120,000 cells loaded, above this cell number there was saturation of the signal. Reliable signal detection in the linear range was demonstrated for 15,000-30,000 cells. These experiments used IARC 273 cells, a Epstein-Barr immortalised human B-lymphoblastoid cell line. Clearly far fewer cells were needed than the 6×10^5 cells for a reliable radiolabel PARP activity assay.

5.2 Poly(ADP-ribose) detection in L1210 and PBL cell preparations

Preliminary experiments were carried out to assess whether the established QC cells (L1210) and human PBLs could be reacted, blotted onto a membrane and polymer detected. These initial experiments were performed using a standard 96-well manifold rather than the custom-made 24 well manifold designed by Professor Bürkle.

Early experiments were performed using the isotonic buffer and permeabilisation buffer described in the published method (Pfeiffer, Brabeck et al. 1999). However it was found that the long permeabilisation incubation and further centrifugation required in this method significantly contributed to the background on the immunoblot (see section 5.4). The method which is described in detail in chapter 3 is the final validated protocol being used in the clinical trial. This method uses the same isotonic buffer as in the [³²P] NAD⁺ incorporation PARP activity assay, with the omission of DTT and a short permeabilisation with digitonin. In addition NAD⁺ was prepared fresh on the day of each experiment and added to the reaction buffer to ensure that there was no degradation of this substrate with storage and that it was present in excess in the reaction, the concentration of oligonucleotide in the final reaction has also been reduced compared to the published assay (Pfeiffer, Brabeck et al. 1999). These changes are also discussed in section 5.4.

5 ml of whole blood was taken from healthy volunteers and PBLs obtained by lymphopreparation. Either the whole blood prior the lymphopreparation or the washed PBLs were exposed to 100 nM AG014699 (1% DMSO only added to controls) for 15 minutes at 37°C. Whole blood was lymphopreped, the cells were permeabilised with the published permeabilisation buffer (10 mM Tris-HCL pH 7.8, 1 mM EDTA, 4 mM MgCl₂, 30 mM 2-mercaptoethanol supplemented with 0.015% (w/v) digitonin), then reacted in the presence of oligonucleotide and NAD⁺ for 6 minutes. The reaction was stopped by the addition of 400 µl ice cold 6.25 µM AG014361 and placing on ice. The cell density in the reaction was counted. The dot-blot 96 well manifold was set up, a suitable sized piece of filter paper and Hybond-N membrane were rehydrated in PBS then clamped into the manifold. 5000, 10000 and 20,000 cells from the reaction

mixture (diluted in PBS to a final volume of 50 μ l) were loaded into the wells, fixed and exposed to primary and secondary antibody as described in section 3.4.

After exposure to ECL for 1 minute the blot was exposed to film to see if PAR could be detected in human PBLs with 10H and whether inhibition with AG014699 was detectable. This experiment was repeated three times, a sample visual blot is shown below (figure 5.1). Triplicate samples of different cell numbers have been loaded, it can be seen that there is an increase in the amount of chemiluminescence detected as the cell number increases, and that this is reduced in the presence of the inhibitor.

Figure 5.1

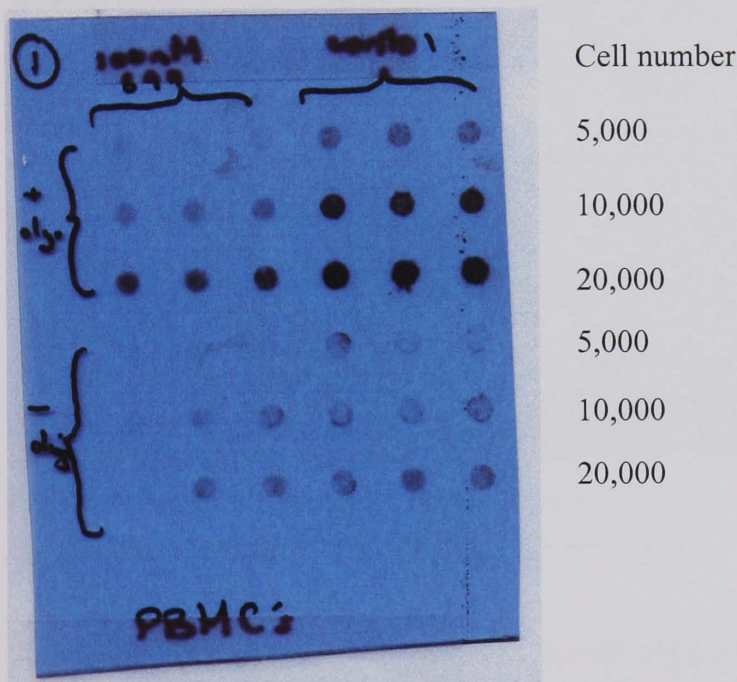


Figure 5.1 Scanned film showing detection of PAR in PBLs, in the presence or absence of 100 nM AG014699. Cell number loaded shown beside.

A similar experiment was performed using L1210 cells. This was done in parallel with a $[^{32}\text{P}] \text{NAD}^+$ incorporation PARP assay as part of the investigation into whether enzyme inhibition was preserved with frozen storage (section 4.4.2, figure 4.6). L1210 cells were exposed to 0, 10, 50 and 100 nM AG014699 for 15 minutes at 37°C, the inhibitor removed and samples frozen in medium + 10% DMSO. At the 8 week time point a small aliquot of the defrosted sample was removed prior to the $[^{32}\text{P}] \text{NAD}^+$ incorporation assay. This was washed, permeabilised and reacted as described

above. Varying cell numbers were again loaded onto the 96-well dot-blot manifold and exposed to primary and secondary antibody.

The results are shown in figure 5.2. These correspond to the 8 week data on figure 4.6. The increase in chemiluminescence with cell number and decrease with increasing concentration of inhibitor are evident, the change with inhibitor was most obvious when only 1000 or 2000 cells were loaded.

Figure 5.2

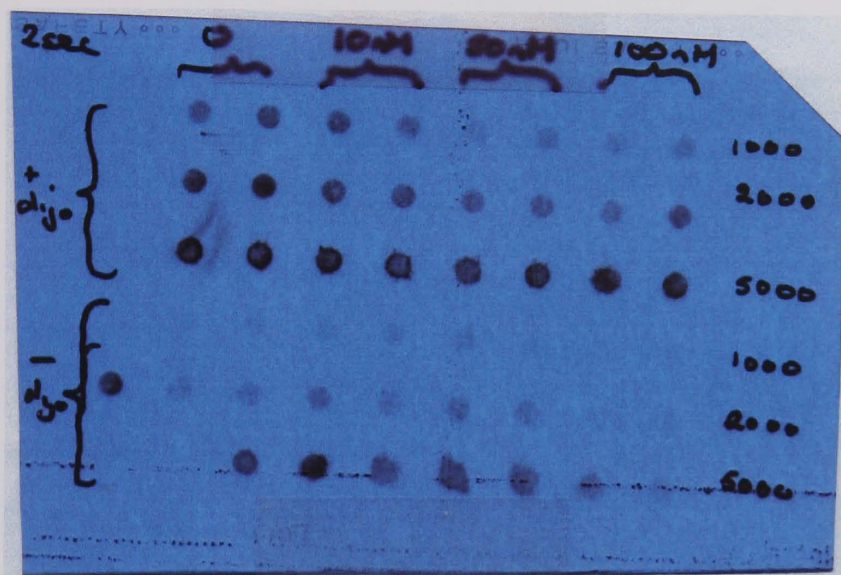


Figure 5.2 Scanned film showing detection of PAR in L1210 cells inhibited with varying concentration of AG014699 (shown across top of film), cell number on RHS.

Having verified that the technique worked with human PBLs and the proposed QC cell line additional work was undertaken to establish the quantification of these matrices using the digital chemiluminescence detector. The original report for the technique used a customised 24 well manifold with a blotting area of $>100 \text{ mm}^2$, allowing loading of a larger volume of cells. Pfeiffer and colleagues reported that permeabilised cells tended to cluster and the larger loading area allowed averaging of this clustering effect.

Initially a 24-well manifold was borrowed from Professor Bürkle's group; subsequently one was made in 18 mm Perspex by Forge House Group, Darlington (figure 5.3). The chemiluminescence detection apparatus initially used was a Fuji

LAS 1000 in Professor Bürkle's laboratory, later we purchased the LAS 3000 model which was used in later experiments and all clinical trial work. The image detected was digitised then interpreted using the Aida Image Analyser, version 3.28.001 software package. An example of the output obtained and defined as source data for the clinical trial is shown below (figure 5.4). The final numerical output is described as "densitometry", the camera detection unit takes a digital picture of the chemiluminescence from the exposed blot, this digital picture is imported into the Aida software as a grey scale image and the densities measured from this image.

Figure 5.3

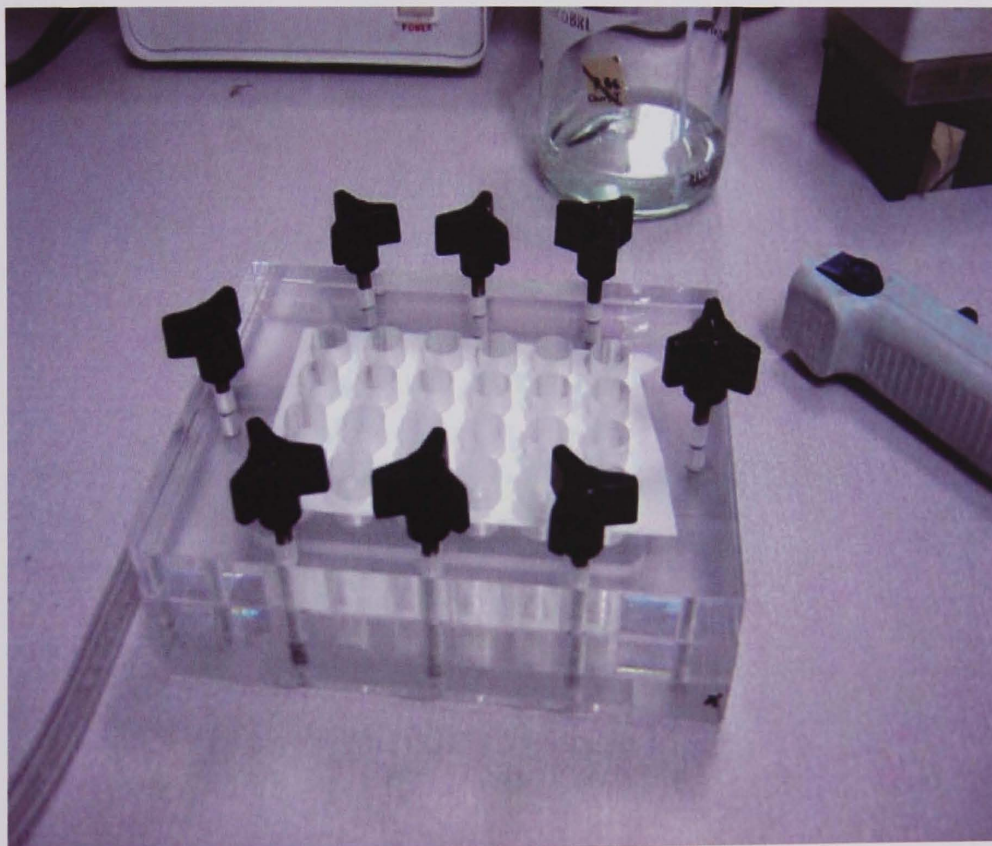
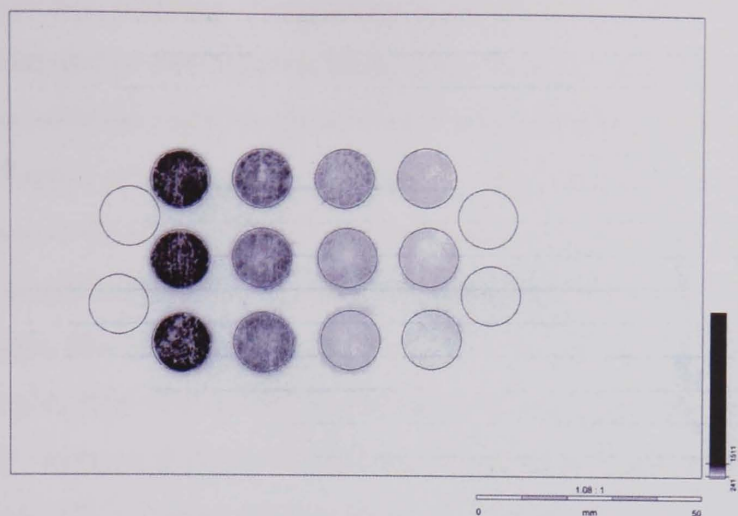


Figure 5.4



Region Report

No	Grp	Type	Area [mm ²]	Integral [LAU]	Integral-Bkg [LAU]	Integral/Area-Bkg [LAU/mm ²]
1	0		134.4	14271223.0	11384458.0	84724.39
2	0		134.4	14692623.0	11805858.0	87860.49
3	0		134.4	13835854.0	10649089.0	81484.32
4	0		134.4	9147751.0	6260986.0	46594.94
5	0		134.4	8681804.0	5795039.0	43127.32
6	0		134.4	8649163.0	5762398.0	42884.40
7	0		134.4	6626955.0	3740190.0	27834.90
8	0		134.4	5925250.0	3038485.0	22612.74
9	0		134.4	4769233.0	1882468.0	14009.53
10	0		134.4	4498424.0	1611650.0	11994.14
11	0		134.4	4213074.0	1326309.0	9870.54

Figure 5.4 Example of output from Aida software following exposure of Fuji LAS 1000. Serial dilution of QC cells, loading pattern being (left to right) 100,000, 50,000, 25,000, 12,500 in triplicate. 4 background areas also measured, see text.

The problem of clustering of cells and pooling of chemiluminescence was observed in early experiments. This was overcome by using two pieces of filter paper as a base to the Hybond-N membrane so that a tighter seal was obtained, and also by diluting small volume samples up to 400 μ l with PBS prior to loading.

Serial dilution of both L1210 cells and human PBLs confirmed that the chemiluminescence detected was proportional to the cell number loaded, a linear relationship observed up to 100,000 L1210 cells and 50,000 PBLs (figure 5.5). Data are mean and standard deviation of triplicate samples. Pfeiffer et al (1999) report similar results with the same detection system, with a linear relationship up to 120,000 IARC 273 cells. The upgrade to the Fuji LAS 3000 system meant that the arbitrary densitometry units were increased 50 fold because of the increased

sensitivity of the machine. All clinical trial samples are being analysed on the more sensitive machine. It must also be noted that the data in the graphs in figure 5.5 were analysed on two separate blots, using the Fuji LAS 1000 analyser. Given the multiple variables in any biological assay it is not possible to compare directly between assays in terms of absolute LAU readings. The purpose of these two separate experiments was to demonstrate the linear relationship between cell number and chemiluminescence detected. Whenever PBLs and L1210 cells were analysed on the same blot it is clear that the maximally stimulatable PARP activity in L1210 cells is higher than that in PBLs confirming the findings with the radiolabel assay. When the QC samples from serial patient samples were compared, corrected to LAU per 20,000 cells PBLs given a reading about 27% of the concomitantly analysed L1210 QC sample.

Figure 5.5

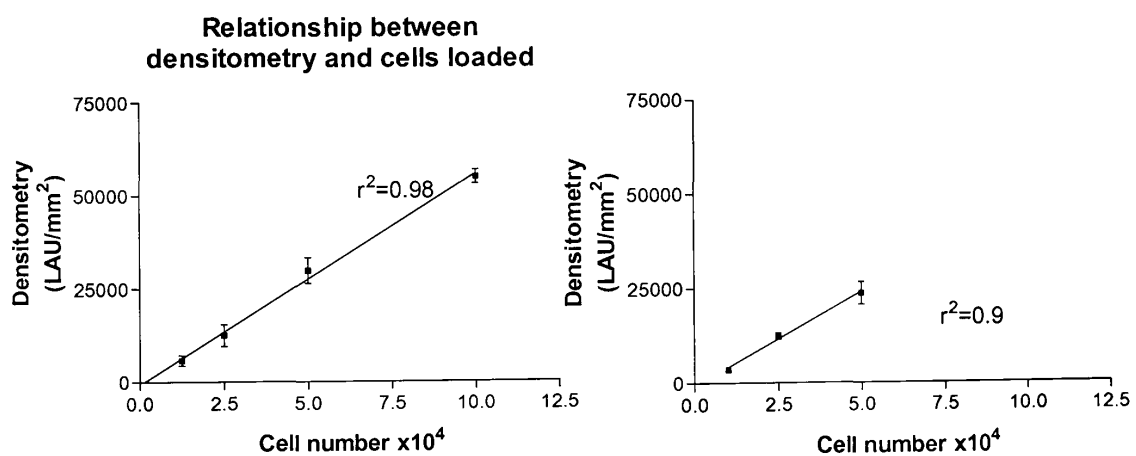


Figure 5.5 Means and standard deviation of triplicate samples of a serial dilution of L1210 cells (LHS) and PBLs (RHS).

These experiments suggested that the method was adaptable as a pharmacodynamic assay using far fewer cells and therefore more suitable for repeated blood sampling procedures. Further investigation was necessary however to establish a standard curve to allow quantification of the polymer formed, to investigate the nature of any background staining and to validate the assay to include QC samples.

5.3 Identification and characterisation of a poly(ADP-ribose) standard curve

In order to apply the immunoblot to clinical trial samples from sequentially treated patients it is necessary to be able to compare between assays performed on different days. The use of QC samples in parallel with the clinical samples allows demonstration that the individual assay had given a valid result and the validation of L1210 cells as QC samples for this assay is described below. It was also considered desirable that an absolute numerical value could be given to the maximally stimutable PARP activity in the PBLs in terms of the amount of polymer formed to allow such inter-patient comparison. The validated [³²P] NAD⁺ incorporation assay expresses results in terms of pmol NAD⁺ incorporated per million cells allowing comparison of different assays. It was hoped to establish a similar method of relating the measured chemiluminescence to an absolute amount of substance.

Standard curves from antibody detection of *in vitro* synthesised polymer have been reported (Affar, Duriez et al. 1998) showing a linear relationship between the detected chemiluminescence and the amount of polymer loaded. They reported the reliable detection of as little as 1 fmol ADP-ribose equivalent polymer using a digital imaging system.

A similar method has been applied to the quantification of this assay. Purified poly(ADP-ribose) polymer is available commercially from BIOMOL Research Laboratories. The polymer consists of branched and linear polymer with an average chain length of 25 ADP-ribose monomers (range 3-100). The concentration of the polymer is expressed in pmol ADP-ribose monomer equivalent and is supplied as a 10 µg/ml solution. 1 µg is equivalent to 2000 pmol ADP-ribose monomer. The product information sheet states that the product contains <0.1% ADP-ribose, and is completely degraded by poly (ADP-ribose) glycohydrolase (PARG).

A standard curve which included 6 values was generated, initially over the range 1-50 pmol monomer equivalent. It was suggested (Shah, Midha et al. 1992) that between five and eight concentrations will define a standard curve in many biological assays. The amounts of PAR loaded as each point on the standard curve were based partly on an estimate of the amount of polymer that would be formed by 100,000 maximally

stimulated PBLs if the mean amount of NAD^+ incorporated into one million PBLs is 24.5 pmol NAD^+ as determined using the [^{32}P] incorporation assay but also utilising a range that allowed several standard curves to be obtained from one batch of commercially produced PAR which is supplied in 100 μl aliquots

It is generally accepted that repeated freeze thaw cycles of the purified PAR polymer should be avoided to preserve its integrity. Therefore a standard curve was designed such that all polymers had two freeze thaw cycles only. On receipt of a new batch of polymer it was aliquoted appropriately and refrozen. When required an aliquot was defrosted and serially diluted on the day of experiment. Due to the limitations on number of wells on the blot apparatus one standard curve was set up for each blot of patient samples, and the number of standards limited to 6 as discussed above. This occupied one complete row on the 6 by 4 manifold. For trial samples all the samples from one patient in one complete 24 hour sampling period were loaded onto one blot.

Purified polymer was diluted to obtain a solution containing 50 pmol monomer equivalent in 100 μl solution in sterile water. This was serially diluted and a standard curve loaded with the values 50, 25, 12.5, 6.25, 3.125, 1 pmol monomer equivalent. These standards were loaded onto a membrane which was processed according to the SOP. The chemiluminescence signal detected was proportional to the amount of polymer loaded. To further investigate the relationship between chemiluminescence and [PAR] and to determine whether the standard curve could be used to both read off unknown results in terms of polymer formed, and then to compare these values with those from assays performed on different days the data from serial blots processed on different experimental days were compared. All standard curves were set up and loaded as described above. Comparison of single standard curves from immunoblots developed on separate days shows that there was a good correlation with the densitometry reading obtained indicating that the polymer is stable when aliquoted and stored as described above and gives reproducible results (figure 5.6). The best fit for the data generated from the standard curve is non-linear. Statistical analysis was performed by non-linear regression using a one-site binding model, which is reported as best modelling the binding of receptor to ligand, in this case secondary antibody to the 10H primary antibody bound to its polymer binding site. The equation used to calculate the non-linear curve fit (one site binding) is $Y=(B_{\text{max}} \cdot X)/[K_d+X]$. Where X

is the concentration of PAR, Y is the luminescence detected following exposure of the bound secondary antibody to ECL. B_{max} is the maximum chemiluminescence, the point where the gradient of the standard curve becomes zero with all PAR present bound to antibody complexes. K_d is the equilibrium dissociation constant, the concentration of PAR at which half is bound to antibody complex at equilibrium.

Figure 5.6

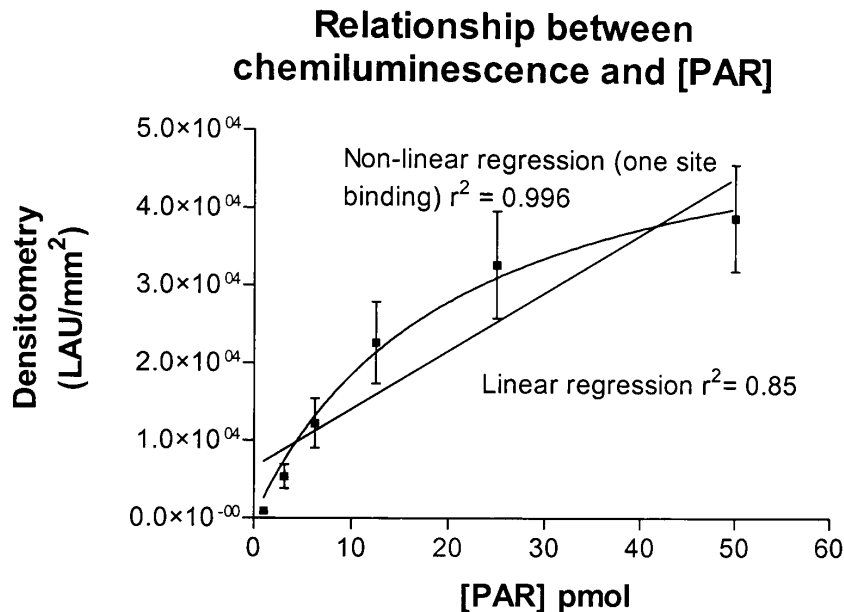


Figure 5.6 Means and standard errors of 11 repeats of PAR standard curve, each standard being run in a separate assay (Note: all data from cell dilution experiments and initial work on the standard curve used a Fuji LAS1000 digital camera. All subsequent experiments were performed with the more sensitive upgraded Fuji LAS3000, there is a consequent change in the range of the digitised output (LAU/mm²) with the scale on the y-axis being much larger).

Regression analysis of the standard curve generated over the range 1-50 pmol PAR suggested that the portion between 1 and 25 pmol was linear. There appeared to be a saturation of the antibody binding and chemiluminescence signal between 25 and 50 pmol. This was not due to the limit of detection of the digital camera; comparison of the densitometry values shown on the y-axis in figures 5.6 and 5.5 shows that more intense signals can be detected and there was not a saturation of detection with increasing cell number. The plateau effect on the standard curve may be due to the mechanism of antibody binding to polymer.

Initial analysis of patient PBL samples after treatment with a PARP inhibitor showed that significant PARP inhibition was caused even with low doses of the drug. Dose escalation decisions will be made based on the degree of PARP inhibition caused; therefore defining the lower limit of quantification was felt to be important. The range of the standard curve was therefore extended to include a “blank” or no polymer well to define the point where the standard curve cuts the y-axis, chemiluminescence signal equivalent to this being due to noise/background. The dilutions were altered so that most standards were at the lower end of the scale, the new standard curve being over the range 0-25 pmol monomer equivalent, with data points at 0, 0.04, 0.2, 1, 5 and 25. The same equation for best fit describes this curve.

Figure 5.7 gives the mean and standard error of 10 separate standard curves set up using this new protocol. These were the standard curves used to derive the PAR values measured from PBLs during the TemoCOMET study (see chapter 6). Each individual standard curve had a coefficient of regression (r^2) of 0.95 or greater. When the data was pooled together $r^2 = 1.000$, confirming that when analysed using a one-site binding non-linear regression model there was a good relationship between the concentration of PAR and measured densitometry on different days.

Figure 5.7

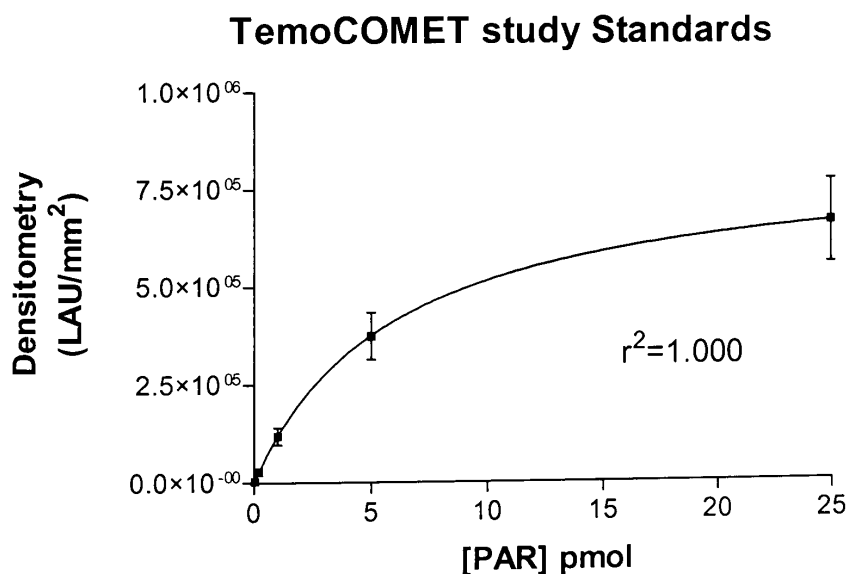


Figure 5.7 Pooled data from 10 individual standard curves run with patient samples during analysis of samples from TemoCOMET study. Mean and SEM.

There is a background chemiluminescence detected by the camera from the Hybond-N membrane itself. When the data was analysed 4 readings were taken of this background and the mean of these reading subtracted from the chemiluminescence detected from the area of each well of the manifold. To establish the lower limit of detection, the PAR standard was diluted further and compared with the blank standard well (400 μ l PBS) in two independent experiments. The practical work for these two experiments was carried out by Dr Chris Jones. Firstly the 5 replicate PAR samples of concentrations 0, 0.01 and 0.05 pmol PAR were blotted onto a membrane and analysed. The limit of detection was found to lie somewhere between 0.01 and 0.05, there was no significantly detectable difference between 0.01 and 0 ($p=0.225$, unpaired t-test, figure 5.8).

To further define the lower limit of detection 5 replicate samples over the range 0 pmol to 0.04 pmol in 10 fmol steps were loaded onto one blot and analysed in the usual way. The results are shown in figure 5.9 where it can be seen that polymer levels of fmol amounts can be distinguished from zero. Statistical analysis of the groups using one-way ANOVA to establish whether the mean values of the groups are statistically different gives $p < 0.01$ when comparing either all 5 groups or the three lowest groups, showing that the chemiluminescence detected for these low standards can be distinguished from zero. It was felt, on the basis of these two experiments, that one could be confident that the chemiluminescence from 0.02 pmol PAR could be reliably distinguished from zero.

Figure 5.8

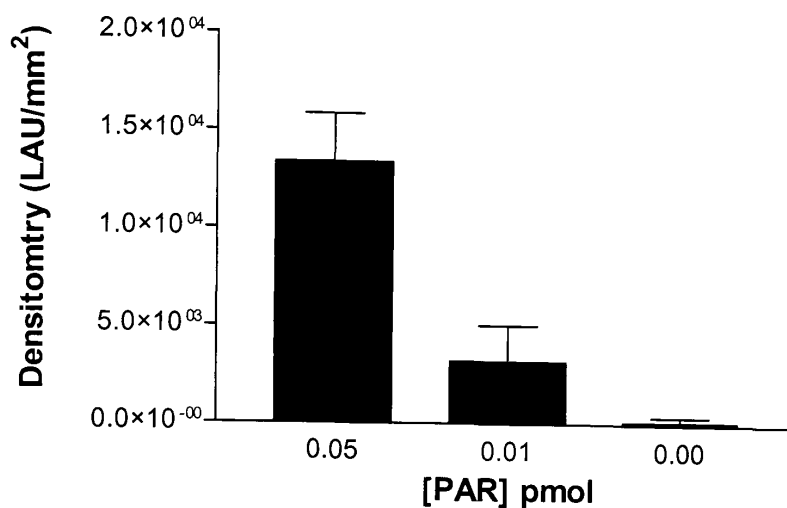


Figure 5.8 Mean and SEM of quintuplet samples of polymer, the difference between 0.01 pmol PAR and 0 is not significant ($p=0.225$, unpaired t test).

Figure 5.9

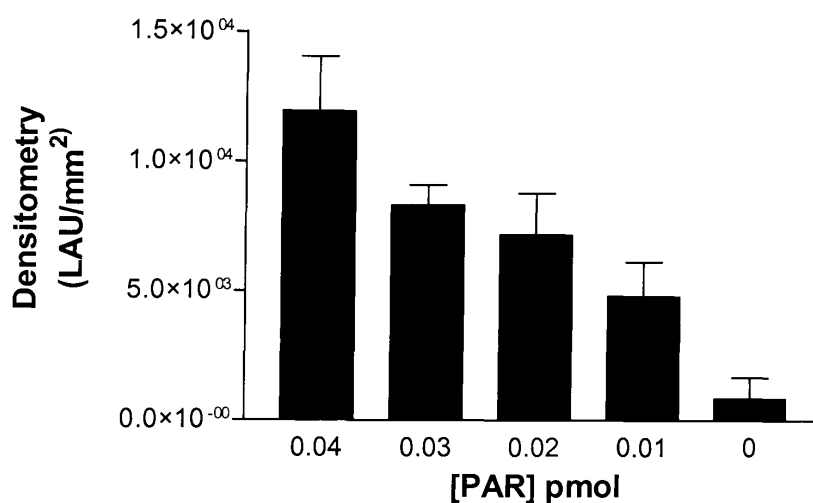


Figure 5.9 Densitometry readings from quintuplet samples, mean plus SEM shown.

Having established a standard curve which allowed the translation of chemiluminescence detected from the unknown samples into an amount of PAR polymer present it was necessary to establish how many human PBLs and L1210 QC cells needed to be loaded to detect a signal within the standard curve range. QC samples were loaded to demonstrate that a given blot has given a valid or “expected”

result. The amount of polymer formed within these cells when maximally stimulated for 6 minutes should be within the standard curve.

Likewise the baseline blood sample taken prior to the PARP inhibitor infusion should give the maximum value for that set of patient samples. This value should also lie below the upper limit of the standard curve to avoid extrapolation being needed. Serial dilution of volunteer PBLs or frozen L1210 cells and also the initial clinical samples studied using this assay (from the TemoCOMET study, chapter 6) suggest that between 5,000-10,000 L1210 cells will give values in the required range (mean PAR per 5000 L1210 cells = 22.2 ± 5.6 pmol, CV(%) = 25%, n=6) and that between 10,000 to 20,000 PBLs (mean PAR = 15.4 pmol/10,000 cells, range 5.6-20.0, n=6) should be loaded onto the blot.

5.4 Modifications to the assay protocol during validation experiments

The aim of the PARP activity determination within the clinical trial setting is to measure PARP inhibition following treatment with AG014699. This measure is obtained by quantifying the amount of polymer formed after a 6 minute period of maximal enzyme stimulation with oligonucleotide. However, the primary antibody against PAR, 10H, will bind to any polymer present within the permeabilised cell, not discriminating between that formed during the reaction period and that present due to existing DNA strand breaks. The existing polymer could potentially contribute to the signal when PBLs are obtained from patients who have received chemotherapy and consequent DNA damage. The effect of this endogenous polymer formation on existing strand breaks, whether caused by chemotherapy or cell handling was demonstrated in an experiment where a direct comparison was made between the radiolabel PARP activity assay and the immunoblot.

Exponentially growing L1210 cells were harvested, washed and then exposed to 0 nM (DMSO only), 10 nM, 50 nM and 100 nM AG014699 for 15 minutes at 37°C. The cells were then washed, permeabilised and assayed for PARP activity using both the [³²P] NAD⁺ incorporation and immunoblot assay. It was observed that, although there was a similar pattern of inhibition, the two curves were parallel, with that from the immunoblot lying above (figure 5.10). On the immunoblot samples were loaded

which had been “spiked” with an identical number of unreacted but permeabilised cells to give a measure of this endogenous PAR. When the mean of this background (non-stimulated) polymer signal was subtracted the two curves to come close together and gave very similar IC₅₀ values. (13.2 cf 12.7 nM)

Figure 5.10

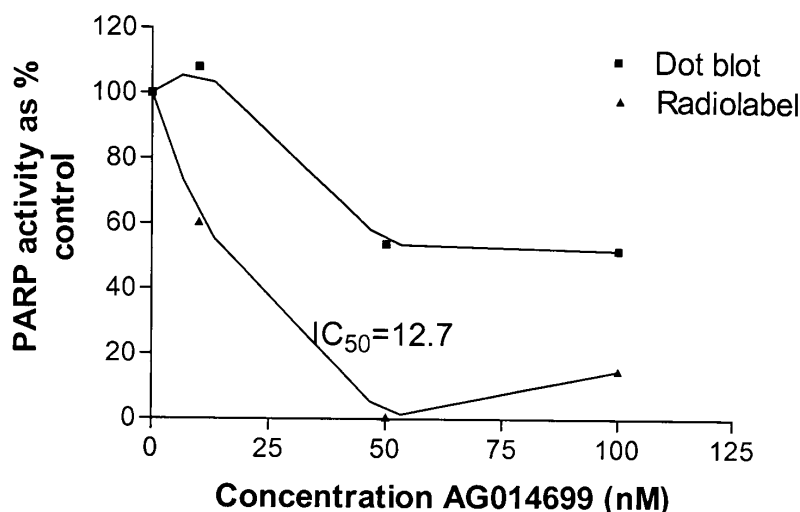


Figure 5.10 PARP activity as %control for parallel [³²P] NAD⁺ incorporation and immunoblot of L1210 cells inhibited with AG014699. % calculated from mean of triplicate samples.

The assay methodology was changed to include “T0” i.e. unreacted samples so that the contribution of this endogenous polymer could be evaluated and excluded from the measure of enzyme activity for all clinical samples. The T0 samples loaded were taken from the permeabilised cell suspension held on ice, and same number of cells loaded into the T0 wells as were placed in the reaction samples. Triplicate T0 samples were loaded from each cell suspension and the mean chemiluminescence detected from these subtracted from the reaction samples before calculation of PAR levels.

The initial description of the PARP immunoblot used an isotonic buffer containing 2-mercaptoethanol, and the permeabilisation step involved supplementation of this buffer with digitonin, incubation for 1 minute then a 10 minute centrifugation step at 0°C. Two problems were encountered when analysing either L1210 or PBLs with this

method. Firstly the degree of permeabilisation was variable and could be as low as 20%, and secondly there was a high background staining in the T0 cells. It was found that samples prepared using the same isotonic buffer as described in the [³²P] NAD⁺ incorporation PARP assay and utilising 0.15 mg/ml digitonin permeabilisation method showed ~100% permeabilisation and background T0 staining was much lower. It is presumed fewer DNA strand breaks are introduced during cell handling with the removal of the prolonged 0°C centrifugation step. The assay method was changed to adopt digitonin permeabilisation and to use the alternative isotonic buffer.

The other significant adaptation to the assay method was reduction in the concentration of oligonucleotide in the reaction. In the published immunoblot PARP activity assay the concentration of oligonucleotide in the final reaction volume was 50 µg/ml (or 1.95 mM). The amount present in the [³²P] NAD⁺ incorporation assay was much lower (2.5 µg/ml) and an experiment was undertaken to investigate whether decreasing the amount of oligonucleotide in the reaction mixture would affect the amount of polymer produced.

Frozen QC cells were defrosted, washed and permeabilised with digitonin. The reaction tubes were set up with a range of oligonucleotide concentrations added to the tubes in a final reaction volume of 100 µl in isotonic buffer. 5000 permeabilised L1210 cells were added to each reaction tube, the reaction carried out for 6 minutes before stopping with excess inhibitor. The contents of the tubes were loaded onto a membrane and immunoblotted in the usual way. The results (mean and standard deviation, n=3) are shown in figure 5.11. There was no suggestion that reducing the amount of oligonucleotide present compromises PARP-1 ability to form polymer.

Figure 5.11

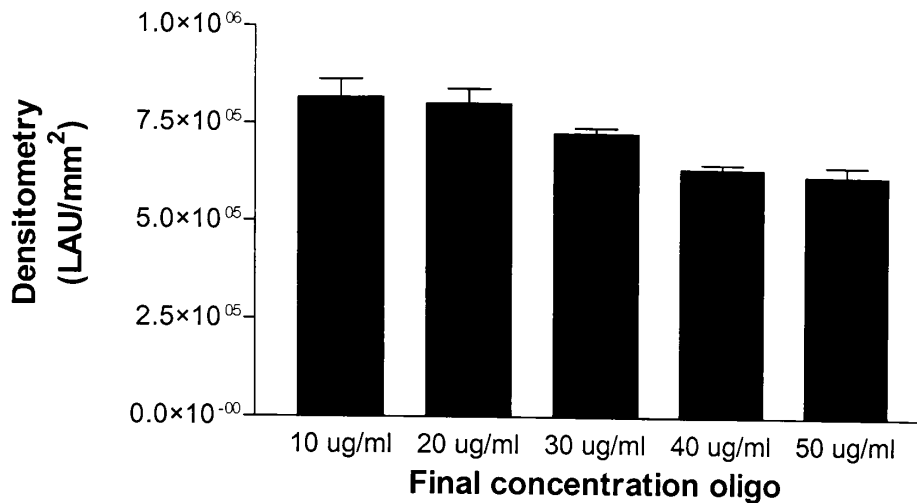


Figure 5.11 Relationship between densitometry and concentration of oligonucleotide in reaction. Mean + SD, n=3.

Pfieffer and colleagues (Pfieffer, Brabeck et al. 1999) described the prototype assay using a reaction buffer which contained 1 mM NAD⁺. This buffer was made in advance and stored over a number of weeks at 4°C (Dr Ragen Pfieffer, personal communication). When planning to establish an assay that was to be validated to GLP-like standards and produce data that could be used for regulatory purposes there were concerns about the stability of NAD⁺ in this solution. To be able to measure maximal PARP-1 activity the reaction solution must contain NAD⁺ at a concentration which is at or near the K_m for the enzyme. The protocol was modified to that described in section 3.6 so that NAD⁺ was made up fresh on the day of reaction from frozen anhydrous stocks, the molarity calculated from the optical density and sufficient added so that the final concentration in the reaction mix was 350 μM. Use of a 7 mM NAD⁺ stock allowed as little as 5 μl to be added to the reaction mix, giving a greater flexibility on the volumes of cell suspension that could be added, keeping the final volume at 100 μl. This was particularly useful if a low cell harvest was obtained and the permeabilised cell suspension more dilute than anticipated.

The reaction phase of the assay was carried out in a water bath at 26°C. The reaction solution containing oligonucleotide, NAD⁺ and reaction buffer was allowed to come to this temperature to ensure optimal reaction conditions. Permeabilised cells were held on ice throughout the assay to prevent autolysis. Since the cell suspension

represents 40% of the reaction mix cells were routinely pre-warmed to 26°C for 7 minutes prior to addition so as not to cool the reaction. There was concern that the pre-warming might contribute to an increased background chemiluminescence from pre-formed polymer.

This potential effect was investigated using L1210 cells. Frozen L1210 cells from the prepared QC stocks were defrosted, washed and permeabilised. The permeabilised cells were counted and cell suspension diluted such that 10,000 cells would be added to the reaction in a volume of 40 µl. Triplicate reaction tubes were set up containing oligonucleotide, NAD⁺ and reaction buffer to a total volume of 60 µl or isotonic buffer only as a control. All tubes were warmed to 26°C. One aliquot of permeabilised cells was held on ice until addition to the reaction volume or isotonic control, and one portion of cells was pre-warmed for 7 minutes prior to addition to the reaction to allow temperature equilibration.

The immunoblot was loaded with control cells which had been held on ice throughout the experiment (T0) and the 4 different experimental preparations, ice cold cells – blank reaction, ice cold cells – full reaction mix, pre-warmed cells – blank reaction, pre-warmed cells – full reaction mix. The results are shown in table 5.1. There were three findings, firstly there was minimal PAR formation due to endogenous ADP-ribosylation at existing strand breaks when cells were maintained on ice. Secondly that pre-warming of the cells is essential if a true measure of maximal PARP-1 activity is required. There was a 25% reduction in the maximally stimulated value when pre-warming was omitted. Finally the pre-warming step did not increase the endogenous PAR *per se* (pre-warm isotonic control).

Table 5.1

Cells	Reaction mixture	Densitometry (LAU/mm²) per 10,000 cells
Ice cold	T0	156±131
Ice cold	Isotonic only	353±485
Ice cold	Full reaction mix	11461±990
Pre-warm	Isotonic only	84±137
Pre-warm	Full reaction mix	15161±561

The result found in this experiment was confirmed by Dr Chris Jones using both freshly grown and frozen stocks of L1210 cells, no difference being observed between the fresh or frozen samples. Therefore, in frozen samples too, pre-warming does not have a major impact on the endogenous PAR formation. Pre-warming of cell suspensions is essential as loading of ice cold cells results in a 25-40% reduction in PAR formation compared to pre-warmed cells.

The results of all the experiments described in this section were all taken into account during the evolution of the final validated standard operating procedure for the immunoblot PARP activity assay.

5.5 Immunoblotting for tumour/tissue samples

In part 2 of the trial tumour biopsies will be taken before and after AG014699 administration not only to determine PARP inhibition of the target tissue but also to determine any correlation with PARP inhibition in PBLs from the same patient. Any pharmacodynamic assay therefore needs to be feasible using both experimental matrices, PBLs and homogenised tissue.

Studies were undertaken to investigate whether the immunoblot technique could be used to detect PAR formed by a tumour/tissue homogenate, and to establish the dilution of the homogenate required so that the chemiluminescence detected would lie within the standard curve.

The experimental protocol was used as described in section 3.8. 50 μ l of homogenate were added to 5 μ l 7 mM NAD⁺ and 45 μ l reaction buffer in all experiments. Oligonucleotide was not necessary in the reaction as explained above (section 4.5.1).

The principle of the assay is the same as for the determination of PARP activity in permeabilised cells in that it measures the amount of polymer formed in a fixed period by the PARP enzyme in the homogenate in the presence of added substrate (NAD⁺). The reaction is stopped with excess AG014699 and the product detected as described

in section 5.2. Pre-existing polymer, formed in response to DNA damage in the presence of endogenous NAD^+ , is corrected for by the subtraction of the measured chemiluminescence from an identical volume of un-reacted homogenate (T0). The data is expressed in terms of pmol monomers of ADP-ribose detected in polymer per mg protein added to the reaction.

All experiments undertaken to establish and investigate the use of the immunoblot with homogenised tissue were performed using homogenised mouse liver as a surrogate sample. It was not ethical or possible to get tumour biopsies to perform this validation work. The established quality control (QC) standards (L1210 cells) will be run with each assay so that individual test run acceptance criteria can be defined as well as enabling inter-assay comparison.

Mouse liver was snap frozen in liquid nitrogen and maintained at -80°C until homogenisation. This mimics the treatment of tumour samples. When thawed prior to homogenisation the wet weight was determined and the specimen homogenised in 3 volumes of isotonic buffer giving an initial dilution of 1 in 4. This preparation was serially diluted to obtain 1 in 100, 1 in 1,000 and 1 in 10,000 dilutions. These were incubated with reaction buffer as described above and blotted. Triplicate samples were loaded, including triplicate T0 (unreacted homogenate) from each dilution. As can be seen in table 5.2, there was a high background chemiluminescence signal measured in the T0 samples as expected. This is due to endogenous polymer formation due to DNA damage induced by the homogenisation procedure. This background signal could be kept to a minimum by ensuring that, except during the pre-warm phase and reaction phase of the assay all tissue homogenate was kept on ice to prevent enzyme activity (personal observation, data not shown).

Subtraction of the T0 endogenous staining gives a clearer picture of the amount of additional polymer that can be made by the enzyme in the presence of NAD^+ at the dilutions investigated (column 3, table 5.2). There did not appear to be a linear relationship between the dilution of homogenate and chemiluminescence signal over this range of dilutions, suggesting that there may be saturation of the signal at higher concentrations.

Table 5.2

Homogenate dilution	Densitometry (LAU/mm ² x10 ⁵)		
	Endogenous PAR	Total PAR	PAR formed during reaction
1:100	10.22	18.18	7.96
1:1,000	3.22	6.53	3.31
1:10,000	0.15	0.32	0.17

To establish the optimum dilution of homogenate, such that PAR formation fell within the range of the standard curve, serial dilutions of frozen mouse liver homogenate were reacted as described above and the standard PAR polymer curve loaded onto the blot. 1 in 100, 1 in 1,000 and 1 in 2,000 dilutions were set up. The mean PAR formed (after subtraction of background) was measured and is shown below (figure 5.12)

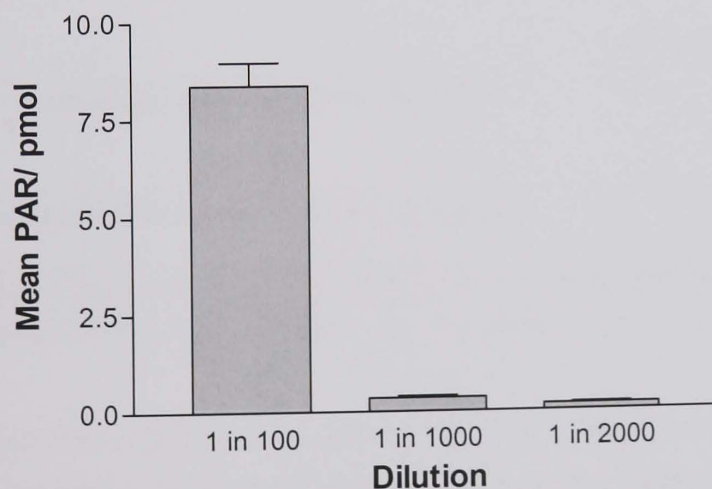
Figure 5.12

Figure 5.12 Mean + SEM of triplicate readings of serially diluted homogenised liver.

The absolute values obtained for PAR amount are shown in table 5.4. Although the 1 in 1000 dilution and 1 in 2000 dilutions gave readings at the lower end of the standard curve 1 in 1000 was selected as the initial dilution to be tried with any tumour samples. Xenograft experiments using the [³²P] NAD⁺ incorporation assay had shown that much higher PARP activity was seen in xenografts compared to normal mouse

liver (1230 pmol NAD⁺/mg protein cf 39.0 pmol NAD⁺/mg protein), this was also observed with xenografts analysed with the immunoblot (Chris Jones, personal communication). Preliminary results from the TemoCOMET study (data in table 5.4, trial discussed in chapter 6) had suggested the measured PARP-1 activity was significantly higher in human tumour samples than in normal tissue when compared on a per mg protein loaded basis. It was therefore felt safer to opt for a higher dilution rather than to risk all baseline samples being without the range of the standard curve.

Table 5.3

Preparation	Mean PAR ± SEM (pmol)
Mouse liver 1 in 100	8.37 ± 0.59
Mouse liver 1 in 1000	0.3 ± 0.04
Mouse liver 1 in 2000	0.16 ± 0.02

Table 5.4

	Liver	Tumour
	Mean ± SD	Mean ± SD
Radiolabel assay (pmol NAD⁺/mg protein)	39 ± 9 (n=9)	1229 ± 26 (n=3)
Immunoblot (pmol PAR/mg protein)	26 ± N/A (n=1)	828 ± 599 (n=9)

Summarised results from individual tumours/livers analysed by the different PARP-1 assays.
n=number livers/tumours studied, each measured in triplicate.

Previous experiments using the [³²P] NAD⁺ incorporation PARP activity assay had established that PARP-1 enzyme activity within tissue cells was stable with frozen storage, and also that PARP inhibition was maintained with storage (see sections 4.5.3 and 4.5.2). It was felt unnecessary to repeat these studies with the immunoblot assay.

As part of the parallel laboratory studies, which are being performed along side the PARP inhibitor clinical study, nude mice bearing SW620 human colon cancer xenografts were treated with a single intra-peritoneal injection of AG014699 and sacrificed at various times after doses. Groups of 3 mice were treated. Xenograft

homogenates from these mice were diluted to 1 in 1000 or 1 in 2000 and an immunoblot performed as per the protocol. It was clearly possible to measure the degree of PARP inhibition in these samples, which varied with dose (figure 5.13). These data are generously supplied by Dr Chris Jones.

Figure 5.13

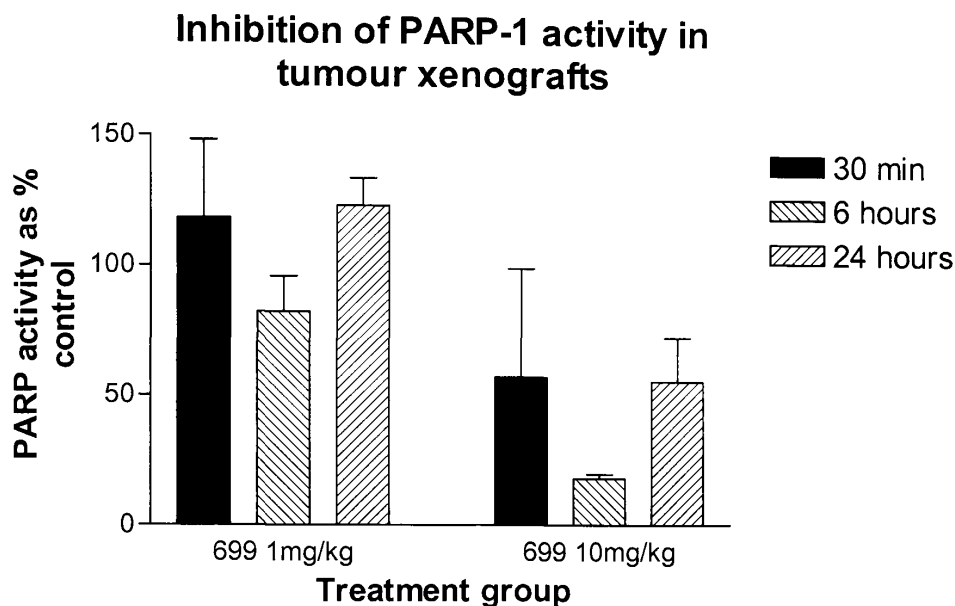


Figure 5.13 PARP activity expressed as a % that measured in matched controls in SW620 xenografts treated with AG014699. Mean + SEM of three tumours, each measured in triplicate

Having established that the immunoblot could be used as a PARP-1 activity assay in both human PBLs and tissue samples further experiments were undertaken to elucidate the nature of the antibody binding. These are described below.

5.6 Investigation of the nature of 10H antibody binding/chemiluminescence detection

10H is a monoclonal antibody which is reported to bind to poly(ADP-ribose) polymer 15-20 ADP-ribose monomers in length. The published characterisation of the antibody has been discussed in section 5.1. The objective whilst developing this assay has been to accurately and reliably obtain a measure of PARP-1 activity in the presence or absence of inhibitor. The measure of activity is quantified by allowing the

enzyme to synthesise polymer in a maximally stimulated state for a defined period of time.

There will be some polymer present in cells, particularly if there is any DNA damage (either due to cytotoxic drug or cell handling procedures). The T0 samples loaded in triplicate for each cell suspension allow for any antibody binding and detection of this background polymer to be excluded from the quantitative assay results.

The contribution of non-specific binding of either the primary or secondary antibody to the membrane or the some component within the cells loaded to the chemiluminescence detected was investigated. Any non-specific binding will be a possible cause of inaccuracy in quantification of unknowns. The potential contribution of the secondary antibody to this was investigated by setting up two identical blots by loading L1210 cells which had been inhibited with AG014699 and a standard curve. One blot was incubated in primary antibody over 48 hours whilst the other was stored in PBS. The blots were then returned to the same container for the secondary antibody incubation and washes. After staining with ECL there was no detectable pattern of staining coinciding with the location of the manifold on the secondary only blot.

By carefully lining up the marked areas of the identical blots it was possible to compare the digitally measured chemiluminescence from 5 wells on the intact blot where the signal was strongest (those loaded with L1210 cells) with the same areas on the secondary only blot. Despite being certain that these would be areas where there were cells present, indicated by the dense chemiluminescence on the complete blot, there was very little detection from the secondary-only blot. It was calculated that for these wells any contribution to the densitometry reading over and above background from non-specific signal due to secondary antibody was $0.18 \pm 0.03\%$ (mean \pm SD, $n=5$).

The signal detected from background areas (areas not loaded with cells) was very similar for both blots described above and represents luminescent pixels detected from the nitrocellulose membrane. The low background densitometry suggests that non-specific binding of either antibody to the nitrocellulose membrane is low. To

correct for any such binding the mean of three background areas is automatically subtracted from all densitometry readings. With the evolution in assay methodology during the validation process and despite the introduction of the more sensitive Fuji LAS 3000 this background detected remains a small contribution to the overall densitometry. When the mean background figure for 12 successive experiments was compared to the chemiluminescence detected from 12.5 pmol PAR the background contribution to the chemiluminescence was in the order of 6%.

The nature of the T0 background signal, i.e. endogenous polymer, was examined by adding a known number (100,000) of permeabilised cells to each standard. Antibody binding to a known amount of polymer was compared in the presence or absence of these cells. The chemiluminescence measured in the spiked standards was higher than that from the control standards but the correlation between chemiluminescence and concentration of PAR was unchanged (table 5.5, $r^2=0.95$ and 0.96 , non-linear regression one site binding). This suggested that the primary/secondary antibody complex detected by ECL in the cells was binding to a consistent feature in those cells which was the same antibody interaction as the known standard, i.e. the polymer.

Table 5.5

[PAR] standard (pmol)	LAU x10 ⁵		
	Standard alone	Standard + cells	Cells alone
1.5	0.03	0.7	0.7
3.125	0.1	1.2	1.2
6.25	0.3	1.7	1.4
12.5	0.6	1.8	1.3
25	0.9	2.6	1.7
50	0.9	2.4	1.5

The specific background binding of the primary antibody to any existing polymer (endogenous, i.e. T0 samples) was further investigated by exposing permeabilised fresh L1210 cells to purified PARG enzyme (2 mU/ μ l) in the presence and absence of excess PARP inhibitor. Purified PARG was obtained from BIOMOL research laboratories Inc (catalogue N^o SE-179, Lot N^o P6321). 2.5 μ M AG01-4699 or an

equivalent 0.25% DMSO alone as control was added to aliquots of 100,000 permeabilised L1210 cells on ice (final total volume 400 μ l). The addition of AG014699 was to prevent further polymer formation during the exposure to PARG. The permeabilised cells were warmed to 37°C and 6 mU PARG added. 1 U PARG is defined as the amount of enzyme which will produce 1 nmol ADP-ribose per minute of reaction at 37°C in a solution of 10 μ M [³²P] PAR. No oligonucleotide was added. After incubation for 5, 10 or 30 minutes the cells were placed back on ice and blotted.

The cells where PARP-1 had been inhibited prior to warming to a temperature at which mammalian enzymes are functional gave a very low signal for polymer. This low signal was further reduced by approximately 30% after incubation with purified PARG, providing evidence that species bound by 10H is degraded by PARG and therefore likely to be PARP. It proved much more difficult to significantly reduce the much higher signal in non-inhibited control cells with the commercial PARG preparations available.

5.7 Evaluation of PARP knockout cells or animal tissue using immunoblot

The gene coding for PARP-1 has been successfully inactivated in mice and PARP-1^{-/-} BalbC mice are readily available. In addition there are established cells lines from these mice which can be studied in vitro. This provides a further mechanism for investigating the nature of the chemiluminescence staining detected using the immunoblot. The other members of the PARP enzyme family are intact in the PARP-1 knockout animals/cells, so poly(ADP-ribose) can be formed in response to the correct stimulus. PARP-2 is the only other PARP enzyme in the cells known to be activated by DNA damage, however PARP-2 activity is not stimulated by blunt ended oligonucleotide, the activator in the permeabilised cell assay (de Murcia, personal communication).

In the first series of experiments PARP-1^{-/-} cultured mouse fibroblasts were grown in Eagles medium and harvested at a cell density of 8 x 10⁶/ml. L1210 cells were used as a positive control as there were no available stocks of PARP-1^{+/+} cells. The cells were harvested, washed and permeabilised with 0.15 mg/ml digitonin as described before. Triplicate samples were set up including + **oligo** (oligo, reaction buffer,

NAD⁺) - **oligo** (NAD⁺, reaction buffer and PBS control) and **inhibited** (NAD⁺, oligo, reaction buffer, with AG014699 stop solution added prior to permeabilised cells). Following cell warming and the 6 minute reaction period blots were loaded including a PAR standard curve, T0 samples in triplicate (permeabilised cell suspension only, pre-warmed then replaced on ice) and each reaction tube. 100,000 cells were loaded per replicate; larger numbers were used because of the expected low levels of polymer formation by the PARP-1^{-/-} cells. It was accepted that 100,000 L1210 cells would take the chemiluminescence out of the range of the standard curve, however the known linear relationship between cell number and chemiluminescence at this number of cells meant a valid measure of polymer formation could be made and enabled comparison of like numbers of cells for the positive and negative groups.

The data from the PARP-1^{-/-} and L1210 cells are shown in table 5.6. Mean and standard error of triplicate samples are given. It can be seen that the levels of chemiluminescence detected from PARP-1^{-/-} cells were very low when compared to similar data from the positive controls. There was some background (T0) endogenous polymer present, it would appear that there was some increase in the polymer present when the cells were warmed to 26°C for the reaction, the differences between the +oligo, - oligo and inhibited columns were not statistically significantly different from one another (p=0.09, one way ANOVA). Polymer in these cells would largely be formed by PARP-2, which is not stimulated by blunt ended oligonucleotide. In this experiment the amount of polymer formed by 100,000 PARP-1^{-/-} cells in the presence of oligonucleotide was 2.5 ± 1.2 pmol; in the absence of oligonucleotide it was 1.2 ± 0.5 pmol/100,000 cells with a similar amount being made in those cells where the PARP-1 inhibitor was added to the reaction mix prior to the addition of the cells (1.7 pmol/100,000 cells). This compared to an average polymer formation of 22.0 pmol by 5000 L1210 positive control cells (440 pmol/100,000 L1210 cells) in the presence of oligonucleotide, indicating <1% of the measured polymer formation was due to PARP-2 activity.

Table 5.6

	LAU/mm ² /100,000 cells	
	L1210	PARP-/-
T0	50697	1941
+oligo (-T0)	146719 ± 53122	3964 ± 1426
- oligo (-T0)	73218 ± 99499	1539 ± 627
+699 (-T0)	-5228 ± 18313	1889 ± 1176

These preliminary experiments suggested that the polymer detected using the immunoblot was largely formed by PARP-1 when stimulated by oligonucleotide. Studies using the PARP-1^{-/-} knockout model were extended to include a comparison of PARP-1 activity in mouse PBLs and homogenised liver from matched groups of PARP-1^{-/-} mice and PARP-1^{+/+} mice treated with saline vehicle or AG014699. These experiments were performed as part of the validation process for the immunoblot PARP activity assay in homogenised tissue, and also to establish whether PARP activity and inhibition could be measured in mouse PBLs after lymphopreparation.

PARP-1^{-/-} and PARP-1^{+/+} male and female mice were obtained from Gilbert de Murcia and housed under standard conditions. Groups of three PARP-1^{-/-} male and female mice were sacrificed by cervical dislocation, then immediately exsanguinated by cardiac puncture. A total of 4-5 ml of whole blood was obtained from the group, pooled and then diluted 1 to 1 with PBS and lymphoprep using the method described for human blood in chapter 3. The PBLs were frozen in medium + 10% DMSO as described in the method. Groups of three PARP-1^{+/+} male and female mice were treated with a single intra-peritoneal injection of AG014699 dissolved in sterile water (or vehicle control) 30 minutes prior to sacrifice. Blood was obtained and prepared as described above. Murine PBLs are smaller than human PBLs, and mouse-specific lymphoprep is available. However, for reasons of expediency and consistency the human lymphoprep was used to prepare the mouse cells. The difference in density between the two lymphopreparations is small, and adequate cell harvests were made with the human preparation.

From one animal in each group the liver was removed and snap frozen for later homogenisation and assay.

The results from the mouse PBLs for all groups is shown in figure 5.14, all values are expressed in terms of pmol PAR formed by 10^6 cells in the 6 minute reaction time. Mean and SEM of triplicate readings are given. It can be seen that in the control PBLs from PARP-1^{-/-} mice there was again little polymer formation when stimulated with blunt ended oligonucleotide. The measured polymer formation appeared higher in the male animals when compared to the females in all treatment groups. This observation is, however, based on a small sample size and did not reach statistical significance. There was no evidence of a variation of PARP activity in human PBLs with gender. Inhibition of PARP-1 with AG014699 was demonstrated, being more profound in male compared to female animals at both doses of AG014699.

Figure 5.14

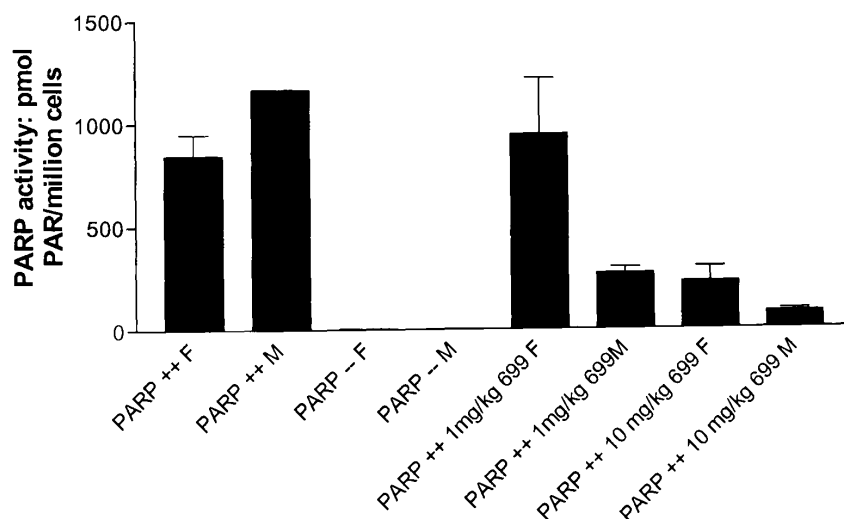


Figure 5.14 Polymer formation in mouse PBLs in PARP ^{-/-} animals and PARP ^{+/+} animals treated with AG014699. Mean and SEM of triplicate samples expressed as per million cells

Frozen livers were defrosted, weighed and homogenised as described in section 3.7. An initial dilution of 1 in 1000 was made with isotonic buffer. However the PARP activity in the inhibited livers was undetectable with this standard dilution. The samples were re-assayed using a 1 in 100 and 1 in 50 but once again PARP activity was undetectable. The results from the standard 1 in 1000 dilution are shown in figure 5.15.

Figure 5.15

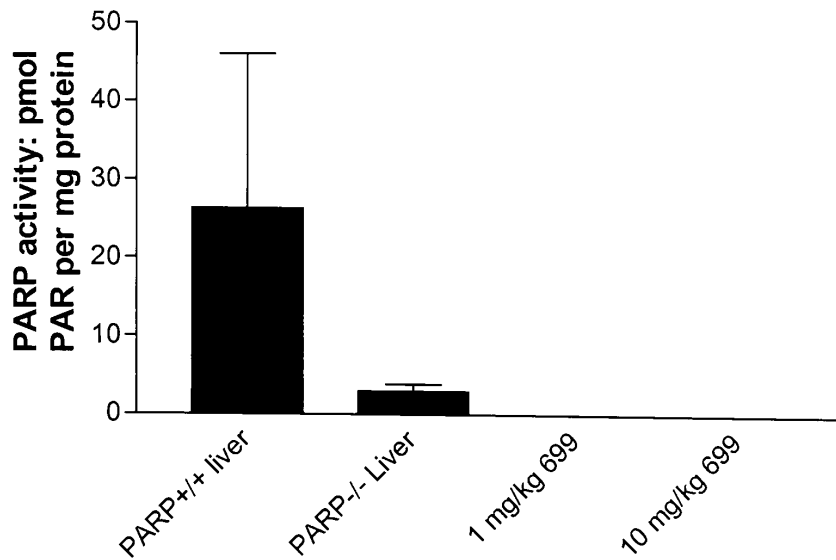


Figure 5.15 Mean and SEM of triplicate reading from homogenised liver from PARP -/- and PARP +/+ animals (+/- 699)

Data are expressed in terms of pmol PAR formed in the reaction period per mg protein in the homogenate. Polymer formation was detectable in the homogenised liver from PARP-1^{-/-} animals using the immunoblot assay. This value represents polymer formation during the reaction period as background T₀ (endogenous polymer) chemiluminescence was subtracted in the usual manner. Homogenisation introduces multiple DNA strand breaks, both single and double; during the reaction period PARP-2 will be active in the presence of substrate (NAD⁺) and an activation stimulus. This explains why in these knock out animals there was more polymer formation in the homogenised liver than was detectable in permeabilised PBLs where the stimulus to PARP activity is exogenous blunt ended double stranded oligonucleotide. The amount of polymer formed during the reaction period (3.0 pmol/mg protein) was similar to that detectable in the unreacted homogenate (6.0 pmol/mg protein) which had been held on ice during preparation, warmed to 26°C for 7 minutes, and then replaced on ice. It is accepted that the warming period will allow polymer formation using endogenous NAD⁺, hence the exclusion of this polymer by the subtraction of the T₀ samples. In the case of the PARP-1^{-/-} liver homogenate, the amount polymer formed during the reaction period is low and the background polymer detected similar, indicating that low PARP activity overall is seen in these

cells compared to PARP-1^{+/+} animals where the background polymer formation was 7.3 pmol/mg protein and that formed in the presence of added NAD⁻ was 26.3 pmol/mg protein. All these observations are preliminary because of the small number of animals studied.

It was unexpected that the degree of PARP inhibition in liver would be so great in the animals treated with AG014699 at 1 mg/kg and 10 mg/kg. Previous experiments studying the degree of inhibition in human tumour xenografts in these animals had not showed such dramatic inhibition at this time point. This marked inhibition, greater than that observed in the PBLs could be due to first pass metabolism of the AG014699. The drug was given as an intra-peritoneal injection; the liver will therefore be the first organ to be exposed to inhibitor and would be expected to have the most marked PARP-1 inhibition. It may also reflect the observed lower PARP activity in normal liver compared to tumour xenografts. This observation is given support by the finding that normal human liver biopsies have lower poly(ADP-ribosylation) capacity than biopsies from hepatocellular carcinomas (Shiobara, Miyazaki et al. 2001).

5.8 Discussion

The results presented in this chapter describe the development and subsequent validation of an immunoblot PARP activity assay for use with human samples, both PBLs and homogenised tumour. The established and validated radiolabel PARP activity assay was initially considered for use in the PARP clinical study, however there were problems with this assay which have been discussed in chapter 4 (section 4.7). It was because of these problems that a robust assay using fewer PBLs was sought. The issues pertaining to validation of a pharmacodynamic biological assay were also examined in section 4.7. During development of this new assay an attempt has been made to address the principles to be used for establishing a valid method defined in the 1990 AAPS International Workshop report (Shah, Midha et al. 1992); see discussion of chapter 4. The way each of these principles has been addressed is discussed below.

- a) Detailed Standard Operating Procedures have been produced for all procedures.
- b) The nature and degree of non-specific antibody binding, both of the primary and secondary antibodies has been investigated. Levels of this are low, and have been excluded from the calculation of polymer formed by the subtraction of background chemiluminescence before generation of the standard curve and reading of results.

The major difference between this and the [^{32}P] NAD^+ incorporation PARP activity assay is that the primary antibody (10H) will bind to any polymer present, whether formed during the reaction period, during cell preparation or prior to blotting on the membrane. Attempts have been made to reduce this endogenous background by maintaining all cells on ice except during the warming and reaction phases, and changing the permeabilisation technique to minimise cell handling. The loading of identical numbers of unreacted cells allows exclusion of any endogenous polymer from the analysis of enzyme activity thus reducing the influence of these variables. Without these T0 samples there would be much greater for potential variation between samples, in particular when considering PBLs. The lymphopreparation method introduces some DNA damage, the fact that during the clinical trial this will be done at three centres, by different personnel and with potential variation in the time whole blood is held on ice before processing would mean that the scope for variation in endogenous polymer would be very high and it is important to exclude this.

- c) The pharmacodynamic effect which is measured by the immunoblot PARP activity assay is the number of pmol polymer formed during the 6 minute reaction period over background endogenous polymer. The assay, therefore, directly measures the product of PARP activity and is specific for PARP-1 alone (PBLs stimulated with oligonucleotide) or with a minor contribution from PARP-2 (homogenates). The activity of the drug which the assay has been designed to assess is inhibition of the PARP-1 enzyme and thus a reduction in the ability to form polymer.

The nature of 10H binding is well established in the literature. Attempts have been made to examine this further in the immunoblot assay by the addition of additional PARG to alter the balance between polymer formation and breakdown, and also by

the use of PARP knockout animals and cells. It would appear that the primary antibody binds to purified polymer in a reproducible way, and that it binds to the reaction product formed when permeabilised cells are incubated with a powerful PARP-1 activator (oligonucleotide) and the PARP enzyme substrate (NAD⁺). It is therefore concluded that the major ligand-receptor binding species detected with chemiluminescence is poly(ADP-ribose) bound to 10H antibody. This conclusion is supported by the work of Affar et al (Affar, Duriez et al. 1998) who demonstrated the detection of purified poly(ADR) using a similar immunoblot using both 10H and a polyclonal antibody against PAR, L896-10.

e) One issue for concern with the immunoblot assay is the degree of variation between assays. There was reasonable reproducibility with replicate samples performed on the same day within the same assay, and between standard curves but considerable variation could be seen between different assay runs studying activity in similar cell samples (for example QC cells). This highlights again the difficulty of standardising a biological assay, Miller et al (Miller, Bowsher et al. 2001) state that “detection of a macromolecular analyte generally occurs in a complex biological milieu... methods tend to have poorer batch-to-batch reproducibility. During analysis of clinical trial samples attempts have been made to reduce factors which typically affect reproducibility (listed in Huber 1998), by defining a detailed SOP with consumable sources prescribed, one operator for all samples and use of a water bath to avoid room temperature variation. It is impossible to exclude all external variables, different personnel who prepare the blood samples, transport of these samples may take varying times and inter-patient variability is an unknown quantity at any given dose of the PARP inhibitor. It is recognised that inter-assay variation is the greatest source of imprecision in immunoassays (Findlay, Smith et al. 2000). The AAPS Bioanalytical Methods validation workshop reached a consensus opinion that minimal acceptance limits for ligand-binding assays should be set at 30% for accuracy (mean bias) and precision with greater limits being permissible if agreed upon by the end users of the data.

f) A standard polymer curve has been established which is reproducible and allows quantification of the results in terms of pmol polymer formed. The validation

of the assay has been audited by Cancer Research UK and by Pfizer GRD and found to be suitable for regulatory purposes and to be performed to GLP-like standards.

The established QC cell line (L1210) has been validated for use in this assay, the more sensitive nature of the assessment means far fewer cells need to be blotted, only 5,000-10,000 cells being required to produce polymer within the limits of the standard curve. PARP-1 activity in tissue homogenates again can be measured with the assay, a 1 in 1000 dilution of the homogenate being required rather than 1 in 40 for the radiolabel PARP activity assay.

Choice and definition of the reference standard are known to have a large impact on the integrity of bioanalytical data (Miller, Bowsher et al. 2001) and it is suggested that the reference sample be procured from a certified reference standard or commercial supplier. The standard curve should contain 5 to 8 points, excluding blanks, with single or replicate samples and covering the entire range of expected concentrations (Shah, Midha et al. 1992; 2001). The mathematical model used to describe the standard curve should be that which best describes the fit, rather than enforcing a linear model. It is recognised that the concentration-response curve for a typical ligand-binding assay is seldom linear throughout its range, but more frequently hyperbolic (Findlay, Smith et al. 2000; Miller, Bowsher et al. 2001). In the immunoblot assay the standard curve is of the appropriate number of points, it is reproducible between assays (see figure 5.9). The number of L1210 QC cells and human PBLs which should be applied to give PAR formation within the standard curve has been defined. When samples fall outside these limits the blot will be repeated with an appropriate number of cells.

In conclusion, an immunoblot method for the detection and quantification of poly(ADP-ribose) has been developed and validated. An appropriate standard curve has been identified, QC samples established and the working range of the assay defined.

Having established this pharmacodynamic assay potentially suitable for use with clinical samples whilst the PARP inhibitor clinical protocol was still under development it was felt that it would be valuable to be able to confirm the assay

validation using some clinical samples. At an early stage of the PARP inhibitor trial protocol development the possibility of running a short pilot study prior to the main trial protocol was discussed with the PARP development team. It was felt that such a trial would be valuable for a number of reasons, and a phase II protocol using full dose temozolomide alone in patients with metastatic malignant melanoma was submitted to the Local Research Ethics Committees of the three centres who would be participating in the main clinical study. Eligible patients would agree additional blood tests on the first cycle for analysis of PARP activity and DNA damage and to two tumour biopsies under local anaesthetic. It was hoped that the trial would address the following points:-

- 1 It would allow the confirmation of PARP activity assay validation with analogous clinical samples
- 2 It would give comparative data on DNA damage after temozolomide with and without a PARP inhibitor
- 3 It would allow the three centres to work together before committing to a clinical trial with complex pharmacokinetic and pharmacodynamic sampling schedules.

This phase II preliminary study was conducted in 12 patients with malignant melanoma, the further rationale for this trial and the results are discussed in chapter 6.

Chapter 6

Clinical and Laboratory results for a Phase II mechanistic study of temozolomide in advanced malignant melanoma

6.1 Introduction

During the protocol development and preclinical evaluation of the PARP inhibitor clinical candidate, AG014699, it was felt that a clinical study evaluating both DNA damage and PARP activity after a standard dose of temozolomide in patients would provide valuable information which could be used to interpret the results of the First-in-Human PARP inhibitor study. The effect of temozolomide alone on the two pharmacodynamic endpoints defined for the trial had not been determined and a phase II study was designed to address these issues.

The mechanism of action of temozolomide has been discussed in chapter 1 of this thesis. It is an orally available mono-functional DNA alkylating agent which is used to treat gliomas and malignant melanoma. Temozolomide is rapidly absorbed and undergoes spontaneous breakdown in the plasma to form the active species MTIC (monomethyl triazene 5-(3-methyl-1-triazeno)imidazole-4-carboxamide). This forms a number of DNA methylation products including O⁶-methylguanine, N⁷-methylguanine and N³-methyladenine. There is evidence that the cytotoxic lesion is O⁶-methylguanine (Stevens, Hichman et al. 1987) which is repaired by ATase (Margison, Koref et al. 2002); N⁷-methylguanine and N³-methyladenine lesions rapidly being repaired by BER (as discussed in chapter 1). It is thought that the potentiation of temozolomide cytotoxicity observed in preclinical work with potent PARP-1 inhibitors is largely due to the inhibition of BER increasing the level of cytotoxicity due to incomplete processing of N⁷-methylguanine and N³-methyladenine lesions.

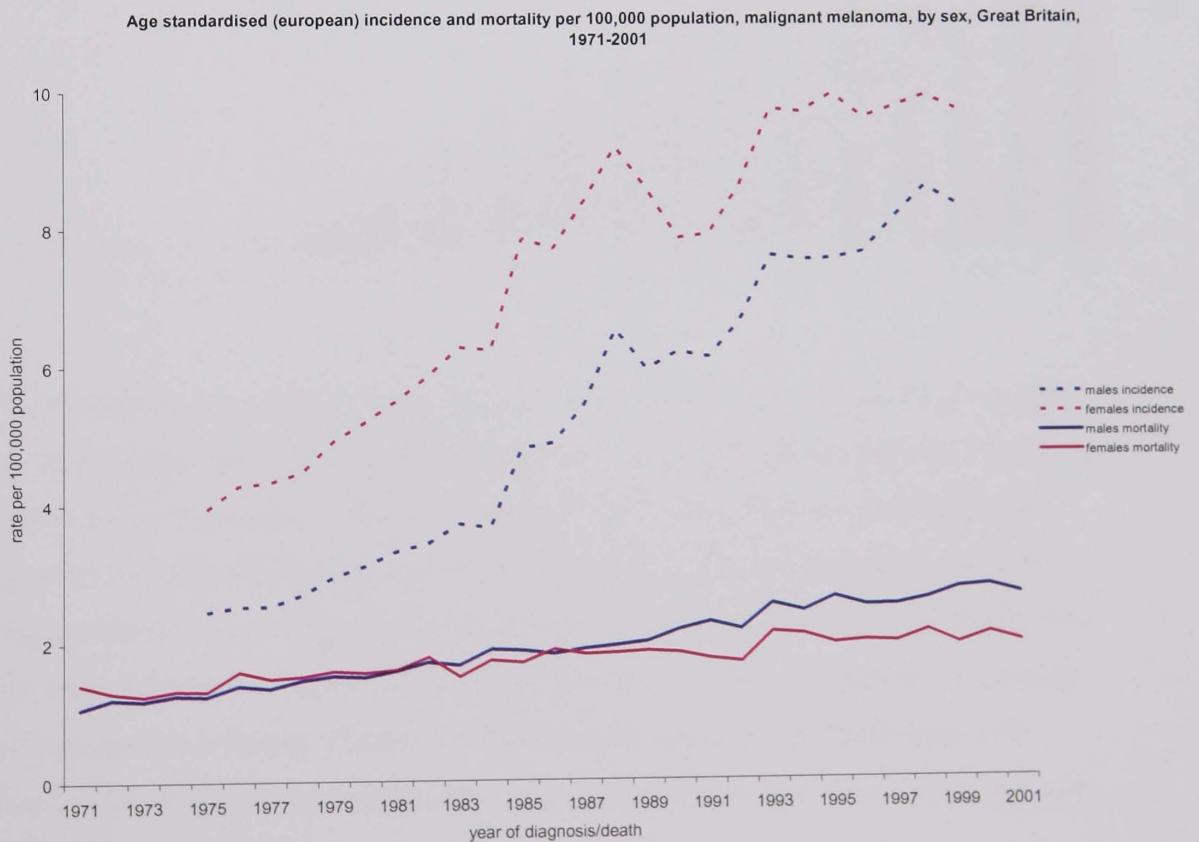
The First-in-Human study of a PARP inhibitor will be in combination with temozolomide and a primary endpoint of the study includes the demonstration of inhibition of PARP-1 in human PBLs and tumour samples. It is not known what the effect of dosing with temozolomide alone or indeed any cytotoxic agent has on basal cell PARP activity. This enzyme is widely expressed throughout human tissues. It would not be expected that chemotherapy-induced DNA damage would significantly alter the PBL's ability to form poly(ADP-ribose) but there was no data from human studies in the literature available. A secondary PD endpoint of the First-in-Human study is the measurement of DNA strand breaks. It was also felt useful to evaluate the

DNA damage caused by temozolomide in human PBLs as a surrogate tissue, but also in tumour samples if possible. It was planned that this work would be carried in The Cancer Research Laboratories in Oxford under the supervision of Dr Mark Middleton.

To address these issues a small phase II study in patients with metastatic malignant melanoma was designed and submitted to the Local Research Ethics Committees at the same three clinical centres cooperating during the First-in-Human PARP inhibitor trial. The study was entitled “Temozolomide induced DNA damage in Advanced Malignant Melanoma: A phase II study”. The study was approved by the local ethics committees and accrual began in June 2002.

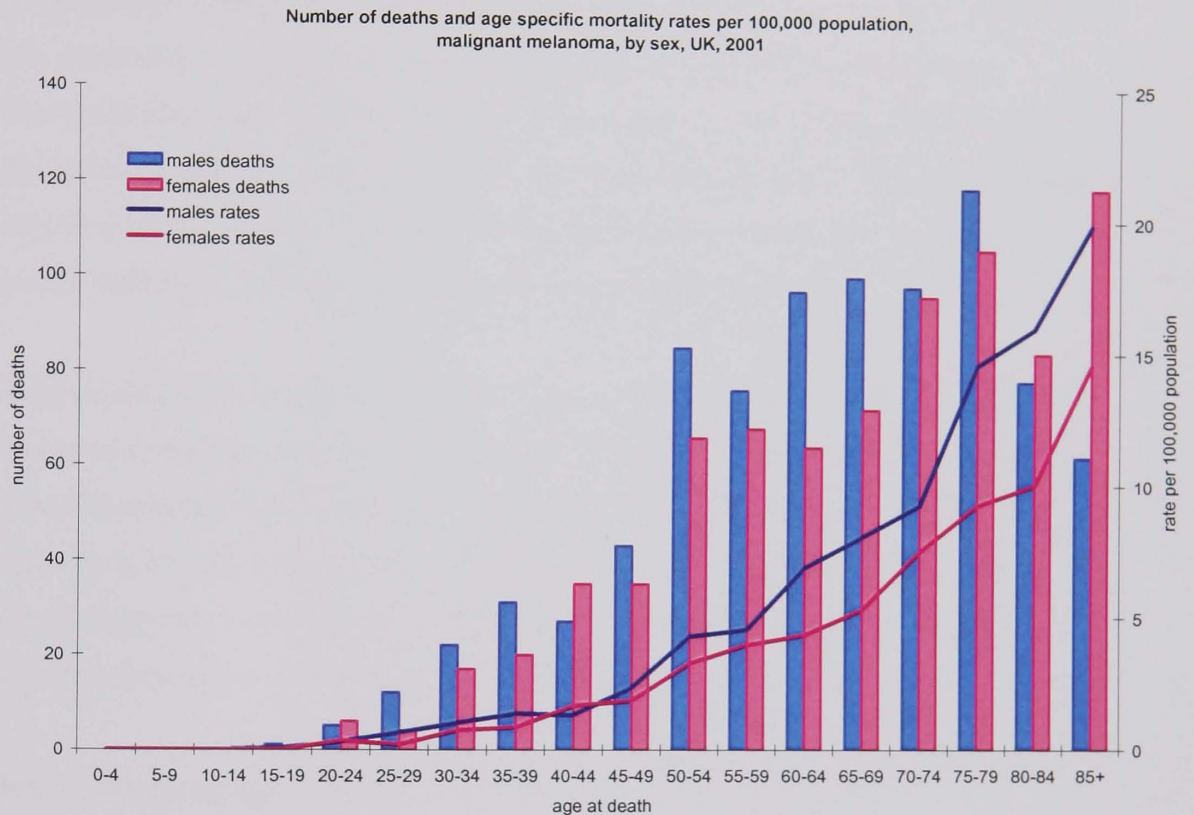
Malignant melanoma is becoming increasingly more common as seen in figure 6.1. The disease is more common in women than in men (57% versus 43%), the incidence rising with age. Despite this it is the third most common cancer diagnosed in those aged 15-39 (source www.cancerresearchuk.org).

Figure 6.1



It is estimated that 1600 lives a year are lost due to this disease, 1% of all cancer deaths. The number of deaths and age specific mortality in the UK for 2001 is shown in figure 6.2. Survival and risk of recurrence after primary resection are strongly associated with thickness of the tumour at the time of diagnosis. 5 year survival in primary melanomas less than 1.5 mm thick is greater than 90% whereas 5 year survival in tumours thicker than 3.5 mm is approximately 45%.

Figure 6.2



There has been some improvement in the 5 year survival over the last 15 years, this has been largely due to improved awareness of the disease allowing primary resection to be curative in a larger number of cases. There is some evidence that high dose adjuvant interferon following resection of high risk malignant melanoma increases progression free and overall survival (Kirkwood, Ibrahim et al. 2001) but this therapy has yet to be widely adopted in the United Kingdom. Treatment options for patients with advanced metastatic disease are limited, with palliative chemotherapy with dacarbazine (DTIC) or temozolomide being the standard therapy, with response rates in the order of 15-20%.

The trial reported in the chapter offers patients treatment with a standard regimen for malignant melanoma, all the patients were aware that therapy would not be curative and at best would improve the length and quality of their survival. Patients with asymptomatic brain metastases were allowed to enter into the study. There is some evidence that temozolomide will cross the blood brain barrier more effectively than the parent drug DTIC (Stevens, Hickman et al. 1987). There is, however, no published clinical data to support this proposal. The phase II study of temozolomide in malignant melanoma included 4 patients with brain metastases, a partial response was seen only in one patient who had a small solitary brain lesion (Bleehen, Newlands et al. 1995), patients with brain metastases were excluded from the phase III study (Middleton, Grob et al. 2000). It was felt that patients with brain metastases should not be excluded from this trial if their performance status was adequate to justify palliative chemotherapy because of this theoretical benefit

Trial coordination, patient recruitment and analysis of PARP activity in both PBLs and tumour biopsies were undertaken as part of this MD thesis. Analysis of DNA strand breaks following treatment were performed by Anna Olsen in Oxford, and changes in O⁶-alkylguanine-DNA alkyltransferase (ATase) levels analysed by Dr Geoff Margison in Manchester. Data from these experiments are included for completeness and to aid discussion of the study results.

6.2 Study Design

6.2.1 Protocol design

The study was a non-randomised trial involving 12 patients with advanced malignant melanoma who had had no prior therapy for their metastatic tumour. All patients received temozolomide at a dose of 200 mg/m²/day for 5 days of a 28 day cycle. Response to therapy was assessed every 2 cycles and patients were treated until progression. Inclusion criteria included age ≥18years, histologically proven advanced metastatic melanoma, assessable disease, and adequate haematological and biochemical parameters. Patients could have received previous radiotherapy or adjuvant therapy with biological agents, must use an acceptable method of birth control and give written informed consent to all study procedures. Patients with uncontrolled vomiting such as to make treatment with an oral agent impractical or

those who had received a biological therapy with 4 weeks of starting treatment were excluded. In addition subjects who were known to be pregnant or breast feeding, or HIV positive were not entered.

The primary objectives for the study were defined as:-

- 1 To assess DNA damage (O⁶ and N⁷ methylation of guanine and single strand breakage) in tumour biopsies and peripheral blood lymphocytes after a single 200 mg/m² dose of temozolomide
- 2 To determine PARP activity and ATase activity in these tissues after dosing

The secondary objectives were stated as:-

- 1 To determine tissue DNA repair capacity by observing changes in repair protein level over time
- 2 To relate biological measures to clinical outcomes (toxicity and tumour response)

6.2.2 Sampling schedule and methods

To achieve these objectives patients were consented to undergo a complex schedule of additional blood tests on days 1 and 2 of the first cycle of treatment only. Patients were assessed clinically on day 1 of every cycle and attended for weekly full blood counts and toxicity monitoring throughout the study. In addition, the first 9 patients treated agreed to two tumour biopsies under local anaesthetic, one prior to starting treatment and a second biopsy either 4 or 24 hours after the first dose of temozolomide. Repeat radiological assessment or clinical measurement by the same method as that performed at baseline was performed every two cycles. All toxicity was graded according to CTC criteria (version 2.0).

At each major sampling time point (baseline, 4-6 and 24 hours) 55 ml of whole blood was drawn and divided between the various analysis sets, 5 ml being placed in pre-chilled heparinized tubes and processed for temozolomide PK, and the rest being anticoagulated in pre-prepared EDTA vacutainers and processed as described in table 6.1. Patients treated in Newcastle had temozolomide PK samples taken at the three PD time points only. The six patients treated in Oxford had a more extensive

temozolomide pharmacokinetic sampling schedule (pre, 30, 60, 120, 240, 360 and 1480 minutes after treatment) and the same PD sampling.

Table 6.1

Sampling time	Pre-treatment	4-6 hours	24 hours
PARP activity	10 ml whole blood diluted with PBS and lymphopreped as described in section 3.2		
COMET assay	20 ml whole blood lymphopreped without dilution in PBS, stored in PBS + 10% DMSO at -80°C		
ATase assay	10 ml whole blood lymphopreped without dilution in PBS, stored as a washed cell pellet at -80°C		
DNA concentration	10 ml whole blood frozen at -80°C		
Temozolomide PK	Plasma from 5 ml blood acidified in phosphoric acid and stored at 20°C in pre-weighed containers		

Following sample preparation at the clinical sites all temozolomide PK samples and PBLs for PARP activity were transferred on dry ice to NICR, Newcastle, for processing. COMET samples were transferred to Oxford and ATase and DNA concentration samples to Manchester.

Where tumour biopsy specimens were available these were collected from the theatre into sterile ice cold PBS. The sample was kept on ice and processed for storage as soon as possible. The specimen was divided into two using a sterile scalpel blade, and one half wrapped in aluminium foil, labelled and snap frozen in liquid nitrogen before storing at -80°C for PARP activity analysis. The other half of the sample was minced using crossed scalpels in a small volume of ice cold medium + 10% DMSO + 20% foetal calf serum. The suspension was centrifuged to precipitate larger particles and the supernatant removed and frozen at -80°C. These samples were transferred to Oxford for analysis using a COMET assay to assess the number of strand breaks formed after treatment with temozolomide. Data from these samples was extremely variable due to the problems with isolating intact tumour cells from the melanoma tumour biopsy. Once it became clear that it would not be possible to perform this

assay on these samples the final few patients were recruited to the study without mandatory biopsies.

6.2.3 Laboratory methods

PBLs and tumour samples for PARP activity analysis were analysed as described in sections 3.6 and 3.7. Temozolomide plasma concentrations were measured using a published High Performance Liquid Chromatography method (HPLC) (Shen, Decosterd et al. 1995). The pharmacokinetics of the drug have been characterised by non-compartmental analysis with the calculation of the area under the plasma concentration time curve (AUC).

6.2.2.1 Sample analysis performed outside NICR

The assays for DNA concentration, DNA methylation and COMET analysis were performed by co-investigators on the clinical trial. Brief summaries of the methods are given below although the practical work for these assays was outside the scope of this thesis.

COMET analysis

The COMET assay is an established method for measuring DNA damage within individual cells (Olive, Chan et al. 1988). Single cells are suspended in a thin layer of agarose, lysed and an electrical current applied across the slide. Alkaline conditions in the assay allow separation of the DNA strands so single strand breaks can be estimated. Negatively charged DNA is drawn towards the anode by electrophoresis, the distance moved being proportional to the size of the fragment of DNA.

Fragmentation of the DNA due to strand breaks therefore results in greater migration in a given time and the “comet” or “tail” is formed ahead of the embedded nucleus.

The amount of DNA damage can be expressed either in terms of Olive Moment, the product of tail length and the proportion of total DNA in the tail, or simply as % tail DNA (Fairburn, Olive et al. 1995).

The method used was a modification of that described by Olive et al (Olive, Chan et al. 1988) with assay conditions optimised for measuring substantial DNA damage after chemotherapy. Stored PBMCs/tumour suspensions were thawed, diluted 1:4 in phosphate buffered saline (PBS), and mixed with an equal volume of 2% low melting

point agarose at 40°C. One ml of the suspension was layered onto polylysine coated slides (BDH Laboratory supplies; Poole, U.K.), lowered into lysis buffer (0.3M NaOH/ 1M NaCl/ 0.1% N-lauroylsarcosine, pH 11.5) and left in the dark for one hour to lyse cells and remove most of the proteins. Salt was removed with 2 x 30 minute washes in 0.3M NaOH/ 2mM EDTA. This wash time provides 1 hour DNA unwinding time which has been shown to be important in the detection of DNA damage. The slides were electrophoresed at 40 mA for 25 minutes in the lysis buffer at pH 11.5 and the DNA was stained with 1% propidium iodide and examined under a confocal microscope (MRC 600, excitation wavelength 480 nm, magnification x 100). The area and mean pixel intensity of the head and the tail of the comets were measured to determine the percentage DNA in the tail for each individual cell. In each patient sample a total of 50 cells, from 2 slides, were measured and the mean DNA damage determined from all the cells examined.

DNA methylation (O^6 methyl guanine)

The method used has been previously published (Middleton, Lee et al. 2000). Briefly DNA was isolated from whole blood using a modified phenol extraction method. DNA concentration was estimated as below. Various quantities of DNA, made up to a standard final concentration with calf thymus DNA, were incubated with recombinant human ATase under substrate limiting conditions at 37°C for 1 hour before the addition of an excess of [3 H]methylated DNA substrate and further incubation for 30 minutes. The radioactivity transferred to protein was plotted against sample DNA concentration and the concentration required to halve the radioactivity transferred determined. This was compared with the corresponding value with a standard DNA preparation to determine the sample O^6 -methylguanine content, which was expressed as fmole/mole deoxyguanosine.

ATase measurement

The method involved measuring [3 H]methyl group transfer to ATase protein from [3 H]methylated DNA substrate under protein limiting conditions (Lee, Thatcher et al. 1991). The substrate provided was diluted to a concentration of 100 µg/ml and 100 ml incubated at 37°C for 30 minutes with varying amounts (up to 200 µl) of tissue extract. At least three different volumes were used for each extract. In each case, the

total volume was made up to 300 μ l with bovine serum albumin (BSA) 1 mg/ml in buffer I. After incubation 100 μ l BSA 10 mg/ml in were added with perchloric acid (100 μ l of 4 M acid and 2 ml of 1 M). The mixture was incubated at 75°C for 50 minutes to hydrolyse the DNA substrate. Protein was recovered by centrifugation at 2100g for 10 minutes at room temperature. The resulting pellet was resuspended in 4 ml 1M perchloric acid and centrifuged at 2100g for a further 10 minutes at room temperature. The second pellet was resuspended in 300 ml NaOH 10 mM and 3 ml Ecoscint scintillation fluid added (Mensura Tech) before thorough mixing. Samples were counted over 5 minutes each on a Rackbeta (LKB) scintillation counter. Counts per minute were plotted against the volume of extract used and specific activity calculated from a minimum of three points on the linear part of the curve. Activity was expressed as fmoles [³H]methyl transferred to protein per μ g DNA in the extract.

DNA concentration measurement

The quantitative fluorescent DNA stain Hoechst 33258 was prepared as follows: 1 ml Hoechst 33258 (bisbenzamide; Sigma, UK) 1 mg/ml diluted 1 in 100 in double distilled water and added to 1 ml 10x TNE buffer (100 mM Tris, 10 mM EDTA, 2 mM NaCl, pH 7.4) and 9 ml double distilled water. The DNA content was measured by adding 2 μ l of extract to 2ml of dye solution and measuring the fluorescence in a TKO 100 mini-fluorometer, which was calibrated using a calf thymus DNA standard with each use. Measurements were taken in duplicate for each sample, with the machine reading giving an estimate of DNA concentration in μ g/ml.

6.3 Patient demographics and clinical data

6.3.1 Patient demographics

12 patients with advanced metastatic malignant melanoma were recruited. 5 female and 7 male patients were treated with temozolomide. The mean age of the patients was 57, and the predominant site of metastatic disease was in the liver. All patients had undergone previous surgical excision of their primary tumour and had subsequently developed metastatic disease. The median time to development of metastatic disease was 24 months. However, excluding the one patient whose disease recurred more than 13 years after the primary was excised, the mean time to

development of metastatic disease is much shorter, 10.8 months, range 1-44. These data are summarized in table 6.2. The performance status of all patients was good on entry into the study.

Table 6.2 Patient demographics

		Number	%
Mean age (range)		57 (39-82)	-
Male/female		7/5	-
WHO Performance status at entry	(0/1/2)	4/6/0 (2 not stated)	-
Site of metastatic disease	Liver	8	67
	Lung	5	42
	Bone	1	8
	Skin/lymph nodes	6	50
	Brain	2	17

Four patients had received adjuvant biological therapy and one patient adjuvant radiotherapy to the axilla, this is documented in table 6.3. 2 patients had received radiotherapy in the palliative setting, one to whole brain following resection of an isolated brain metastasis and one to a painful bone lesion. All patients were chemotherapy naïve.

Table 6.3 Previous therapy

	N° of patients
Adjuvant high dose interferon	4
Adjuvant radiotherapy	1
Palliative radiotherapy	2
No previous therapy	6

Although this is a small study this patient group would appear representative of patients who accept palliative chemotherapy for metastatic malignant melanoma.

6.3.2 Treatment and toxicity summary

All patients completed their first cycle of treatment, allowing collection of all the planned pharmacokinetic and pharmacodynamic blood samples. Two patients were withdrawn after one cycle of treatment with early progressive disease, in previously resected brain metastases and liver metastases respectively, one patient withdrew after the first cycle because he could not tolerate oral medication but not due to nausea. 9 patients received at least 2 cycles of treatment and had objective response assessment. The number of cycles given is summarised in table 6.4.

Table 6.4

Number of Cycles	1	2	4	6	>6
Number of patients	3	5	2	0	2

The treatment was well tolerated with no incidence of greater than CTC grade 1 nausea and vomiting. Fatigue was the most commonly reported adverse event with two patients grading this as grade 2. One patient required a dose reduction for myelosuppression with grade 2 neutropaenia and grade 3 thrombocytopenia on the first cycle. Her second treatment was delayed by 10 days and she received a dose reduction to 150 mg/m²/day as per the protocol. One patient had a prolonged response to temozolomide and went on to receive a total of 9 cycles of full dose treatment without significant myelotoxicity being observed, having two brief, uncomplicated records of grade 3 neutropaenia during the 9 months treatment. All CTC grade 3 toxicity and greater is listed in table 6.5.

Table 6.5

Toxicity	N^o patients with CTC grade 3/4 toxicity	% of cycles given (32)
Thrombocytopenia	1	3
Neutropaenia	2	6
Headache (disease related)	1	3

The degree of toxicity observed is in line with that published (references as below). The phase II study of temozolomide in metastatic melanoma reported mild toxicity with 3% grade 4 thrombocytopenia and 3% grade 3 neutropenia with no grade 4 neutropenia. Grade 1 nausea was the most common adverse event, reported in 30% of patients (Bleehen, Newlands et al. 1995). The larger phase III study of temozolomide against DTIC reported 2% grade 4 neutropenia and 5% grade 4 thrombocytopenia (Middleton, Grob et al. 2000). Nausea was again the commonest non-haematological toxicity, but was mild in the majority of cases, being grade 2 in one patient, grade 1 in two patients only; there was no vomiting reported.

6.3.3 Response data

All patients were assessed for response after every two cycles of treatment unless they had been withdrawn from treatment because of clinical deterioration and early disease progression. Response was assessed either by clinical measurement of skin lesions/lymph node recurrence or by radiological documentation of disease. Where radiological assessment of response was made the same scanning modality was used throughout treatment, and scans were evaluated according to WHO Guidelines.

9 out of 12 patients were assessable for response. Three patients did not receive their second cycle of treatment as documented above and are therefore not assessable for response. 5 patients demonstrated progressive disease after 2 cycles and were withdrawn from treatment. A further 2 patients had disease stabilisation after 2 cycles but progressive disease after 4 months of treatment. 1 patient had a prolonged response achieving a PR and received 8 cycles of treatment and 1 patient had an excellent response to treatment with a complete radiological response in her lung metastases, and resolution of subcutaneous metastases. Her scan showed continuing response after 6 cycles of treatment, she had suffered no haematological toxicity and a decision was made to treat with 3 further cycles of temozolomide. A CT scan after 9 cycles confirmed the resolution of lung metastases, but showed a fracture through an isolated pelvic bone metastasis. She was withdrawn from the study at this point to receive palliative radiotherapy to this painful area.

The overall response rate was 22%, with a clinical benefit rate (response plus disease stabilisation for at least 2 months) of 44% in the assessable patients. However including those with early proven progressive disease the response rate fell to 18% with 36% clinical benefit.

The phase II study of temozolomide in metastatic melanoma reported a response rate of 21% with an overall clinical benefit rate of 36% (Bleehen, Newlands et al. 1995). In the phase III study comparing temozolomide with DTIC the overall response rate to temozolomide was 13.5% and 12.1% to DTIC, with clinical benefit in 31.4% and 27.9% of patients respectively (Middleton, Grob et al. 2000).

6.4 Plasma temozolomide pharmacokinetics

Plasma temozolomide levels were measured in all patients. A limited sampling schedule only was passed by the ethics committee in Newcastle so 5 of the 6 subjects recruited in this centre had acidified plasma samples for temozolomide analysis at base line, 4 and 24 hours after temozolomide dosing on day 1 of cycle 1 only (4 hour data included in table 6.6). PK samples were not available for one patient recruited at this centre. Limited conclusions can be drawn from these data. The 6 patients recruited in Oxford had more extensive pharmacokinetic sampling and concentration time plots can be calculated. These are shown below in figure 6.3. The limited data available shows a pattern of absorption and rapid clearance similar to that observed and published in the phase I (Newlands, Blackledge et al. 1992), and phase III studies of temozolomide (Middleton, Grob et al. 2000) although in the later study PK sampling was done on day 4 of treatment.

Figure 6.3

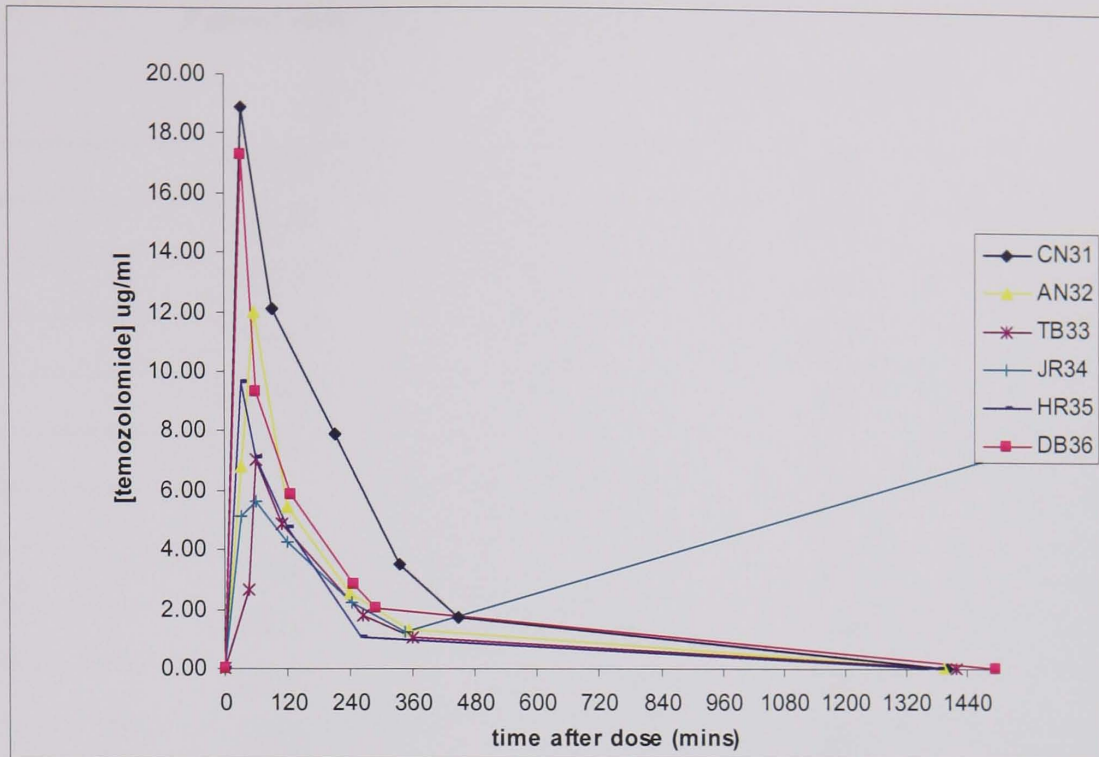


Figure 6.3 Plasma temozolomide concentrations against time from dosing. Concentration/time curve for 6 patients. Note patient HR35 received second dose of temozolomide before 24 hour PK sample taken.

Plasma temozolomide concentrations 4 hours after drug administration for all patients are given in table 6.6. In all patients no temozolomide was detectable by HPLC measurement before treatment and in 11 patients 24 hours after first dose and before receipt of the second dose; consistent with the published clearance of this drug (NB 1 patient inadvertently took his tablets prior to the 24 hour sample). The values measured at 4 hours are consistent with those found in the patients with more extensive sampling.

Table 6.6 Plasma temozolomide at 4 hours in all patients

Patient code	Plasma temozolomide concentration at 4 hours (µg/ml)
SA11*	3.67
HS12*	3.72
RQ13*	2.12
UD14*	2.70
JOCP16*	2.55
CN31	3.50
AN32	2.52
TB33	1.79
JR34	2.23
HR35	1.04
DB36	2.82

* Limited sampling patient

6.5 PARP activity in human PBLs and the effect of temozolomide

Isolated PBLs were obtained from all patients at baseline, 4 and 24 hours after the first dose of temozolomide. When the study was initiated it was hoped that the radiolabel PARP assay used in all the preclinical studies would be suitable for a clinical PD assay. It became clear that low cell harvests compromised the reproducibility of the radiolabel PARP activity assay and the immunoblot assay was developed during the recruitment of this precursor study. The first 3 patient samples were initially analysed using the radiolabel assay, the cell recovery was so low that a range of between 0.015×10^6 to 0.366×10^6 cells could be loaded. All these values lie outside the validated range of cell numbers for the assay. PBLs were prepared from 10 ml whole blood in this study, it was proposed that only 5 ml of blood would be available for lymphopreparation during the Phase I PARP inhibitor study to minimise the total blood volume drawn from patient whilst maximising the number of different PK and PD assays. The problem of low cell harvest would be more acute with the lower volume of blood therefore it became clear that a change in assay technique was required.

The duplicate samples from these first three patients were analysed on a prototype of the immunoblot assay. The assay methodology was identical to the final validated version and appropriate QC samples loaded; however the purified PAR standard curve had not been established at this stage so polymer formation can not be expressed in terms of pmol PAR formed for these three patients. It is, however, possible to compare changes in polymer formation over the baseline value, expressing chemiluminescence detected as a percentage baseline.

All other patient samples were analysed using the final validated protocol for the immunoblot with QC samples and a PAR standard curve (section 3.6). All samples from each patient were loaded in triplicate onto one blot so the any variation in processing and washing was eliminated. A typical blot and Aida output are show in figure 6.4.

Figure 6.4

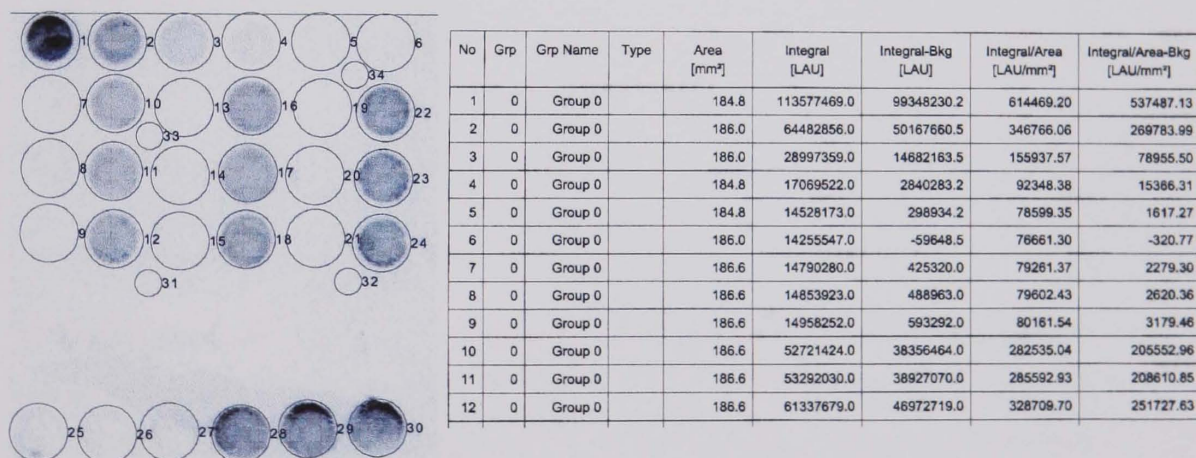


Figure 6.4 Illustrative blot showing standard curve (wells 1-6), T0 samples (7-9, 13-15, 19-21), triplicate patient samples (10-12, 16-18, 22-24) and QC samples (25-30). Areas 31-34 represent background areas for the blot subtracted from all readings. The Aida digital readout is illustrated below the blot, the final column of data (Integral/Area-bkg, LAU/mm²) is used in all subsequent calculations.

The results from all 12 patients are summarised in table 6.7. Data are expressed both as amount of PAR formed per 10⁶ PBLs and also as a percentage of the baseline level for each individual patient.

Table 6.7

Patient ID	Mean PAR formed per 20,000 PBMCs/pmol monomer equiv			As % baseline		
	Baseline	4 hours	24 hours	Baseline	4 hours	24 hours
CN31				100	275	No cells in sample
AN32				100	91	43
TB33				100	No cells in sample	105
JB34	20	130	10	100	603	55
HR35	135	695	195	100	515	144
DB36	20	100	15	100	447	75
SA11	90	75	20	100	84	20
HS12	165	225	70	100	136	42
RQ13	170	205	275	100	122	165
UD14	285	555	500	100	197	177
JR15	185	1160	100	100	636	55
JOCP16	120	80	No cells in sample	100	66	No cells in sample

The mean baseline PARP activity in this patient population who had not previously received chemotherapy was 130 ± 185 pmol/ 10^6 cells (mean \pm SD) with a range 20 – 285. These values are similar to those observed in healthy volunteers with a mean PAR formation of 160 ± 145 , range 15-615 pmol/ 10^6 cells (Dr Chris Jones, personal communication). A significant increase in PARP activity was detected at 4 hours ($p=0.033$: 2-tailed Wilcoxon signed rank test) at the time when temozolomide-induced DNA strand breaks would be expected to peak. There was no statistical difference between the paired baseline and 24 hour samples.

6.6 PARP activity in homogenised human tumour biopsies

9/12 patients consented to tumour biopsies under local anaesthesia before and at one time after receiving their first dose of temozolomide. Patient RQ13 had a groin node biopsy prior to treatment which bled significantly after the procedure and required hospitalisation. It was felt inappropriate to ask him to undergo a further biopsy and risk of re-bleeding.

All experiments were performed using the method described in section 3.7. The results following immunoblotting of the tumour homogenate are shown in table 6.8. Data are expressed in term of the mean amount of PAR formed per mg protein in the tumour homogenate from triplicate samples.

Table 6.8

Patient ID	Mean PAR formed per mg protein (pmol monomer equiv)			As % baseline		
	Baseline	4 hours	24 hours	Baseline	4 hours	24 hours
CN31	463.4		495.5	100		106.8
AN32		2.5			-	
TB33	1.65		18.4			
JB34	2754.2		29.3	100		1.1
HR35	818.6	2926.2		100	375.7	
DB36	606.1		2875.0	100		474.5
SA11	1311.2		258.7	100		19.7
HS12	3609.1	2058.9		100	57.2	
RQ13	3596.2		No biopsy taken			

Note TB33 had melanotic tumour, results given but comparison not made, see below. AN32 baseline biopsy too small to homogenise

There was a considerable range of values for PARP activity in the homogenised tumour samples. This could be due to true variation in the amount of PARP active in the tumour, or due to the biopsy process.

Where two biopsies were obtained these were either different subcutaneous nodules, or in the case of two patients liver biopsies with a tru-cut needle. Tumour

heterogeneity would mean that, even if the same lesion had been biopsied there could be significant variation in the amount of viable tumour in the sample. To allow comparison between samples all data were expressed in terms of mg protein added to the blot. The protein concentration varied between tumours with a range of 0.031-0.55 mg/ml in a 1 in 1000 homogenate. The majority of values lay at the lower end of this scale. One patient (TB33) had a very melanotic tumour and it may be that the pigment interfered with the protein assay giving an unreliable reading. Although there was variation in protein concentration between patients, when the two samples from the same patient were compared there was no significant difference in the protein concentration of their biopsies ($p=0.81$, Wilcoxon signed rank test, 2-tailed p value). The variation in protein levels should not, therefore affect the comparison of PARP activity between tumour biopsies on the same patient.

When tumour PAR formation was expressed as a percentage of the control there was no clear pattern of change in PARP-1 activity at either 4 or 24 hours after dosing. Although the ability to form polymer varied between tumours comparison of the paired samples showed no significant difference after a dose of temozolomide ($p \approx$, Wilcoxon signed rank test, 2-tailed p value).

6.7 Investigation of DNA damage and repair

6.7.1 COMET assay for DNA breaks

Initially both PBLs and tumour samples were prepared for analysis of DNA strand breaks by COMET assay. However it proved impossible to obtain a suitable preparation of isolated tumour cells and there are no data from this matrix. Frozen PBLs were transferred from the clinical centres to the laboratory in Oxford where the COMET assays were performed by Dr Anna Olsen. The summarised results are shown below.

The results from the 12 patients treated are shown in figure 6.5. giving the mean Olive moment at the three time points from individual patients. The mean of 50 COMETs with the standard error of the mean is shown. In the 6/10 of patients the expected rise in DNA damage was observed 4 hours after dosing with temozolomide with a fall

towards baseline at 24 hours, prior to the next dose. The mean values confirmed a general trend towards increased strand breaks at 4 hours (table 6.9). However, due to the variability of the data this increase was not significant ($p=0.15$: Student's t test).

Figure 6.5

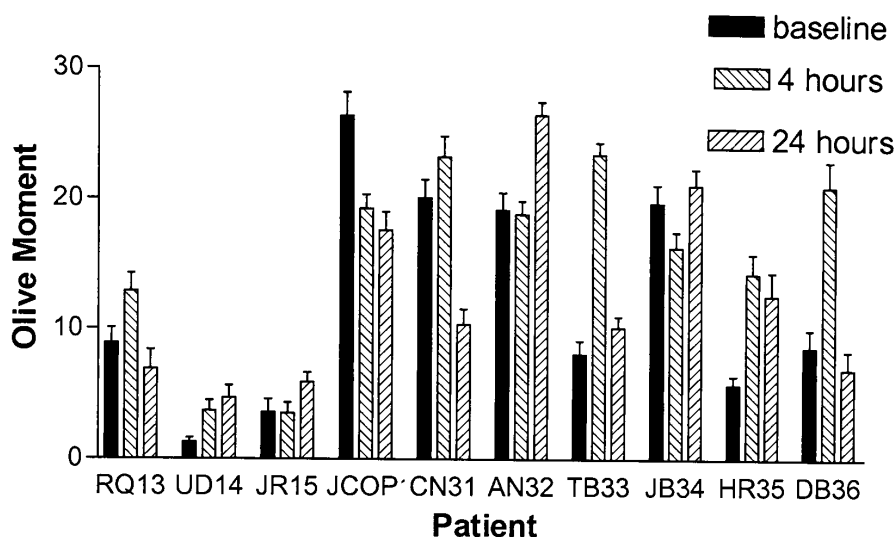


Figure 6.5 Olive tail moments for patient samples at baseline, 4 and 24 hours after 200 mg/m² temozolomide. Mean and SEM, 50 COMETs measured. Data from 10 patients, 2 sets of samples unsuitable for analysis

Table 6.10

Time point	Mean Olive moment	95% confidence interval
Baseline	12.2	6.1-18.2
4 hours	15.7	10.5-20.9
24 hours	12.3	7.1-17.5

6.7.2 ATase

PBLs were prepared by lymphopreparation and washed cell pellets frozen for ATase measurement. All assays were performed by Dr Geoff Margison at the Paterson Institute for Cancer Research, Manchester. As discussed in chapter 1 O⁶-alkylguanine alkytransferase (ATase) is a DNA repair protein which is endogenously expressed and

removes methyl groups from O⁶methyl guanine after exposure to temozolomide. ATase levels would be expected to fall after induction of DNA damage by temozolomide as this protein is also the acceptor for the methyl group in the repair of cytotoxic lesions and once methylated becomes a target for proteolytic degradation (D'Incalci, Citti et al. 1988; Lee, Thatcher et al. 1994).

The results obtained from the patient samples are summarised in figure 6.6, mean and SEM are given, with ATase activity expressed in terms of fmol/ μ g DNA. The expected fall was seen at 4 hours and levels had not recovered to baseline by 24 hours post treatment.

Figure 6.6



Figure 6.6 Mean and SEM of ATase activity in human PBLs after temozolomide dosing (n=8)

Comparison of change in ATase level at 4 hours and pre-treatment is shown in figure 6.7, no correlation has been observed with these samples.

Figure 6.7

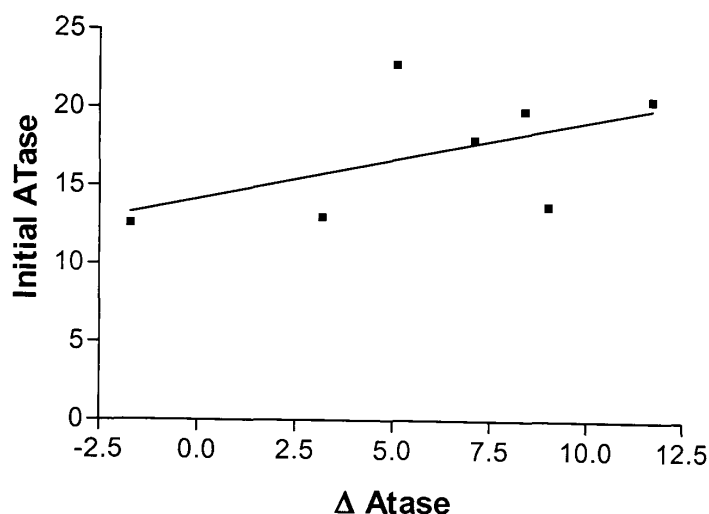


Figure 6.7 Correlation between Initial ATase level and the change 4 hours after treatment with temozolomide. ATase expressed in fmol/ μ g DNA, (n=7)

6.8 Discussion

This chapter reports the clinical and laboratory results of a small phase II study of temozolomide in patients with advanced metastatic melanoma. The study was proposed as a precursor study to the main PARP-1 inhibitor/temozolomide combination study to obtain clinical data to aid validation of the laboratory methods to be used in that study. Additionally it was intended to provide control data for the PD endpoints for the First-in-Human study of AG014699 in combination with temozolomide.

The clinical efficacy and toxicity data obtained in this study is in line with that in the published literature meaning this small study is representative of the typical toxicities and responses reported. The dose limiting toxicity of temozolomide is myelosuppression (reviewed in (Newlands, Stevens et al. 1997) and other toxicities are mild. This was borne out in this study where only one patient required a dose reduction for myelosuppression and otherwise the treatment was well tolerated. The response rate observed was similar to that published for the phase II and phase III trials of this drug (Bleehen, Newlands et al. 1995; Middleton, Grob et al. 2000) with a number of patients deriving clinical benefit from the treatment. The relatively high

rate of early withdrawal from the study (after 2 or fewer cycles) confirms the poor prognosis of this disease, rather than being a reflection on toxicity of the treatment.

The limited pharmacokinetic results are consistent with the well established profile of this compound (Newlands, Blackledge et al. 1992; Danson and Middleton 2001). All patients absorbed the oral preparation rapidly, and no subject showed prolonged retention of the drug in the plasma. It is unfortunate that the only patient who showed significant myelosuppression on the first cycle had their PK sampling omitted.

PARP-1 activity was measured in PBLs from all patients and in tumour samples in 9 out of 12 patients. The variation in this untreated patient population was similar to that observed in healthy volunteers. An important piece of information gained from these results is that PARP-1 activity shows a small but significant increase at 4 hours after a single exposure to temozolomide. It is unclear why this should be, there being no other data available measuring PARP-1 activity in patients receiving chemotherapy.

PARP-1 retains its activity following a round of activation, automodification and removal of the polymer. Therefore, it would not be expected that this enzyme would be depleted following DNA damage. In fact, a small rise in maximally stimulated PARP-1 activity was observed in this study. There is no comparable data in the literature. In a study of the potentiation of temozolomide by the novel PARP inhibitor CEP 6800 a similar increase in PAR accumulation in xenografts was observed 4 hours after treatment with a single dose of temozolomide or irinotecan compared to vehicle control (Miknyoczki, Jones-Bolin et al. 2003). These authors measured endogenous PAR in xenografts as a measure of enzyme activity. This differs from the experiments reported above where the ability of the enzyme to form polymer *ex vivo* was measured

PARP-1 is a nuclear enzyme which is constitutively expressed in the majority of human cells with an average of one copy per 1000 base pairs. Following activation by DNA single strand breaks there is rapid synthesis and degradation of polymer and proposed re-cycling of the enzyme. The half-life of poly(ADP-ribose) is known to be a matter of minutes, with the polymer rapidly removed from its acceptor proteins by

PARP. Given the high endogenous expression of enzyme and this dynamic equilibrium it would not be expected that further enzyme would be synthesised in response to DNA damage. It could be either that there are inactive PARP-1 enzymes sequestered within the cell which are released following temozolomide that could explain the small rise in maximal ability to form polymer or post-translational modification (?phosphorylation) that activates PARP-1 after temozolomide exposure.

The vital piece of evidence gleaned from this study is that there was no fall in PARP-1 activity with cytotoxic drug treatment. In the first in human PARP inhibitor study the primary endpoint is proof of PARP inhibition by the novel agent. For ethical reasons a combination study with a cytotoxic agent is being proposed rather than a single “novel agent” study. Hence it was important to prove that the cytotoxic treatment on its own would not cause a depletion of PARP-1 activity and hence potentially confound the results of the inhibitor study. The fact that a small rise is observed will allow greater certainty of the effect of AG014699 when PARP inhibition is achieved in human PBLs with this drug.

PARP activity was also measured in human tumour samples. There was wide variation in the amount of PARP activity detected in the tumour biopsies, reflecting the heterogeneity of tumours. Preclinical data in human tumour xenografts indicated that there were high levels of PARP activity in tumours when compared with a “standard” tissue such as liver when PARP activity was measured using the [³²P] NAD⁺ incorporation PARP activity assay and with the immunoblot (table 5.5). There is also evidence to confirm this from human liver biopsies, where normal liver shows lower levels of PARP-1 activity than hepatocellular cancer (Shiobara, Miyazaki et al. 2001). The majority of the melanoma biopsies obtained in this study also showed comparatively high levels of PARP enzyme activity. If this high PARP activity contributes to tumour resistance to temozolomide then it is hoped that use of a PARP inhibitor in combination with temozolomide will allow increased tumour effect without increased toxicity.

Pre-clinical evidence shows that inhibition of PARP and hence BER following temozolomide treatment increases peak levels of strand breaks and the persistence from repair of intermediate N-methyl purines (Boulton, Kyle et al. 1999). However,

results from the analysis of DNA single strand breaks with the alkaline COMET assay show a disappointing level of variation with this method. Nevertheless it would appear that there was some evidence of the expected rise in the amount of DNA damage after temozolomide and that this was repaired over the 24 hour period before repeat dosing. It is hoped that further validation of this method will allow its use in studies to support the First in human study of a PARP-1 inhibitor with temozolomide. The inherent variability in the assay is an important reason why this pharmacodynamic endpoint was defined as a secondary not primary endpoint in the PARP-1 inhibitor study.

The primary endpoints of the study have been achieved with the assessment of the DNA damage caused by full dose temozolomide and measurement of PARP-1 and ATase activity after treatment. These enzymes are involved in the two major DNA repair pathways utilised by cells after temozolomide to repair methylated DNA, BER and direct repair. ATase is inactivated by this process hence a fall in levels after treatment is observed, to approximately 60% at 4 hours.

In the phase II study reported here ATase levels fell by $\approx 40\%$ 4 hours after temozolomide therapy. Similar observations were made by Lee et al (Lee, Thatcher et al. 1994) who found that where ATase levels were measured in PBLs from 8 patients after dosing with temozolomide (150 mg/m^2) depletion of ATase was observed within 4 hours of the first dose of temozolomide with a median nadir of 52.9% baseline 2-6 hours post-treatment with levels not returning to normal by 24 hours. This earlier study showed an eight-fold variation in pre-treatment levels of ATase (69 to 593 fmol/mg protein) The different units of measurement do not allow direct comparison with the values found in the current study for the majority of patients, pre-treatment values range from 12.6-22.8 fmol/ μg DNA. In the final 4 patients data was expressed in terms of fmol/mg protein and a similar range is observed to that published (81-535). A similar time course of depletion in tumours has been demonstrated in a mouse xenografts model (Middleton, Kelly et al. 2000) with complete depletion of the enzyme by 4 hours after a single i.p. injection of 100 mg/kg temozolomide. When animals received 5 daily doses of temozolomide (same dose and route) ATase recovery was not complete until day 16 after treatment. Previous studies have demonstrated a relationship between the extent of ATase

depletion and the pre-treatment values in patients receiving temozolomide (Lee, Thatcher et al. 1994). However, in the study reported here, there was no correlation between initial ATase activity and the extent of its depletion (see section 6.7.2), which was largely a reflection of the limited samples points. .

The secondary objectives of the TemoCOMET trial included relating the biological measures of DNA damage and PARP activity to clinical outcome. This has proved difficult because of sample handling problems, however limited conclusions can be drawn. In terms of toxicity there was little significant toxicity observed in this small group of patients. The drug was well tolerated. A correlation has been demonstrated between level of DNA damage and toxicity, in particular nausea (Braybrooke, Houlbrook et al. 2000). No significant emetogenesis was observed in this study. The one patient who developed dose limiting myelosuppression had low mean Olive moments without a significant increase after temozolomide (patient JR15).

4 patients demonstrated clinical benefit with disease stabilisation for 4 months or more. Two of these patients had baseline ATase levels at the bottom of the range observed (13.3 and 12.2 fmol/ μ g DNA) and one at the upper end (17.7 fmol/ μ g DNA), no data is available for the patient who had a prolonged response due to a sample transport problem. The two patients who had early progression of disease (after 1 cycle of treatment) had high/normal initial ATase levels (20.7 fmol/ μ g DNA and 219 fmol/mg protein respectively) and high PARP-1 activity at baseline (135 and 120 pmol PAR/ 10^6 cells). A correlation has previously been demonstrated between high tumour ATase activity and poor response to temozolomide in patients with malignant glioma (Friedman, McLendon et al. 1998) but no correlation with response in biopsy samples from patients with metastatic melanoma (Middleton, Lunn et al. 1998).

In conclusion this Phase II study has provided a valuable forum for the clinical centres to work together, ironing out problems in the complex sampling schedules which it planned to use as part of the dose defining process in the novel PARP inhibitor study. Additional data in human samples has been obtained to complete the validation of the immunoblot as a suitable method for measuring PARP-1 activity to an acceptable standard of accuracy. It has also been shown that PARP-1 activity shows a small

increase after doing with temozolomide, meaning that there will be greater certainty that any measured decrease in the inhibitor study is due to AG014699.

Chapter 7

Summary

7.1 Introduction

Inhibition of PARP was suggested as a potential clinical drug target in 1980, when the first evidence that poly(ADP-ribosylation) was involved in DNA repair was reported (Durkacz, Omidiji et al. 1980). Development of potent PARP inhibitors was identified as one of the Newcastle University Cancer Research Unit's drug development targets in 1990. Over the next 13 years potent inhibitors were developed, latterly in collaboration with Agouron Pharmaceuticals (currently part of Pfizer GRD) and the clinical candidate to emerge from this research entered First-in-Human clinical trials in 2003.

The work described in this thesis was performed during the late stages of the drug development project and included the drafting of the First-in-Human phase I trial protocol and close involvement with the design of this trial. Laboratory studies were based around the validation of an established assay of PARP activity for use as a clinical pharmacodynamic method and the subsequent development of a quantitative immunological PARP-1 activity assay based on polymer detection. A small phase II clinical trial has been supervised to obtain suitable clinical samples which have provided additional validation evidence for the assays but also clinical data to support the subsequent First-in-Human PARP-1 inhibitor trial.

7.2 Protocol development

The development of the phase I clinical trial protocol for a combination study of AG014699, a novel, potent PARP-1 inhibitor and temozolomide is discussed in chapter 2. The final design was for a 2 part study, escalating first the dose of AG014699 until PARP-1 inhibition was proven and subsequently escalating the dose of temozolomide to define a maximum tolerated dose. The majority of the work performed during the early stages of this MD project involved authorship of the first draft of the trial protocol, liaison with other investigators and final collaboration with the teams both in the Drug Development Office, Cancer Research UK, and at Pfizer GRD to produce a protocol for submission to Cancer Research UK's CIRB, the Northern MREC and LRECs for Belfast, Oxford and Newcastle.

There are a number of features in the final study design which are atypical, these have been discussed in chapter 2 and are summarised below.

Unusual features of the study

1. Starting dose of AG014699 was not defined as is usual in a phase I trial as 1/10th of the toxic dose low (TDL) in most sensitive species. Efficacy data was taken in to account to suggest a lower starting dose which is 1/40th TDL in rats.
2. The decision to stop escalation in part 1 of the study is defined by pharmacodynamic indices rather than toxicity. It would not be anticipated that AG014699 and half-dose temozolomide would cause significant toxicity before a PARP inhibitory dose was reached. If significant PARP inhibition is observed in PBLs, sustained out to 6 hours after dosing and with a plateau in magnitude between 2 dose levels escalation of AG014699 would stop at this point and phase 2 of the study entered even if no significant toxicity were reported.
3. Single agent dosing with AG014699 is planned in a run-in period prior to starting the combination to allow the generation of PK and PD single agent data and avoiding the ethical difficulties of proposing a study of the novel agent alone when this would be predicted to be ineffective.

7.3 Pharmacodynamic assay validation

The majority of the work undertaken has been directed towards establishing and validating a pharmacodynamic assay which can be used with clinical samples, both PBLs and tumour biopsy specimens.

Initially an assay based on the incorporation of [³²P] NAD⁺ into poly(ADP-ribose) which was already well established in the Drug Development Laboratory, NICR was adapted and validated for use with human PBLs. This assay proved robust and was suitable for analysis of PBLs and homogenised tumour, whether analysed on the day of harvest or after storage for up to 3 months. However, during the validation process

it became clear that the variability in results was unacceptably high if low numbers of cells were harvested, subsequent experiments have suggested that similar increased variability was an issue with tumour biopsy specimens that have been diluted below 1 in 80 and work is on-going to clarify this.

In the light of the problems with low cell harvest an alternative assay was sought and an immunoblotting technique, first reported by Professor Bürkle's group, adapted for use with human PBLs and tumour homogenate. The various stages of this assay were examined and modified to reduce potential variability, a standard polymer curve established to allow quantification of results and the direct comparison of data from different patient samples.

The salient facts established during the validation of these two assays are listed below.

Salient features established during assay validation

1. PARP enzyme activity in isolated cells, snap frozen tissue or homogenised tumour is not destroyed by freezing at -80°C for up to three months, allowing storage and transport of clinical samples from disparate clinical sites for analysis. Additionally, the degree of enzyme inhibition with AG014699 and AG014361 appears to be preserved when frozen, meaning there is no concern that variation in storage time might affect the degree of inhibition measured in clinical samples.
2. The [^{32}P] NAD^+ incorporation PARP activity assay is a robust assay giving reproducible results providing sufficient cell numbers are available for analysis.
3. A mouse leukaemia cell line, L1210, has been established as suitable cells to use as QA samples to validate an individual assay run.
4. Purified poly(ADP-ribose) can be commercially obtained and used to set up reproducible standard curves allowing quantification of the immunoblot and hence inter-blot comparison.
5. Studies using PARP-1 "knock-out" animals have demonstrated that PARP-1 activity is detected and measured with the immunoblot.

7.4 Assay evaluation within a phase II clinical trial

Having established a potential PD assay which could be used in the First-in-Human PARP inhibitor clinical trial a phase II mechanistic study of temozolomide in patients with advanced malignant melanoma was written and submitted to LREC in Newcastle, Belfast and Oxford. The aims of this study were to investigate indices of DNA damage and PARP activity following full dose temozolomide in a small cohort of patients.

The clinical and laboratory results of this study are discussed. The observed toxicity and response rates were comparable with those reported in the literature, temozolomide at a dose of $200 \text{ mg/m}^2 \times 5$ days every 28 days was well tolerated and >30% patients gained a clinical benefit from treatment.

Pharmacodynamic assays were performed using isolated PBLs. Maximally stimutable PARP-1 activity increased slightly 4 hours after temozolomide dosing, falling to baseline prior to re-dosing on day 1 of cycle 1. COMET assay analysis of DNA single strand breaks suggested that these peak at 4 hours after dosing consistent with reports in the literature. ATase levels fell after temozolomide exposure and had not recovered by 24 hours.

The critical piece of data generated by this study was that maximally stimulated PARP-1 activity did not fall following treatment with temozolomide. During the First-in-Human PARP inhibitor trial study endpoints rely on the demonstration of the degree of PARP inhibition caused by AG014699, it would be more difficult to define these endpoints if they were confounded by changes in enzyme activity due to the chemotherapeutic agent.

7.5 Conclusions and future directions

The development of 2 different pharmacodynamic assays alongside the authorship of the phase I protocol in which the assays would be used allowed the maximum consideration of the practical issues surrounding the treatment of patients at a vulnerable stage in their lives whilst ensuring that scientifically valid endpoints were

defined, appropriate sampling times were selected and translational research was facilitated.

The conduct of a “run-in” study not only provided valuable information but also encouraged co-ordination between the centres and built up an understanding between key personnel in the three centres. This meant that a good working relationship was established before the centres embarked on a complicated trial taking a drug from a new class of agents into the clinical for the first time with all the associated risks.

The final few patients were recruited on to the TemoCOMET study as the First-in-Human study of AG014699 and temozolomide commenced in June 2003. This study is recruiting successfully, PARP inhibition has been demonstrated in PBLs using the immunoblot assay and the study should move into its second stage early in 2004.

On-going laboratory work is focussing on the reproducibility of the assay, in particular that of the standard polymer curve and the background polymer staining in homogenised tissue samples. It is planned that a second phase I combination study of AG014699 with irinotecan will start soon after completion of the temozolomide combination study.

References

- (1992). The health of the nation: a strategy for health in England. London, HMSO.
- (1996). Note for guidance on validation of analytical procedures: methodology, European Agency for the Evaluation of Medicinal Products: Human Medicines Evaluation Unit: 1-9.
- (2001). Guidance for Industry Bioanalytical Method Validation, U.S Food and Drug Administration: Center for Drug Evaluation and Research: 1-16.
- Aboul-Ela, N., E. Jacobson, et al. (1988). "Labelling methods for the study of poly- and mono(ADP-ribose) metabolism in cultured cells." Analytical Biochemistry **174**: 239-250.
- Affar, B., R. G. Shah, et al. (2002). "Role of poly(ADP-ribose) polymerase in rapid intracellular acidification induced by alkylating DNA damage." Proc Natl Acad Sci U S A **99**(1): 245-50.
- Affar, E. B., P. Duriez, et al. (1998). "Immunodot blot method for the detection of poly(ADP-ribose) synthesised in vitro and in vivo." Analytical Biochemistry **259**: 280-283.
- Alvarez-Gonzalez, R. and F. R. Althaus (1989). "Poly(ADP-ribose) catabolism in mammalian cells exposed to DNA-damaging agents." Mutat Res **218**(2): 67-74.
- Ame, J. C., V. Rolli, et al. (1999). "PARP-2, A novel mammalian DNA damage-dependent poly(ADP-ribose) polymerase." J Biol Chem **274**(25): 17860-8.
- Ames, B. N. and L. S. Gold (1991). "Endogenous mutagens and the causes of aging and cancer." Mutation Research **250**: 3-16.
- Banasik, B., H. Komura, et al. (1992). "Specific inhibitors of poly(ADP-ribose) synthetase and mono(ADP-ribosyl) transferase." J Biol Chem **267**: 1569-1575.
- Belanich, M., M. Pastor, et al. (1996). "Retrospective study of the correlation between the DNA repair protein alkyltransferase and survival of brain tumor patients treated with carmustine." Cancer Res **56**(4): 783-8.
- Bernardi, R., C. Negri, et al. (1995). "Activation of poly(ADP-ribose) polymerase in apoptotic human cells." Biochimie **77**(5): 378-84.
- Bernstein, C., H. Bernstein, et al. (2002). "DNA repair/pro-apoptotic dual-role proteins in five major DNA repair pathways: fail-safe protection against carcinogenesis." Mutat Res **511**(2): 145-78.
- Blackledge, G., J. T. Roberts, et al. (1989). "A phase II study of mitozolomide in metastatic transitional cell carcinoma of the bladder." European Journal of Cancer and Clinical Oncology **25**(2): 391-392.
- Bleehen, N. M., E. S. Newlands, et al. (1995). "Cancer Research Campaign phase II trial of temozolomide in metastatic melanoma." Journal of Clinical Oncology **13**(4): 910-3.
- Bouchard, V. J., M. Rouleau, et al. (2003). "PARP-1, a determinant of cell survival in response to DNA damage." Exp Hematol **31**(6): 446-54.

- Boulikas, T. (1991). "Relation between carcinogenesis, chromatin structure and poly(ADP-ribose) (review)." Anticancer Res **11**(2): 489-527.
- Boulton, S., S. Kyle, et al. (1999). "Interactive effects of inhibitors of poly(ADP-ribose) polymerase and DNA-dependent protein kinase on cellular responses to DNA damage." Carcinogenesis **20**(2): 199-203.
- Boulton, S., L. C. Pemberton, et al. (1995). "Potentiation of temozolomide-induced cytotoxicity: a comparative study of the biological effects of poly(ADP-ribose) polymerase inhibitors." Br J Cancer **72**(4): 849-56.
- Bower, M., E. S. Newlands, et al. (1997). "Multicentre CRC phase II trial of temozolomide in recurrent or progressive high-grade glioma." Cancer Chemother Pharmacol **40**: 484-488.
- Bowman, K. J., D. R. Newell, et al. (2001). "Differential effects of the poly(ADP-ribose) polymerase (PARP) inhibitor NU1025 on topoisomerase I and II inhibitor cytotoxicity in L1210 cells in vitro." Br J Cancer **84**(1): 106-112.
- Bowman, K. J., A. White, et al. (1998). "Potentiation of anti-cancer agent cytotoxicity by the potent poly(ADP-ribose) polymerase inhibitors NU1025 and NU1064." Br J Cancer **78**(10): 1269-1277.
- Boyum, A. (1968). "Separation of leucocytes from blood and bone marrow." J. Clin. Invest. **21**(suppl 97).
- Brada, M., K. Hoang-Xuan, et al. (2001). "Multicenter phase II trial of temozolomide in patients with glioblastoma multiforme at first relapse." Ann Oncol **12**(2): 259-66.
- Braybrooke, J. P., S. Houlbrook, et al. (2000). "Evaluation of the alkaline comet assay and urinary 3-methyladenine excretion for monitoring DNA damage in melanoma patients treated with dacarbazine and tamoxifen." Cancer Chemother Pharmacol **45**(2): 111-9.
- Brown, J. and R. Marala (2002). "Development of a high-throughput screening-amenable assay for human poly(ADP-ribose) polymerase inhibitors." Journal of Pharmacological and Toxicological Methods **47**: 137-141.
- Budman, D. R., A. H. Calvert, et al. (2003). Introduction. Handbook of Anticancer Drug Development. B. D. R, C. A. H and R. E. H, Lippincott Williams and Wilkins: ix-x.
- Burkle, A. (2000). "Poly(ADP-ribosylation): a posttranslational protein modification linked with genome protection and mammalian longevity." Biogerontology **1**: 41-46.
- Burkle, A. (2001). "PARP-1: a regulator of genomic stability linked with mammalian longevity." Chembiochem **2**(10): 725-8.
- Burkle, A. (2001). "Physiology and pathophysiology of poly(ADP-ribosylation)." BioEssays **29**: 795-806.
- Calabrese, C. R., R. Almassy, et al. (2004). "Anticancer chemosensitization and radiosensitization by the novel poly(ADP-ribose) polymerase-1 inhibitor AG14361." J Natl Cancer Inst **96**(1): 56-67.

- Canan Koch, S. S., L. H. Thoresen, et al. (2002). "Novel tricyclic poly(ADP-ribose) polymerase-1 inhibitors with potent anticancer chemopotentiating activity: design, synthesis, and X-ray cocrystal structure." J Med Chem **45**(23): 4961-74.
- Chambon, P., J. Weil, et al. (1963). "Nicotinamide mononucleotide activation of a new DNA-dependent polyadenylic acid synthesizing nuclear enzyme." Biochem Biophys Res Communications **11**: 39.
- Chatterjee, S. and N. Berger (1998). Poly(ADP-ribose) polymerase in response to DNA damage. DNA Damage and Repair: DNA repair in higher eukaryotes. J. Nickoloff and M. Hoekstra. Totowa, New Jersey, Humana Press. **2**: 487-516.
- Cherney, B. W., O. W. McBride, et al. (1987). "cDNA sequence, protein structure, and chromosomal location of the human gene for poly(ADP-ribose) polymerase." Proc Natl Acad Sci U S A **84**(23): 8370-4.
- Chiarugi, A. (2002). "Poly(ADP-ribose) polymerase: killer or conspirator? The "suicide hypothesis" revisited." trends in Pharmacological Science **23**(3): 122-129.
- Christmann, M., M. T. Tomicic, et al. (2003). "Mechanisms of human DNA repair: an update." Toxicology **19**: 3-34.
- Conde, C., M. Mark, et al. (2001). "Loss of poly(ADP-ribose) polymerase-1 causes increased tumour latency in p53-deficient mice." Embo J **20**(13): 3535-43.
- Curtin, N., L.-Z. Wang, et al. (2004). "Novel PARP-1 inhibitor, AG14361, restores sensitivity to temozolomide in mismatch repair deficient cells." Clin Cancer Res.
- D'Amours, D., S. Desnoyers, et al. (1999). "Poly(ADP-ribosylation) reactions in the regulation of nuclear functions." Biochemistry Journal **342**: 249-268.
- Danson, S. J. and M. R. Middleton (2001). "Temozolomide: a novel oral alkylating agent." Expert Rev Anticancer Ther **1**(1): 13-9.
- Dantzer, F., V. Schreiber, et al. (1999). "Involvement of poly(ADP-ribose) polymerase in base excision repair." Biochimie **81**(1-2): 69-75.
- D'Atri, S., L. Tentori, et al. (1998). "Involvement of the mismatch repair system in temozolomide-induced apoptosis." Molecular Pharmacology **54**(2): 334-41.
- Davidovic, L., M. Vodenicharov, et al. (2001). "Importance of poly(ADP-ribose) glycohydrolase in the control of poly(ADP-ribose) metabolism." Exp Cell Res **268**(1): 7-13.
- de Murcia, G. and J. Menissier de Murcia (1994). "Poly(ADP-ribose) polymerase: a molecular nick-sensor." Trends Biochem Sci **19**(4): 172-6.
- de Murcia, J. M., C. Niedergang, et al. (1997). "Requirement of poly(ADP-ribose) polymerase in recovery from DNA damage in mice and in cells." Proc Natl Acad Sci U S A **94**(14): 7303-7.
- Decker, P., E. Miranda, et al. (1999). "An improved nonisotopic test to screen a large series of new inhibitor molecules of poly(ADP-ribose) polymerase activity for therapeutic applications." Clin Cancer Res **5**: 1169-1172.

- Delaney, C. A., L. Z. Wang, et al. (2000). "Potentiation of temozolomide and topotecan growth inhibition and cytotoxicity by novel poly(adenosine diphosphoribose) polymerase inhibitors in a panel of human tumor cell lines." Clin Cancer Res 6(7): 2860-7.
- DeVita, V. T., S. Hellman, et al. (1997). Cancer Principles and practice of oncology. Philadelphia, Lippincott-Raven.
- Dillon, K., G. Smith, et al. (2003). "A flashplate assay for the identification of PARP-1 inhibitors." Journal of Biomolecular Screening 8(3): 347-352.
- D'Incalci, M., L. Citti, et al. (1988). "Importance of the DNA repair enzyme O⁶-alkyl guanine alkyltransferase (AT) in cancer chemotherapy." Cancer Treatment Reviews 15: 279-292.
- Dinnes, J., C. Cave, et al. (2002). "A rapid and systemic review of the effectiveness of temozolomide for the treatment of recurrent malignant glioma." Br J Cancer 86: 501-505.
- Drummond, J. T., G.-M. Li, et al. (1995). "Isolation of an hMSH2p160 heterodimer that restores DNA mismatch repair to tumour cells." Science 268(1909-1912).
- D'Silva, I., J. D. Pelletier, et al. (1999). "Relative affinities of poly(ADP-ribose) polymerase and DNA-dependent protein kinase for DNA strand interruptions." Biochim Biophys Acta 1430(1): 119-26.
- Du, L., X. Zhang, et al. (2003). "Intra-mitochondrial poly(ADP-ribosylation) contributes to NAD⁺ depletion and cell death induced by oxidative stress." J Biol Chem 278(20): 18426-33.
- Durkacz, B., O. Omidiji, et al. (1980). "(ADP-ribose)_n participates in DNA excision repair." Nature 283: 593-596.
- Fairburn, D. W., P. L. Olive, et al. (1995). "The comet assay: a comprehensive review." Mutation Research 339: 37-59.
- Farrell, A., J. Leighton, et al. (2003). How oncology drug development differs from other fields. Anticancer drug development. D. Budman, H. Calvert and E. Rowinsky, Lippincott Williams and Wilkins: 3-12.
- Findlay, J. W. A., W. C. Smith, et al. (2000). "Validation of immunoassays for bioanalysis: a pharmaceutical industry perspective." Journal of Pharmaceutical and Biomedical Analysis 21: 1249-1273.
- Fink, D., S. Aebi, et al. (1998). "The role of DNA mismatch repair in drug resistance." Clin Cancer Res 4: 1-6.
- Friedberg, E. C., G. C. Walker, et al. (1995). DNA repair and mutagenesis. Washington DC, ASM Press.
- Friedman, H. S., R. E. McLendon, et al. (1998). "DNA mismatch repair and O⁶-alkylguanine-DNA alkyltransferase analysis and response to Temodal in newly diagnosed malignant glioma." J Clin Oncol 16(12): 3851-7.

- Griffin, R. J., L. C. Pemberton, et al. (1995). "Novel potent inhibitors of the DNA repair enzyme poly(ADP-ribose)polymerase (PARP)." Anticancer Drug Des 10(6): 507-14.
- Grube, K., J. Kupper, et al. (1991). "Direct stimulation of Poly(ADP-ribose) polymerase in permeabilised cells by double-stranded DNA oligomers." Anal. Biochem 193: 236-239.
- Hansen, K. and M. Kelly (2000). "Review of mammalian DNA repair and translational implications." Journal of Pharmacology and Experimental Therapeutics 295(1): 1-9.
- Harris, M. T., M. A. Rosenthal, et al. (2001). "An Australian experience with temozolomide for the treatment of recurrent high grade gliomas." Journal of Clinical Neuroscience 8: 325-327.
- Hickman, M. J. and L. D. Samson (1999). "Role of DNA mismatch repair and p53 in signalling induction of apoptosis by alkylating agents." Proc Natl Acad Sci U S A 96: 10764-10769.
- Hoeijmakers, J. H. (2001). "Genome maintenance mechanisms for preventing cancer." Nature 411: 360-374.
- Horng, S., E. J. Emanuel, et al. (2002). "Descriptions of benefits and risks in consent forms for phase 1 oncology trials." N Engl J Med 347(26): 2134-40.
- Huber, L. (1998). Validation of analytical methods: review and strategy. LC.GC International: 96-105.
- Karran, P. and M. Bignami (1992). "Self-destruction and tolerance in resistance of mammalian cells to alkylation damage." Nucleic Acids Res 20: 2933-2940.
- Karran, P. and R. Hampson (1996). "Genomic instability and tolerance to alkylating agents." Cancer Surv 28: 69-85.
- Kawamitsu, H., H.-o. Hoshino, et al. (1984). "Monoclonal antibodies to poly(adenosine diphosphate ribose) recognize different structures." Biochemistry 23: 3771-3777.
- Kirkwood, J. M., J. G. Ibrahim, et al. (2001). "High-dose interferon alfa-2b significantly prolongs relapse-free and overall survival compared with the GM2-KLH/QS-21 vaccine in patients with resected stage IIB-III melanoma: results of intergroup trial E1694/S9512/C509801." J. Clin. Oncology 19(9): 2370-2380.
- Knight, M. I. and P. J. Chambers (2001). "Production, extraction, and purification of human poly(ADP-ribose) polymerase-1 (PARP-1) with high specific activity." Protein Expr Purif 23(3): 453-8.
- Kupper, J. H., M. Muller, et al. (1995). "trans-dominant inhibition of poly(ADP-ribosylation sensitizes cells against gamma-irradiation and N-methyl-N'-nitro-N-nitrosoguanidine but does not limit DNA replication of a polyomavirus replicon." Mol Cell Biol 15(6): 3154-63.
- Lawley, P. D. and D. H. Phillips (1996). "DNA adducts from chemotherapeutic agents." Mutation Research 355: 13-40.

- Lee, S. M., N. Thatcher, et al. (1994). "Inactivation of O6-alkylguanine-DNA alkyltransferase in human peripheral blood mononuclear cells by temozolomide." British Journal of Cancer **69**(3): 452-6.
- Lee, S. M., N. Thatcher, et al. (1991). "O6-alkylguanine-DNA alkyltransferase depletion and regeneration in human peripheral lymphocytes following dacarbazine and fotemustine." Cancer Res **51**: 619-623.
- Li, J.-H. and J. Zhang (2001). "PARP inhibitors." Investigational Drugs **4**(7): 804-812.
- Lindahl, T., P. Karran, et al. (1997). "DNA excision repair pathways." Current Opinion in Genetic Development **7**: 158-169.
- Lindahl, T., M. S. Satoh, et al. (1995). "Post-translational modification of poly(ADP-ribose) polymerase induced by DNA strand breaks." Trends Biochem Sci **20**(10): 405-11.
- Liu, L., P. Taverna, et al. (1999). "Pharmacologic disruption of base excision repair sensitizes mismatch repair-deficient and -proficient colon cancer cells to methylating agents." Clin Cancer Res **5**(2908-2917).
- Lynch, H. T., T. Smyrk, et al. (1996). "Overview of natural history, pathology, molecular genetics and management of HNPCC (Lynch syndrome)." Int J Cancer **69**: 38-43.
- Mahmood, I. (2003). Allometric scaling: Predicting pharmacokinetic parameters of drugs in humans from animals. Handbook of anticancer drug development. D. R. Budman, A. H. Calvert and E. Rowinsky, Lippincott, Williams and Wilkins: 285-296.
- Malanga, M., J. M. Pleschke, et al. (1998). "Poly(ADP-ribose) binds to specific domains of p53 and alters its DNA binding functions." J Biol Chem **273**(19): 11839-43.
- Margison, G., M. S. Koref, et al. (2002). "Mechanisms of carcinogenicity/chemotherapy by O⁶-methylguanine." Mutagenesis **17**(6): 483-487.
- Masson, M., C. Niedergang, et al. (1998). "XRCC1 is specifically associated with poly(ADP-ribose) polymerase and negatively regulates its activity following DNA damage." Mol Cell Biol **18**(6): 3563-71.
- Masutani, M., T. Nozaki, et al. (2000). "The response of Parp knockout mice against DNA damaging agents." Mutat Res **462**(2-3): 159-66.
- Masutani, M., T. Nozaki, et al. (1999). "Function of poly(ADP-ribose) polymerase in response to DNA damage: gene-disruption study in mice." Mol Cell Biochem **193**(1-2): 149-52.
- Masutani, M., T. Nozaki, et al. (1995). "Role of poly(ADP-ribose) polymerase in cell-cycle checkpoint mechanisms following gamma-irradiation." Biochimie **77**(6): 462-5.
- Mendoza-Alvarez, H. and R. Alvarez-Gonzalez (1993). "Poly(ADP-ribose) polymerase is a catalytic dimer and the automodification reaction is intermolecular." J Biol Chem **268**: 22575-22580.
- Middleton, M. R., J. J. Grob, et al. (2000). "Randomized phase III study of temozolomide versus dacarbazine in the treatment of patients with advanced metastatic malignant melanoma." J Clin Oncol **18**(1): 158-66.

- Middleton, M. R., J. Kelly, et al. (2000). "Four-hourly scheduling of temozolomide improves tumour growth delay but not therapeutic index in A375M melanoma xenografts." Cancer Chemother Pharmacol **45**(1): 15-20.
- Middleton, M. R., J. Kelly, et al. (2000). "O(6)-(4-bromothienyl)guanine improves the therapeutic index of temozolomide against A375M melanoma xenografts." Int J Cancer **85**(2): 248-52.
- Middleton, M. R., S. M. Lee, et al. (2000). "O6-methylguanine formation, repair protein depletion and clinical outcome with a 4 hr schedule of temozolomide in the treatment of advanced melanoma: results of a phase II study." Int J Cancer **88**(3): 469-73.
- Middleton, M. R., J. M. Lunn, et al. (1998). "O6-methylguanine-DNA methyltransferase in pretreatment tumour biopsies as a predictor of response to temozolomide in melanoma." Br J Cancer **78**(9): 1199-202.
- Miknyoczki, S. J., S. Jones-Bolin, et al. (2003). "Chemopotentiation of temozolomide, irinotecan, and cisplatin activity by CEP-6800, a poly(ADP-ribose) polymerase inhibitor." Mol Cancer Ther **2**(4): 371-82.
- Miller, K., R. Bowsher, et al. (2001). "Workshop on Bioanalytical Methods Validation for Macromolecules: Summary Report." Pharmaceutical Research **18**(9): 1373-1383.
- Molinete, M., W. Vermeulen, et al. (1993). "Overproduction of the poly(ADP-ribose) polymerase DNA-binding domain blocks alkylation-induced DNA repair synthesis in mammalian cells." Embo J **12**(5): 2109-17.
- Newlands, E. S., G. R. Blackledge, et al. (1992). "Phase I trial of temozolomide (CCRG 81045; M&B 39831; NSC 362856)." British Journal of Cancer **65**(2): 287-91.
- Newlands, E. S., M. F. G. Stevens, et al. (1997). "Temozolomide: a review of its discovery, chemical properties, pre-clinical development and clinical trials." Cancer Treatment Reviews **23**: 35-61.
- Oei, S. L. and M. Ziegler (2000). "ATP for the DNA ligation step in base excision repair is generated from poly(ADP-ribose)." J Biol Chem **275**(30): 23234-9.
- Offer, H., M. Milyavsky, et al. (2001). "Structural and functional involvement of p53 in BER in vivo and in vitro." Oncogene **20**: 581-589.
- Oka, J., J. C. Ueda, et al. (1984). "ADP-ribosyl-protein lyase. Purification, properties and identification of the product." J Biol Chem **259**: 986-995.
- Olive, P. L., A. P. S. Chan, et al. (1988). "Comparison between the DNA precipitation and alkali unwinding assays for detecting DNA strand breaks and cross-links." Cancer Res **48**: 6444-6449.
- Oliver, F. J., G. de la Rubia, et al. (1998). "Importance of poly(ADP-ribose) polymerase and its cleavage in apoptosis. Lesson from an uncleavable mutant." J Biol Chem **273**(50): 33533-9.
- O'Quigley, J., M. Pepe, et al. (1990). "Continual reassessment method: a practical design for phase I clinical trials in cancer." Biometrics **46**: 33-48.

- Pfieber, R., C. Brabeck, et al. (1999). "Quantitative nonisotopic immuno-dot-blot method for the assessment of cellular poly(ADP-ribosylation) capacity." Analytical Biochemistry **275**: 118-122.
- Purnell, M. R. and W. J. D. Whish (1980). "Novel inhibitors of poly(ADP-ribose) synthetase." Biochemical Journal **185**: 775-777.
- Rossi, L., M. Denegri, et al. (2002). "Poly(ADP-ribose) degradation by post-nuclear extracts from human cells." Biochimie **84**: 1227-1233.
- Rubinstein, L. and R. Simon (2003). Phase I clinical trial design. Anticancer drug development. D. Budman, H. Calvert and E. Rowinsky, Lippincott Williams and Wilkins: 297-308.
- Ruf, A., G. de Murcia, et al. (1998). "Inhibitor and NAD⁺ binding to poly(ADP-ribose) polymerase as derived from crystal structures and homology modeling." Biochemistry **37**(11): 3893-900.
- Ruf, A., J. M. de Murcia, et al. (1996). "Structure of the catalytic fragment of poly(ADP-ribose) polymerase from chicken." Proc Natl Acad Sci USA **93**: 7481-7485.
- Sanderson, R. J. and T. Lindahl (2002). "Down-regulation of DNA repair synthesis at DNA single-strand interruptions in poly(ADP-ribose) polymerase-1 deficient murine cell extracts." DNA Repair (Amst) **1**(7): 547-58.
- Satoh, M. S. and T. Lindahl (1992). "Role of poly(ADP-ribose) formation in DNA repair." Nature **356**(6367): 356-8.
- Schreiber, V., J. C. Ame, et al. (2002). "Poly(ADP-ribose) polymerase-2 (PARP-2) is required for efficient base excision DNA repair in association with PARP-1 and XRCC1." J Biol Chem **277**(25): 23028-36.
- Schreiber, V., M. Molinete, et al. (1992). "The human poly(ADP-ribose) polymerase nuclear localization signal is a bipartite element functionally separate from DNA binding and catalytic activity." Embo J **11**(9): 3263-9.
- Shah, G., S. Kaufmann, et al. (1995). "Detection of poly(ADP-ribose) polymerase and its apoptosis-specific fragment by a nonisotopic activity-Western blot technique." Analytical Biochemistry **232**: 251-254.
- Shah, G., D. Poirier, et al. (1995). "Methods for biochemical study of poly(ADP-ribose) metabolism in vitro and in vivo." Analytical Biochemistry **227**: 1-13.
- Shah, V., K. Midha, et al. (1992). "Analytical methods validation: bioavailability, bioequivalence, and pharmacokinetic studies." Journal of Pharmaceutical Sciences **81**(3): 309-312.
- Shall, S. (2002). "Poly(ADP-ribosylation)- a common control process?" BioEssays **24**: 197-201.
- Shall, S. and G. de Murcia (2000). "Poly(ADP-ribose) polymerase-1: what have we learned from the deficient mouse model?" Mutat Res **460**(1): 1-15.

- Shen, F., L. A. Decosterd, et al. (1995). "Determination of temozolomide in human plasma and urine by high-performance liquid chromatography after solid-phase extraction." Journal of Chromatography B: Biomedical Applications **667**: 291-300.
- Shieh, W. M., J. C. Ame, et al. (1998). "Poly(ADP-ribose) polymerase null mouse cells synthesize ADP-ribose polymers." J Biol Chem **273**(46): 30069-72.
- Shiobara, M., M. Miyazaki, et al. (2001). "Hepatocellular carcinoma: treatment and recurrence marker." Journal of Gastroenterology and Hepatology **16**: 338-344.
- Simbulan-Rosenthal, C. M., B. R. Haddad, et al. (1999). "Chromosomal aberrations in PARP(-/-) mice: genome stabilization in immortalized cells by reintroduction of poly(ADP-ribose) polymerase cDNA." Proc Natl Acad Sci U S A **96**(23): 13191-6.
- Simon, R., B. Freidlin, et al. (1997). "Accelerated titration designs for phase I clinical trials in oncology." J Natl Cancer Inst **89**(15): 1138-47.
- Simonin, F. (1993). "The carboxy-terminal domain of human poly(ADP-ribose) polymerase. Overproduction in Escherichia coli. large scale purification and characterization." J Biol Chem **268**: 13454-13461.
- Skalitzky, D. J., J. T. Marakovits, et al. (2003). "Tricyclic benzimidazoles as potent poly(ADP-ribose) polymerase-1 inhibitors." J Med Chem **46**(2): 210-3.
- Smith, S. (2001). "The world according the PARP." Trends in Biochemical Sciences **26**(3): 174-179.
- Soldani, C. and A. I. Scovassi (2002). "Poly(ADP-ribose) polymerase-1 cleavage during apoptosis: an update." Apoptosis **7**(4): 321-8.
- Southan, G. and C. Szabo (2003). "Poly(ADP-ribose) polymerase inhibitors." Curr Med Chem **10**: 321-340.
- Stevens, M., J. Hickman, et al. (1987). "Antitumour activity and pharmacokinetics in mice of 8-carbamoyl-3-methyl-imidazo[5,1-d]-1,2,3,5-tetrazin-4(3H)-one (CCRG 81045; M & B 39831), a novel drug with potential as an alternative to dacarbazine." Cancer Research **47**: 5846-5852.
- Stupp, R., M. Gander, et al. (2001). "Current and future developments in the use of temozolomide for the treatment of brain tumours." The Lancet Oncology **2**: 552-560.
- Tentori, L., G. Graziani, et al. (1995). "Triazene compounds increase apoptosis in O⁶-alkylguanine-DNA alkyltransferase deficient leukaemic cell lines." Leukemia **9**: 1888-1895.
- Tentori, L., C. Leonetti, et al. (2002). "Combined treatment with temozolomide and poly(ADP-ribose) polymerase inhibitor enhances survival of mice bearing hematologic malignancy at the central nervous system site." Blood **99**(6): 2241-4.
- Tentori, L., L. Orlando, et al. (1997). "Inhibition of O⁶-alkylguanine DNA-alkyltransferase or poly(ADP-ribose) polymerase increases susceptibility of leukemic cells to apoptosis induced by temozolomide." Mol Pharmacol **52**(2): 249-58.
- Tentori, L., I. Portarena, et al. (2002). "Potential clinical applications of poly(ADP-ribose) polymerase (PARP) inhibitors." Pharmacol Res **45**(2): 73-85.

- Tentori, L., I. Portarena, et al. (2002). "Poly(ADP-ribose) polymerase inhibitor increases growth inhibition and reduces G(2)/M cell accumulation induced by temozolomide in malignant glioma cells." Glia **40**(1): 44-54.
- Tentori, L., I. Portarena, et al. (2001). "Effects of single or split exposure of leukemic cells to temozolomide, combined with poly(ADP-ribose) polymerase inhibitors on cell growth, chromosomal aberrations and base excision repair components." Cancer Chemother Pharmacol **47**(4): 361-9.
- Tentori, L., I. Portarena, et al. (2002). "Apoptotic and genotoxic effects of a methyl sulfonate ester that selectively generates N3-methyladenine and poly(ADP-ribose) polymerase inhibitors in normal peripheral blood lymphocytes." Cancer Chemother Pharmacol **49**(3): 217-24.
- Tentori, L., M. Turriziani, et al. (1999). "Treatment with temozolomide and poly(ADP-ribose) polymerase inhibitors induces early apoptosis and increases base excision repair gene transcripts in leukemic cells resistant to triazene compounds." Leukemia **13**(6): 901-9.
- Valenzuela, M. T., R. Guerrero, et al. (2002). "PARP-1 modifies the effectiveness of p53-mediated DNA damage response." Oncogene **21**(7): 1108-16.
- Virag, L. and C. Szabo (2002). "The therapeutic potential of poly(ADP-ribose) polymerase inhibitors." Pharmacological Reviews **54**: 375-429.
- Vodenicharov, M. D., F. R. Sallmann, et al. (2000). "Base excision repair is efficient in cells lacking poly(ADP-ribose) polymerase 1." Nucleic Acids Res **28**(20): 3887-96.
- Wang, Z.-Q., B. Auer, et al. (1995). "Mice lacking ADPRT and poly(ADP-ribosylation) develop normally but are susceptible to skin disease." Genes and Development **9**: 509-520.
- Wang, Z. Q., L. Stingl, et al. (1997). "PARP is important for genomic stability but dispensable in apoptosis." Genes Dev **11**(18): 2347-58.
- Wedge, S. R., J. K. Porteus, et al. (1996). "3-Aminobenzamide and/or O⁶-benzylguanine evaluated as an adjuvant to temozolomide or BCNU treatment in cell lines of variable mismatch repair status and O⁶-alkylguanine-DNA alkyltransferase activity." Br J Cancer **74**: 1030-1036.
- Wesierska-Gadek, J., J. Wojciechowski, et al. (2003). "Central and carboxy-terminal regions of human p53 protein are essential for interaction and complex formation with PARP-1." J Cell Biochem **89**(2): 220-32.
- Wieler, S., J. P. Gagne, et al. (2003). "Poly(ADP-ribose) polymerase-1 is a positive regulator of the p53-mediated G1 arrest response following ionizing radiation." J Biol Chem **278**(21): 18914-21.
- Wood, R. D. (1996). "DNA repair in eukaryotes." Annual Review of Biochemistry **65**: 135-167.
- Ying, W., P. Garnier, et al. (2003). "NAD⁺ repletion prevents PARP-1-induced glycolytic blockade and cell death in cultured mouse astrocytes." Biochem Biophys Res Commun **308**(4): 809-13.

- Yu, S. W., H. Wang, et al. (2002). "Mediation of poly(ADP-ribose) polymerase-1-dependent cell death by apoptosis-inducing factor." *Science* **297**(5579): 259-63.
- Yung, W. K., M. D. Prados, et al. (1999). "Multicenter phase II trial of temozolomide in patients with anaplastic astrocytoma or anaplastic oligoastrocytoma at first relapse. Temodal Brain Tumor Group." *J Clin Oncol* **17**(9): 2762-71.